Universidade de Brasília
INSTITUTO DE CIÊNCIAS BIOLÓGICAS
PROGRAMA DE PÓS-GRADUAÇÃO EM BIOLOGIA ANIMAL

Avaliação da atividade imunogênica da terapia fotodinâmica mediada por nanoemulsão de alumínio-ftalocianina em modelo de melanoma murino B16F10

José Athayde Vasconcelos Morais

Brasília
2024

José Athayde Vasconcelos Morais

Avaliação da atividade imunogênica da terapia fotodinâmica mediada por nanoemulsão de alumínio ftalocianina em modelo de melanoma murino

Tese de Doutorado apresentada ao Programa de Pós-Graduação em Biologia Animal da Universidade de Brasília como parte dos requisitos para obtenção do título de Doutor em Biologia Animal.

Orientador: Prof. Dr. Marcio José Poças Fonseca
Coorientador: Prof. Dr. Luis Alexandre Muehlmann

Brasília
2024

“A trabalho duro é a verdade do sucesso. O verdadeiro campeão é aquele que nunca desiste.”

Jesse Owens

RESUMO

O melanoma, a forma mais letal de câncer de pele, representa um grande desafio clínico devido à tendência à formação de metástases e à resistência às terapias tradicionais. Apesar dos avanços na cirurgia, quimioterapia e radioterapia, o tratamento do melanoma avançado ainda carece de alternativas mais eficazes, reforçando a necessidade urgente de mais estudos nessa área. A terapia fotodinâmica (TFD) surgiu há mais de um século como uma alternativa promissora ao tratamento de cânceres. Esse tratamento é baseado na fotoativação de um fotossensibilizante, o qual então converte oxigênio e outras moléculas presentes no tecido alvo a espécies altamente oxidantes, as quais danificam diversas biomoléculas e podem provocar a morte de células afetadas. A eficácia antitumoral da TFD depende de três mecanismos principais: i) citotoxicidade direta às células alvo, ii) colapso da microvasculatura tumoral, com consequente isquemia tecidual, e iii) ativação de respostas imunitárias contra as células tratadas. Ainda, a fotocitotoxicidade dessa terapia é limitada aos tecidos irradiados por luz na sua aplicação, reduzindo a probabilidade de ocorrência de efeitos colaterais negativos. Nesse estudo, foram avaliados os efeitos antitumorais da TFD mediada pelo fotossensibilizante cloreto de alumínio-ftalocianina em modelo de melanoma murino de células B16F10, por meio da indução de morte celular imunogênica (MCI), efeito abscopal e pela alteração de expressão de genes responsáveis pelo processo do sistema imunitário. Concentrações inibitórias (IC) de 50%, 70% e 90% de AlPcNE induziram a exposição de DAMPs pelas células B16F10 após TFD. A aplicação de células B16F10 tratadas com IC50 ou IC70 de AlFtNE-TFD anteriormente ao desafio com células B16F10 viáveis tornou os camundongos C57BL/6 mais resistentes ao desenvolvimento do tumor. Diferentes protocolos de TFD inibiu o crescimento tumoral por ação direta e abscopal. O protocolo de HL_HPS foi capaz de modular a ativação do sistema imunitário levando a significativos aumentos da população sistêmica de linfócitos T CD8 e alterações no perfil de expressão de genes relacionados à resposta imunitária. Essa pesquisa lança luz sobre o potencial de diferentes protocolos de TFD para modular a resposta imunitária e abre caminhos para tratamentos de câncer mais eficazes e direcionados.

Palavras-chave: melanoma; TFD; alumínio-cloro ftalocianina; DAMP; morte celular imunogênica; efeito abscopal; Transcriptoma;

ABSTRACT

Melanoma, the most lethal form of skin cancer, presents a significant clinical challenge due to the propensity for metastasis and resistance to traditional therapies. Despite advances in surgery, chemotherapy, and radiotherapy, the treatment of advanced melanoma still lacks more effective alternatives, underscoring the urgent need for further research in this area. Photodynamic therapy (PDT), which emerged over a century ago, is promising as an alternative cancer treatment. This therapy relies on the photoactivation of a photosensitizer, which then converts oxygen and other molecules present in the target tissue into highly oxidizing species that damage various biomolecules and can induce the death of affected cells. The antitumor efficacy of PDT depends on three main mechanisms: i) direct cytotoxicity to target cells, ii) collapse of the tumor microvasculature, leading to tissue ischemia, and iii) activation of immune responses against treated cells. Additionally, the phototoxicity of this therapy is limited to tissues irradiated by light during its application, reducing the likelihood of adverse side effects. In this study, the antitumor effects of PDT mediated by the photosensitizer aluminum phthalocyanine chloride in murine B16F10 melanoma models were studied, highlighting the role in immunogenic cell death, the abscopal effect, and the expression of genes responsible for immune system processes. Inhibitory concentrations (IC) of 50%, 70%, and 90% of AlPcNE induced the exposure of DAMPs by B16F10 cells after PDT. The application of B16F10 cells treated with IC50 or IC70 of AlPcNE-PDT before the challenge with viable B16F10 cells rendered the C57BL/6 mice more resistant to the tumor devepolment. Different PDT protocols inhibited melanoma tumor growth through both direct and abscopal effects. The HL_HPS protocol was capable of modulating the immune system activation: significant increase in the systemic population of CD8 T lymphocytes and changes in the expression profile of genes related to immune response were detected. This research sheds light on the potential of different PDT protocols to modulate the immune response and opens avenues for more effective and targeted cancer treatments.

Keywords: melanoma; PDT; aluminum chloride phthalocyanine; DAMP; immunogenic cell death; abscopal effect; Transcriptome;

LISTA DE FIGURAS

LISTA DE ABREVIATURAS E SIGLAS

AlPcNE	nanoemulsão contendo o fotossensibilizante alumínio cloro ftalocianina
ANOVA	análise de variância
AO	laranja de acridina
ATP	trifosfato de adenosina
DAMP	do inglês: padrão molecular associado a danos
DEGs	do inglês: genes diferencialmente expressos
DNA	ácido desoxirribonucleico (do inglês desoxiribonucleic acid)
FC	do inglês fold-change
DMSO	dimetilsulfóxido
EPM	Erro Padrão da Média
FS	fotossensibilizante
IC	índice celular
IC_{50}	concentração inibitória para 50% das células
LED	diodo emissor de luz com 25,9 j/cm^2
min	minutos
MCI	morte celular imunogênica
MTT	brometo de 3 (4,5 dimetiltiazol-2il)-2,5-difenil-tetrazólio
PBS	tampão fosfato salina
PDI	índice de polidispersão
PI	iodeto de propídeo
RNA	ácido ribonucleico (do inglês ribonucleic acid)
RNAm	ácido ribonucleico mensageiro
RNAseq	do inglês *RNA sequencing*
RT-qPCR	transcrição reversa seguida de reação em cadeia da polimerase em tempo real (do inglês *Reverse transcription quantitative real time polymerase chain reaction*)
ROS	espécies reativas do oxigênio
SFB	soro fetal bovino
TFD	terapia fotodinâmica
vol	volume

LISTA DE SÍMBOLOS

°C	graus celsius
J/cm^2	Joule por centímetro quadrado
µM	micromolar
µL	microlitros
µg	microgramas
mV	milivolt
nm	nanometros
µm	micrometros
mg	miligramas
mL	mililitros
O_2	oxigênio
%	porcentagem

SUMÁRIO

1. INTRODUÇÃO

O melanoma, apesar de não ser um dos tipos de câncer mais frequentes, é um dos mais agressivos e letais[1,2]. Apesar de corresponder a cerca de 1% dos casos de câncer de pele, o melanoma é responsável por mais de 75% das mortes por cânceres desse órgão[3], o que se deve à alta capacidade metastática. Ainda, o melanoma é um dos poucos tipos de câncer com taxa de incidência crescente no mundo nas últimas décadas, com cerca de 325.000 novos casos em 2020, um aumento de cerca de 41% em relação a 2012 com cerca 230 mil novos casos, e 57.000 mortes relatadas em 2020[3]. Segundo o Instituto Nacional do Câncer (INCA) só em 2022, no Brasil, foram cerca de 8.980 novos casos de melanoma por 100 mil habitantes, desses 4.640 homens e 4.340 mulheres[4]. No Brasil, o câncer de pele é o mais frequente e corresponde a cerca de 30% de todos os tumores malignos[4].

A formação de metástases, responsáveis por mais de 90% das mortes associadas ao câncer, acontece quando as células do tumor primário adquirem a capacidade de se disseminar para outras partes do corpo [5]. A metástase surge por seleção natural de subpopulações celulares com capacidade de infiltração e sobrevivência fora do ambiente tumoral primário[6,7] (Figura 1)[8].

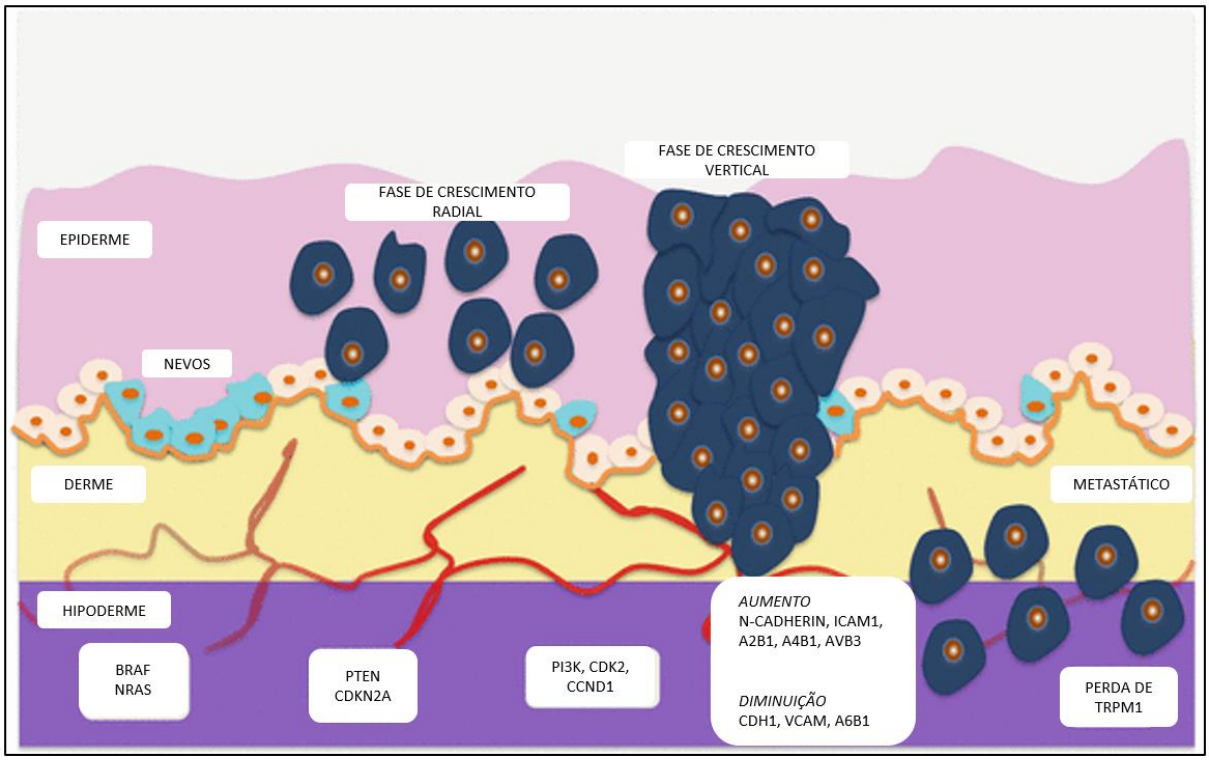

Figura 1. Representação esquemática do modelo molecular de progressão do melanoma em múltiplas etapas. Adaptado de Dakubo 2017.

O diagnóstico precoce e a excisão do tumor primário são eficientes para a maioria dos casos, no entanto a disseminação de células metastáticas é geralmente comum e rápida no melanoma, dificultando o tratamento[1,9].

Os recentes avanços científicos trouxeram um expressivo aumento na sobrevida de pacientes com melanoma metastático, com várias abordagens inovadoras que melhoraram a sobrevivência e a qualidade de vida dos pacientes. Os tratamentos padrões para o melanoma avançado consistem principalmente no uso dos inibidores de "checkpoint" imunológico, as terapias alvo dos inibidores moleculares dos genes *BRAF* e *MEK*, além da terapia combinada entre elas[8].

PD-1 é uma proteína de superfície expressa nas células T ativadas, células B e outras células do sistema imunológico. Já PD-L1 e PD-L2 são ligantes de PD-1, expressos em várias células, incluindo células tumorais, células dendríticas e macrófagos, além de algumas células de resposta à inflamação[1,7]. Quando PD-L1 ou PD-L2 se ligam a PD-1, enviam um sinal inibitório que reduz a resposta imunitária, prevenindo a ativação e proliferação excessiva das células T, que poderia levar a danos teciduais[7]. A ligação de PD-1 a PD-L1/PD-L2 ocorre naturalmente durante a resposta imunitária de modo a regular a atividade das células T e prevenir a autoimunidade. Entretanto, em células tumorais, a expressão de altos níveis de PD-L1 é comum e é uma das principais formas do câncer evadir do sistema imunitário, criando um microambiente imunossupressor, permitindo o crescimento do tumor e a invasão de outros tecidos, sem ser atacado pelo sistema imunológico[10].

Medicamentos como pembrolizumabe e nivolumabe são inibidores de PD-1, já atezolizumabe inibe PD-L1. Essas drogas representam uma abordagem inovadora ao estimular o sistema imunológico do próprio paciente a combater o câncer[11]. De forma semelhante, tem-se o ipilimumabe que inibe CTLA-4 permitindo que as células T permaneçam ativas e proliferem para combater o tumor[7]. CTLA-4 é fundamental como sinalizador inibitório das células T ativadas após a apresentação de antígenos, o que reduz a proliferação e a produção de citocinas.

As terapias alvo direcionadas aos inibidores *BRAF* e *MEK* representam tratamento personalizado dos melanomas que apresentam mutações ativadoras de *BRAF-V600*. Esses representam cerca de 50% do total de melanomas e, em mais de 90% dos casos, ocorre a mutação da valina 600 em ácido glutâmico (V600E)[12]. O gene *BRAF* codifica uma proteína que faz parte da via de sinalização *MAPK/ERK*, responsável por regular a diferenciação, sobrevivência e proliferação celular, e que é normalmente ativada por fatores de crescimento

como VEGF e EGF[12]. Entretanto, mutações no gene BRAF o convertem em um oncogene e levam à ativação da via de sinalização MAPK/ERK, mesmo sem os estímulos fisiológicos normais, o que pode contribuir para a proliferação descontrolada das células tumorais (Figura 2)[12].

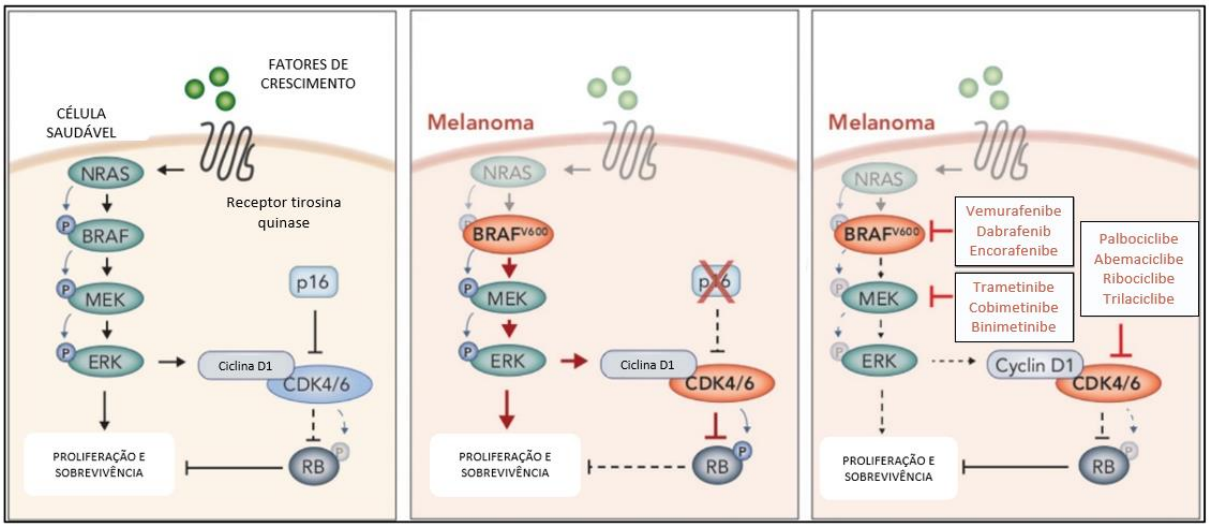

Figura 2. Representação esquemática das Vias de sinalização MAPK/ERK em células saudáveis, no melanoma e no melanoma com inibidores clínicos alvo. Adaptado de Lelliott et al. (2021).

Além da mutação no gene BRAF, outras descobertas genéticas sobre os melanomas vêm sendo alvo de estudos. Algumas mutações em genes específicos estão relacionadas com o risco de desenvolvimento do melanoma ao longo da vida, como por exemplo os genes MITF, CDK4, BAP1 e POT1[13].

Apesar dos progressos, as terapias ainda apresentam limitações quanto à eficácia, principalmente em razão da heterogeneidade genética e da resistência ao tratamento, característicos do melanoma, além dos efeitos colaterais negativos significantes desses tratamentos, prejudicando a qualidade de vida dos pacientes[14].

O sistema imunitário é capaz de detectar e eliminar agentes infecciosos, como vírus e bactérias, bem como células cancerosas[6]. Esta capacidade depende do reconhecimento de padrões moleculares associados a patógenos (PAMPs) ou padrões moleculares associados a danos (DAMPs)[15,16]. Os PAMPs são moléculas de diferentes patógenos, como lipopolissacarídeo ou RNA bacteriano, já os DAMPs são moléculas do próprio organismo que sinalizam algum dano tecidual ou celular, como o ATP extracelular, a calreticulina e HMGB1[17].

À medida que as infecções bacterianas e virais progridem, elas liberam quantidades crescentes desses padrões moleculares que estimulam progressivamente os receptores do

sistema imunitário inato do tipo Toll (TLRs), sinalizando a presença de patógenos invasores. Um mecanismo semelhante acontece com as células cancerosas. Alguns tratamentos antitumorais promovem a liberação de DAMPS que aumentam a apresentação de antígenos tumorais, ativando o sistema imunológico contra aquelas células[18]. Os DAMPs, normalmente se encontram dentro das células e são liberados ou exteriorizados na membrana em condições de estresse celular ou patológicas, sinalizando ao sistema imunológico e aumentando a imunogenicidade do tumor[19]. Isso ocorre por meio da comunicação celular por receptores presentes nas células apresentadoras de antígenos (APCs) como macrófagos e células dendríticas (DC). Os tratamentos antitumorais estão cada vez mais explorando a morte direta de células cancerosas com a capacidade de estimular a imunidade antitumoral por meio da exposição de DAMPs, a chamada morte celular imunogênica (MCI)[20,21].

Essa exposição de DAMPs contribui para a atração de fagócitos para o microambiente tumoral; esses liberam citocinas pró-inflamatórias, como Il-1b e IFN-g, e desencadeiam a apresentação cruzada de antígenos tumorais em moléculas MHC II, nas células T CD4, e MHC I nas células T CD8[22]. Após o reconhecimento do complexo MHC classe I ligado a antígenos intracelulares de células tumorais, as células T CD8 secretam perforinas capazes de induzir poros nas células-alvo induzindo a morte das células[23] (Figura 3)[24].

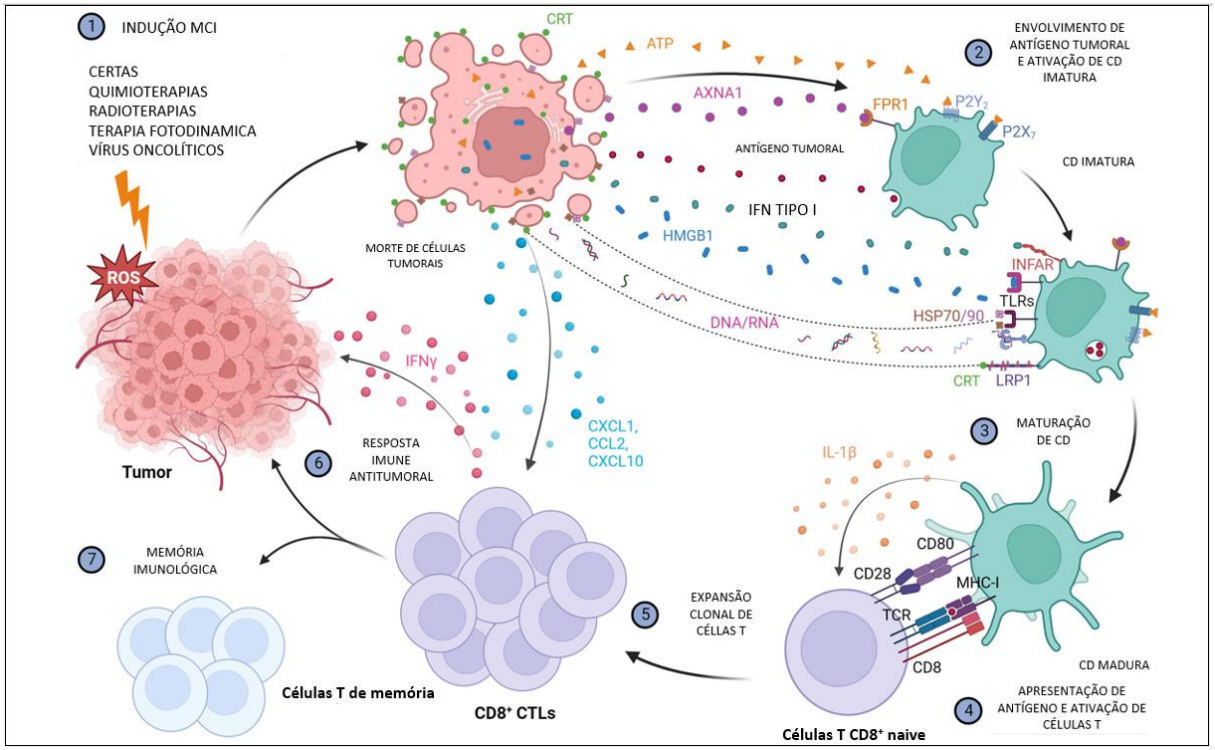

Figura 3. Representação esquemática do mecanismo de morte celular imunogênica e subsequente ativação da resposta imune antitumoral. Adaptado de Palanivelu et al. (2023).

Portanto, o uso de tratamentos que sejam capazes de induzir MCI podem contribuir para uma resposta imunológica mais eficaz contra tumores, em especial, o melanoma. Alguns estudos demonstraram que a indução de estresse oxidativo por espécies reativas de oxigênio (EROs) favorecem a liberação de DAMPs, uma vez que a imunogenicidade da MCI foi prejudicada após a adição de antioxidantes no meio[25]. Dentro desse contexto, um tratamento promissor que vem se destacando é a terapia fotodinâmica (TFD). A TFD consiste na interação entre um agente fotossensibilizante (FS), uma fonte de luz em um comprimento de onda específico e oxigênio molecular[26]. A fonte de luz transfere energia ao FS e esse, em seu estado ativado, transfere energia a diversas moléculas do meio em que se encontram. O oxigênio, no seu estado fundamental, é uma das principais moléculas a serem excitadas, culminando na produção de EROs que por sua vez vão induzir estresse, danos e morte celular (Figura 4)[27].

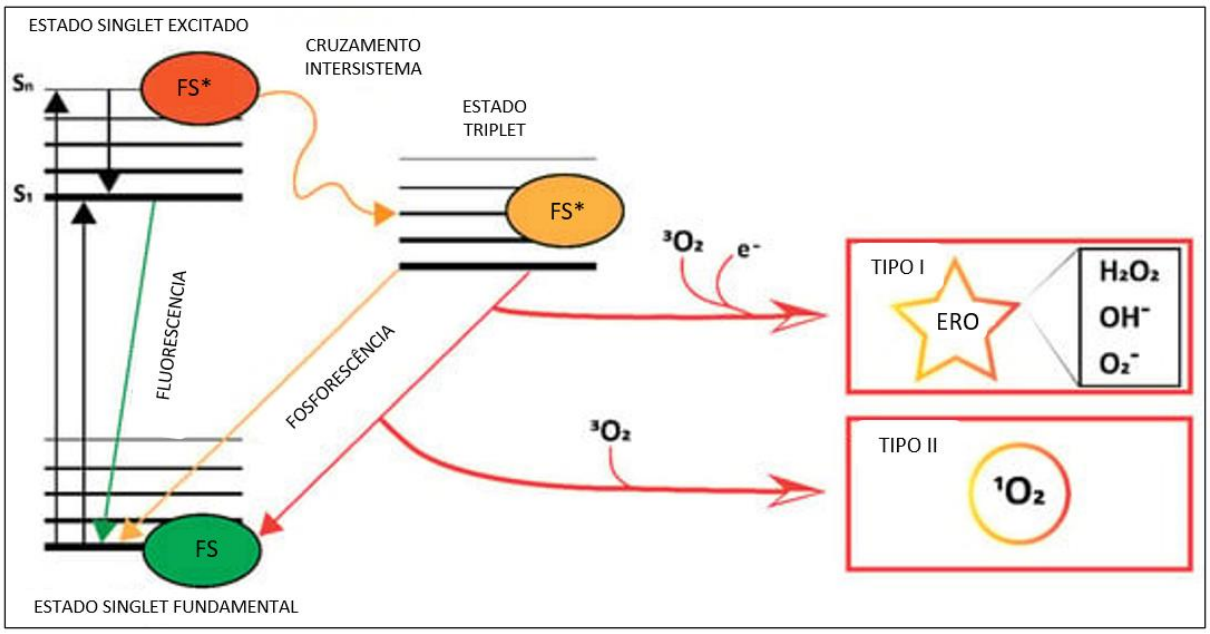

Figura 4. Representação esquemática do Diagrama de Jablonski ilustrando fotorreações tipo I e tipo II de um PS após excitação com luz. Adaptador de Huis in 't Veld et al. (2023).

A geração de EROs na TFD ocorre principalmente em dois tipos de reações. Na reação do tipo I, o fotossensibilizador em estado mais energético reage diretamente com moléculas biológicas, transferindo elétrons ou hidrogênio para formar radicais livres e podem iniciar uma reação em cadeia que danificam componentes celulares essenciais. No mecanismo de tipo II, a transferência de energia ocorre diretamente ao oxigênio molecular, gerando oxigênio singleto, uma forma altamente reativa de oxigênio que causa danos oxidativos severos às células[26,27].

Além de apresentar como vantagem a ação local do tratamento e por ser minimamente invasiva, a TFD pode ser usada como adjuvante à cirurgia e/ou quimioterapias.

Autorizada no Brasil pela Portaria SECTICS/MS Nº 46, de 5 de setembro de 2023, a Terapia Fotodinâmica passou a ser incorporada no Sistema Único de Saúde (SUS) devido a eficácia e segurança sendo uma alternativa para o tratamento de câncer, principalmente para câncer de pele do tipo basocelular superficial e nodular.

A TFD é eficaz devido a capacidade de induzir necrose ou apoptose, destruir a microvasculatura, além de ativar o sistema imunitário[28–30].

A TFD é capaz de induzir a liberação dos diferentes tipos de DAMPs, a depender do tipo de fotossensibilizante e da localização intracelular onde ocorre a geração de estresse oxidativo. A eficácia da TFD depende de vários fatores, principalmente do tipo de FS e sua biodisponibilidade nos tecidos alvo.

Um fotossensibilizante conhecido pela eficiência na geração de EROs é o cloreto de alumínio ftalocianina (AlFt) (Figura 5).

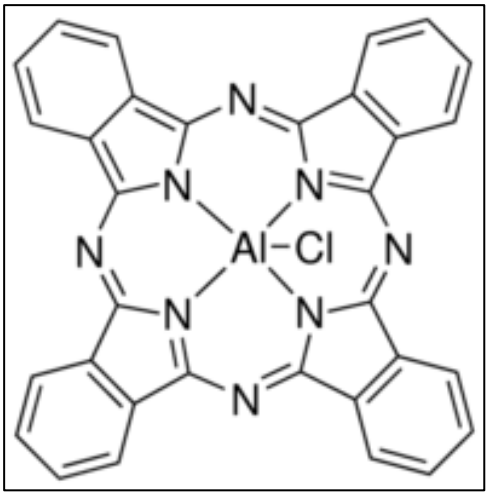

Figura 5. Representação esquemática da estrutura química do fotossensibilizante alumínio cloro ftalocianina.

Esse FS vem sendo utilizado como mediador da TFD no tratamento de diversas doenças, devido a suas propriedades fotoquímicas e fotofísicas. Umas das principais características é o coeficiente de absorção espectral na faixa do vermelho de comprimento de onda, em torno de 600 a 700 nm, um dos comprimentos com maior poder de penetração na pele (Figura 6)[31].

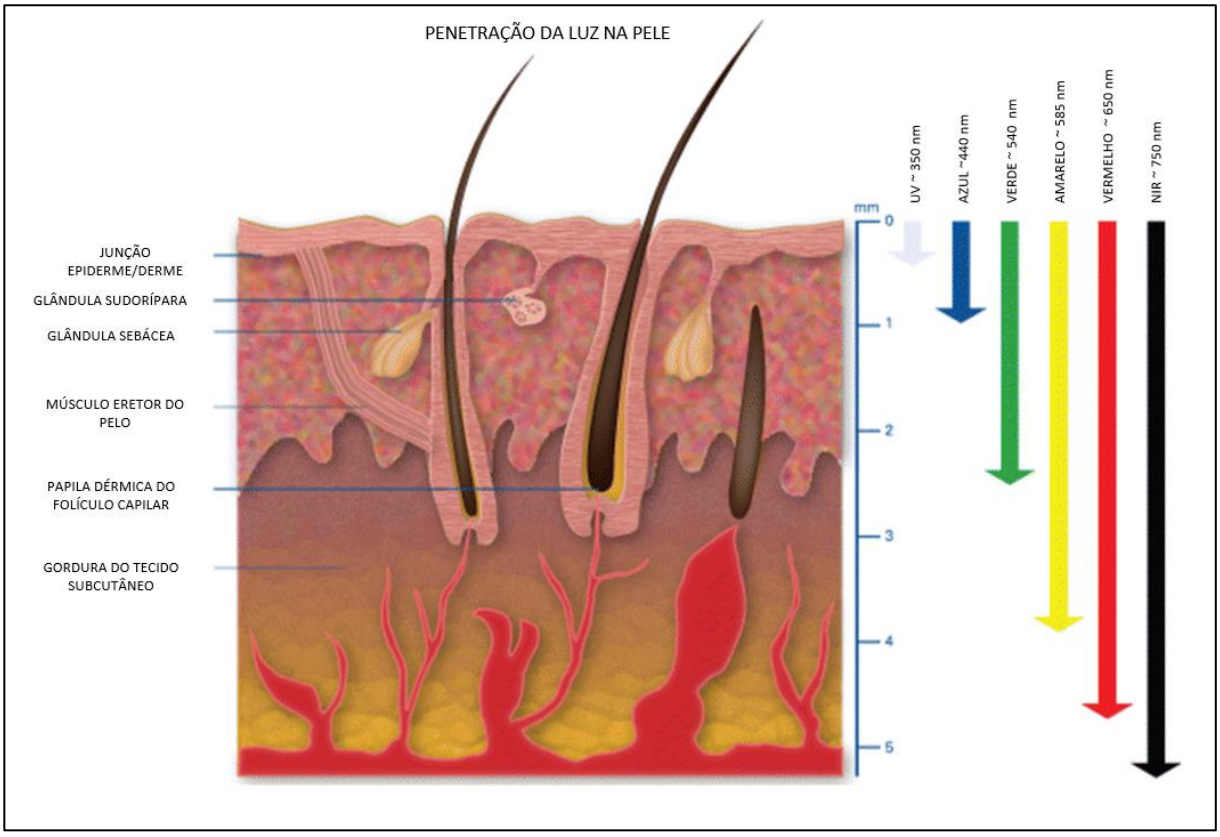

Figura 6. Representação esquemática da penetração da luz na pele ilustrando a profundidade em que os comprimentos de onda penetram. Adaptado de Ash et al. (2017).

A principal dificuldade no uso da AlFt é a baixa solubilidade em meios aquosos devida à hidrofobicidade o que leva à agregação e à perda de eficiência em produção de EROs. Por isso, Muehlmann et al. (2015)[32] desenvolveram uma nanoemulsão espontânea carreando o FS AlFt (AlFt NE). Esta formulação é formada por gotículas de óleo de rícino dispersas em água e estabilizadas pelo tensoativo cremophor ELP®, o que possibilita o carreamento da AlFt, contornando a hidrofobicidade do composto.

A AlFt NE vem se mostrando eficaz como mediador de TFD contra diversos modelos de câncer, entre eles o câncer de colorretal murino e o adenocarcinoma mamário murino[33–37]. Mello e colaboradores (2022) demostraram a eficácia da AlFt em uma nanopartícula lipídica sólida estável e escalonável na redução da viabilidade de células B16-F10 in vitro, induzindo morte celular por apoptose. Apesar disso, ainda há poucos estudos sobre a eficácia antitumoral para tumores como o melanoma, bem como sobre outras propriedades como a capacidade de estimular o sistema imunitário.

Dentro desse contexto, o presente trabalho buscou avaliar se a TFD mediada por AlFt NE induz MCI em células de melanoma B16F10, bem como explorar a atividade antitumoral e

imunogênicas por meio de diferentes protocolos que pudessem otimizar o tratamento do melanoma em modelo de enxerto murino.

2. OBJETIVO GERAL

Investigar a potencial atividade antitumoral e imunogênica da TFD mediada por AlFt NE em células B16F10.

2.1 OBJETIVOS ESPECÍFICOS

1) Avaliar os tipos de morte celular em TFD mediada por diferentes concentrações de AlFt NE;
2) Avaliar a exposição de DAMPs após TFD mediada por diferentes concentrações de AlFtNE;
3) Avaliar a atividade antitumoral de diferentes protocolos de TFD mediada por AlFtNE;
4) Avaliar a atividade imunomodulatória de diferentes protocolos de TFD mediada por AlFtNE;
5) Avaliar o perfil de expressão de genes do sistema imunitário em resposta à TFD mediada por AlFtNE;

3. MATERIAIS E MÉTODOS

3.1 Cultura de células

A linhagem de células de melanoma murino B16F10 foi obtida do Banco de Células do Rio de Janeiro (BCRJ, Rio de Janeiro, RJ, Brasil). As células foram cultivadas em DMEM, com 10% de soro fetal bovino, penicilina (100 U/mL) e estreptomicina (100 μg/mL) (Gibco Invitrogen, EUA), a 37 °C em atmosfera com 5% de CO_2.

3.2 Protocolos de TFD mediada pela AlFtNE

Para o Capítulo 1, células B16F10 foram cultivadas em microplacas de 96 poços e expostas por 15 minutos a diferentes concentrações de nanoemulsão de ftalocianina de alumínio (AlFtNE). Em seguida, as células foram lavadas duas vezes com PBS e mantidas no escuro ou irradiadas com um sistema de iluminação baseado em arranjo de diodos emissores de luz (LED) (660 nm, com densidade de energia de 25,9 J/cm²), que foi gentilmente fornecido pelo Prof. Paulo Eduardo Narcizo de Souza. A AlFtNE foi produzida por emulsificação espontânea, seguindo os protocolos de Muehlmann et al. 2015. Já para o Capítulo 3, os camundongos foram aleatoriamente designados para serem tratados apenas no tumor primário com: PBS, 1) baixa densidade de energia [25 J/cm²] com baixa concentração de AlFtNE [10 nM] (LL_LPS); 2) baixa densidade de energia [25 J/cm²] com alta concentração de AlFtNE [40 nM] (LL_HPS); 3) alta densidade de energia [112 J/cm²] com baixa concentração de AlFtNE [10 nM] (HL_LPS); e 4) alta densidade de energia [112 J/cm²] com alta concentração de AlFtNE [40 nM] (HL_HPS). Como controle, os camundongos receberam uma injeção intratumoral de PBS no dia 12. Para o tratamento TFD, os camundongos foram injetados intratumoralmente com diferentes concentrações de AlFtNE no dia 12. Trinta minutos após a injeção nos tumores do lado direito, estes foram irradiados com LED. Os camundongos foram eutanasiados no dia 18.

3.3 Ensaio de viabilidade celular

Foi utilizado o ensaio de MTT para avaliar a viabilidade celular. Vinte e quatro horas após o tratamento TFD, as células B16F10 (10.000 células por poço em placas de 96 poços) foram incubadas com MTT (0,5 mg/mL) por 2 horas a 37 °C. Depois disso, o meio foi removido, e os cristais de formazan, de cor azul escura, foram dissolvidos com DMSO. A densidade óptica das soluções a 570 nm foi medida com um espectrofotômetro (Spectramax

M2, Molecular Devices, USA), e os resultados foram expressos como uma porcentagem em relação ao controle negativo (células não tratadas). Como controles, usamos células B16F10 tratadas com mitoxantrona por 4 horas (controle positivo de morte celular imunogênica) e cisplatina por 24 horas (controle negativo de morte celular imunogênica). Cada tratamento foi realizado em triplicata e em três experimentos independentes.

3.4 Ensaio de quantificação de morte celular

Quatro horas após o tratamento, a morte celular foi avaliada usando microscopia de fluorescência após exposição a laranja de acridina (AO) (1 μg/mL) e iodeto de propídio (PI) (20 μg/mL). As células foram incubadas com AO/PI por 5 minutos e, em seguida, analisadas em microscópio de fluorescência (EVOS Cell Imaging Systems, ThermoFisher). As contagens foram realizadas por quatro analistas diferentes, de forma duplo-cega.

3.5 Ensaio de liberação de HMGB1

A concentração de HMGB1 (Proteína de Grupo de Alta Mobilidade B1) nos sobrenadantes das células tratadas foi medida 24 horas após o tratamento. Para isso, as células B16F10 foram primeiramente cultivadas e tratadas conforme o protocolo experimental. Após o tratamento, os sobrenadantes das culturas celulares foram cuidadosamente coletados para análise de acordo com as instruções do fabricante (IBL International). Cada tratamento foi realizado em triplicata e em três experimentos independentes.

3.6 Ensaio de detecção extracelular de ATP

A concentração de adenosina 5'-trifosfato (ATP) extracelular nos sobrenadantes das células tratadas foi medida com o kit de ensaio bioluminescente de ATP (Sigma Aldrich, EUA), conforme recomendado pelo fabricante. A bioluminescência foi medida por espectrofotômetro (Spectramax M2, Molecular Devices, EUA) em placas opacas. O ensaio foi realizado em triplicata técnica e em três experimentos independentes.

3.7 Ensaio de exposição de Calreticulina

A exposição de CRT (calreticulina) foi avaliada por microscopia de fluorescência (EVOS Cell Imaging Systems, ThermoFisher), seguindo as instruções do fabricante. Em resumo, as células foram colhidas e lavadas com PBS gelado 4 horas após o tratamento. Em

seguida, foram incubadas com uma solução de BSA 2% (albumina bovina) por 30 minutos para bloquear a ligação não específica, lavadas novamente, e então incubadas com um anticorpo anti-calreticulina (Abcam) por 1 hora a 37°C. Após a incubação com o anticorpo, as células foram lavadas com PBS e analisadas.

3.8 Animais

Todos os procedimentos que envolveram camundongos foram previamente aprovados pelo Comitê de Ética Animal da Universidade de Brasília, conforme o protocolo UnBDOC n.º 46/2019. Os camundongos utilizados eram fêmeas da linhagem C57Bl/6, com idade entre 6 e 8 semanas e peso de 18 ± 2 gramas. Os animais utilizados no Capítulo 1 foram obtidos da Faculdade de Saúde da Universidade de Brasília (UnB/DF), enquanto para os experimentos do Capítulo 3 foram obtidos da Faculdade de Medicina da Universidade Federal de Goiás.

Os camundongos foram mantidos em um ambiente controlado, com temperatura regulada com ciclos de luz e escuridão de 12 horas, com livre acesso a alimento e água.

3.9 Ensaio de imunização-desafio

Em resumo, 5×10^5 células B16F10 foram tratadas *in vitro* com mitoxantrona (MTX) IC50 (4 μM) por 4 horas, cisplatina (CDDP) IC50 (150 μM) por 24 horas, congelamento e descongelamento (F/T) ou quatro protocolos diferentes de TFD-AlFtNE (mediados por AlFtNE nas concentrações IC20, IC50, IC70, IC90). Em seguida, as células foram desprendidas com uma espátula e agrupadas de acordo com o grupo de tratamento em tubos Falcon de 15 mL. As células foram centrifugadas, o *pellet* foi lavado com PBS e as células foram ressuspendidas em PBS na concentração final de 1×10^7 células/mL. Para a imunização dos camundongos, 100 μL da suspensão, contendo 1×10^6 células, foram injetados por via subcutânea no flanco esquerdo dos camundongos. PBS foi injetado como grupo controle negativo de células. Esse procedimento foi repetido uma semana depois. Sete dias após a última injeção, cada camundongo foi desafiado com uma única injeção subcutânea de 1×10^6 células B16F10 viáveis no flanco contralateral. Em seguida, a ocorrência de tumores foi monitorada a cada 2 dias e o crescimento do tumor foi medido. Os camundongos foram eutanizados quando o volume do tumor atingiu o ponto final humanitário (2000 mm²), de acordo com o protocolo aprovado pelo Comitê de Ética Animal.

3.10 Ensaio de modelo tumoral bilateral

Para avaliar os efeitos diretos e abscopais da TFD, foi utilizado um modelo de tumor bilateral. Os camundongos foram injetados subcutaneamente com 5×10^5 células B16F10 no flanco direito (tumor primário). Dois dias depois, 2×10^5 células tumorais foram implantadas no flanco esquerdo (tumor secundário). O tamanho do tumor foi monitorado por medições com paquímetro a cada dois dias. O volume do tumor foi calculado da seguinte forma: volume do tumor (mm^3) = largura (mm) × largura (mm) × comprimento (mm)/2.

3.11 Análise de parâmetros hematológicos

No dia da eutanásia, os animais foram anestesiados com 120 mg/kg de cetamina e 16 mg/kg de xilazina. Em seguida, amostras de sangue foram coletadas por punção cardíaca em microtubos EDTA Vacutte®. Os parâmetros hematológicos, incluindo o número de leucócitos (WBC), eritrócitos (RBC), hemoglobina (HGB), hematócrito (HCT), plaquetas (PLT), volume corpuscular médio (MCV), hemoglobina corpuscular média (MCH) e concentração de hemoglobina corpuscular média (MCHC), foram avaliados pelo contador hematológico automatizado para uso veterinário Horiba ABX Micros ESV 60 (São Paulo, Brasil).

3.12 Avaliação histológica

No dia 18, os camundongos foram eutanasiados e dissecados para coleta dos tumores irradiados e não irradiados. Todos os tecidos foram fixados em formalina a 10% por 24 horas e, subsequentemente, transferidos para etanol a 70%, 80%, 90% e 100%. O material foi submetido a três banhos de parafina em um forno a 58 °C e incluído em blocos de parafina. Seções histológicas de 3 a 4 μm de espessura (Leica® modelo RM2125RT, China) foram fixadas em lâminas de vidro para microscopia, e as amostras foram coradas com hematoxilina e eosina (HE).

3.13 Análise por citometria de fluxo

A suspensão de células únicas de esplenócitos de camundongos foi preparada por digestão mecânica seguida de filtração através de um filtro de células de 40 μm (SPL Life Sciences, Pocheon, Coreia). As amostras de células foram ressuspensas em tampão de lise celular por 10 minutos, lavadas com PBS, centrifugadas e contadas. As células foram transferidas para tubos de polipropileno em 100 μl de PBS + 2% FBS para marcação por 1 hora

no gelo, protegidas da luz, com os anticorpos APC anti-mouse CD3ε, PE/Cyanine7 anti-mouse CD4 e PE anti-mouse CD8b da Invitrogen. Os anticorpos FITC anti-mouse CD45 e PerCP Cy5.5 anti-mouse CD45RA foram usados para o painel de células T ativadas (Painel 1). Os anticorpos FITC anti-mouse CD25 e PerCP Cy5.5 anti-mouse CD62L foram usados para o painel de células T reguladoras (Painel 2). Após lavagens adicionais com PBS contendo 2% FBS, as células foram ressuspensas, adquiridas pelo FACSVerse (BD Biosciences, San Jose, Califórnia, EUA) e analisadas pelo software FlowJo X (BD Biosciences). Células marcadas com anticorpos individuais foram usadas para compensação.

3.14 Análise de expressão gênica

O RNA total foi isolado a partir de amostras independentes homogeneizadas e congeladas de alógrafos de melanoma primários e secundários (n=3 por grupo) usando o kit RNeasy Mini (Qiagen, Hilden, Alemanha), de acordo com as instruções do fabricante. As amostras foram quantificadas pelo método fluorimétrico específico para RNA utilizando o kit Qubit™ RNA High Sensitivity (Invitrogen™), seguindo as recomendações do fabricante. O sequenciamento e análise de bioinformática foi realizado pela empresa GenOne Biotech usando a plataforma Illumina (Illumina, Inc., CA, EUA). De acordo com os requisitos da empresa, apenas amostras com RNA total puro (OD 260/280>2,0) e intacto (com RIN>6,3) foram enviadas para sequenciamento. As amostras deveriam consistir em pelo menos 2 µg de RNA liofilizado. Na análise de bioinformática, primeiro foi realizado o controle de qualidade dos dados; seguido pelo mapeamento das leituras ao genoma de referência. O índice do genoma de referência foi construído usando Hisat2 v2.0.5; a quantificação do nível de transcritos utilizando o *featureCounts* v1.5.0-p3 e, por fim, a análise de expressão diferencial que foi realizada usando o pacote DESeq2 (1.20.0) no R. Os níveis de expressão gênica foram estimados com base na abundância de transcritos, com valores normalizados para FPKM (Fragments Per Kilobase of transcript per Million mapped reads), levando em consideração os efeitos da profundidade de sequenciamento e do comprimento do gene sobre a contagem de fragmentos. Os genes com níveis de expressão significativamente diferentes em várias condições ($|\log2(\text{FoldChange})| \geq 1$ e $\text{padj} \leq 0,05$) foram identificados. Um log2FC > 0 indica maior expressão gênica na condição experimental em comparação com a condição de controle, enquanto um log2FC < 0 indica menor expressão na condição experimental em comparação com o controle. Um log2FC = 0 indica que não há diferença na expressão gênica entre as duas condições.

3.15 Análise estatística

Para registrar todas as diferenças estatísticas, foi utilizado o software GraphPad Prism versão 6.01 para Windows (Califórnia, EUA). As análises estatísticas foram conduzidas empregando testes ANOVA unidimensionais e bidimensionais, seguidos de comparações múltiplas usando o método de Tukey. Os resultados são expressos como média ± erro padrão da média, e a significância foi determinada com um valor de $p < 0,05$.

CAPÍTULO 1 - The induction of immunogenic cell death by photodynamic therapy in B16F10 cells in vitro is effected by the concentration of the photosensitizer

José Athayde Vasconcelos Morais[a,b] , Letícia R. Almeida[a,b] , Mosar C. Rodrigues[a,b] , Ricardo B. Azevedo[b] , Luis A. Muehlmann[a,b].

a. Laboratory of Nanoscience and Immunology, Faculty of Ceilandia, University of Brasilia, Brasilia/DF, 72220-900, Brazil.
b. Departmentof Genetics and Morphology, Institute of Biological Sciences, University of Brasilia, Brasilia 70910-900, Brazil.

Paper published in **Photodiagnosis and Photodynamic Therapy**, 2021.

KEYWORDS: Immunotherapy; Cancer; Aluminum-phthalocyanine; DAMP; Melanoma;

Photodiagnosis and Photodynamic Therapy 35 (2021) 102392

Contents lists available at ScienceDirect

Photodiagnosis and Photodynamic Therapy

journal homepage: www.elsevier.com/locate/pdpdt

The induction of immunogenic cell death by photodynamic therapy in B16F10 cells in vitro is effected by the concentration of the photosensitizer

José Athayde Vasconcelos Morais [a,b], Letícia R. Almeida [a,b], Mosar C. Rodrigues [a,b], Ricardo B. Azevedo [b], Luis A. Muehlmann [a,b,*]

[a] Laboratory of Nanoscience and Immunology, Faculty of Ceilandia, University of Brasilia, Brasilia/DF, Brazil
[b] Laboratory of Nanobiotechnology. Department of Genetics and Morphology, Institute of Biological Sciences. University of Brasilia, Brasilia/DF, Brazil

ARTICLE INFO

Keywords:
Immunotherapy
Cancer
Aluminum-phthalocyanine
DAMP
Melanoma

ABSTRACT

Photodynamic therapy (PDT) can trigger immune responses against cancer cells. The induction of immunogenic cell death (ICD) is one of the possible mechanisms behind this event, but the protocol conditions necessary for a robust induction of ICD by PDT have not been defined. In this work, the immunogenicity of B16F10 melanoma cells treated with different PDT protocols was investigated. The exposure of damage-associated molecules (DAMPs), namely HMGB1, calreticulin and ATP, a hallmark of ICD, and the presence of apoptotic and necrotic cells were assessed after the application of PDT mediated by different concentrations of aluminum-phthalocyanine (AlPcNE) in vitro. Furthermore, the in vivo immunogenicity of PDT-treated B16F10 cells was investigated with an immunization-challenge model in C57BL/6 mice. The percentage of dead cells was directly proportional to the concentration of AlPcNE. The IC_{50}, IC_{70} and IC_{90} concentrations of AlPcNE induced the exposure of DAMPs by B16F10 cells after PDT. In the in vivo model, however, only the B16F10 cells treated with PDT-AlPcNE at the IC_{50} or IC_{70} rendered C57BL/6 significantly more resistant to a subsequent challenge with viable B16F10 cells. Thus, the induction of ICD in B16F10 cells by PDT occurs only at a specific range of AlPcNE concentrations.

1. Introduction

PDT is a clinically established, minimally invasive[1] approach for the treatment of different tumors, including squamous cell carcinoma and bladder cancer[2]. It is based on the production of reactive species following the photoactivation of a photosensitizer[3]. ROS and other reactive species produced during PDT are known to directly kill tumor cells by inducing necrosis or apoptosis[4], to destroy the tumor microvasculature[5], and to activate the immune system against tumor antigens[6].

The immune effects of anticancer PDT have been described by a number of works[7–9]. However, the biological consequence of PDT is greatly effected by parameters such as light dose, photosensitizer concentration, and the interval between the administration of the photosensitizer and the irradiation of the target tissue[8]. Therefore, not surprisingly, many studies report contradictory results in regard to the immune activation by PDT[10–12]. This reflects not only the need to elucidate the immunity-related mechanisms elicited by PDT, but also the necessity of understanding how the protocol parameters affect the activation of these mechanisms.

One of the mechanisms underlying the immune effects of PDT is the induction of immunogenic cell death (ICD). As its name suggests, this modality of cell death renders the cell able to elicit an immune response against its antigens. The induction of ICD can be useful in the treatment of cancers, considering that the malignant cells express tumor-associated or tumor-specific antigens[13,14]. ICD can elicit antitumor immunity by signaling to the immune system by the exposure of different damage associated molecular patterns (DAMPs), such as calreticulin (CRT), adenosine triphosphate (ATP) and "high mobility group" box 1 "(HMGB1)[15,16].

The use of PDT as an ICD-inducing approach can be particularly interesting for the in situ immunotherapy of superficial tumors, such as melanoma. In the case of melanoma, this approach is further justified by the relatively low availability of treatment modalities against this cancer type. Thus, this study aimed at investigating the ICD-inducing potential of PDT protocols with different concentrations of the photosensitizer

* Corresponding author.
E-mail address: luisalex@unb.br (L.A. Muehlmann).

https://doi.org/10.1016/j.pdpdt.2021.102392
Received 8 April 2021; Received in revised form 25 May 2021; Accepted 7 June 2021
Available online 13 June 2021

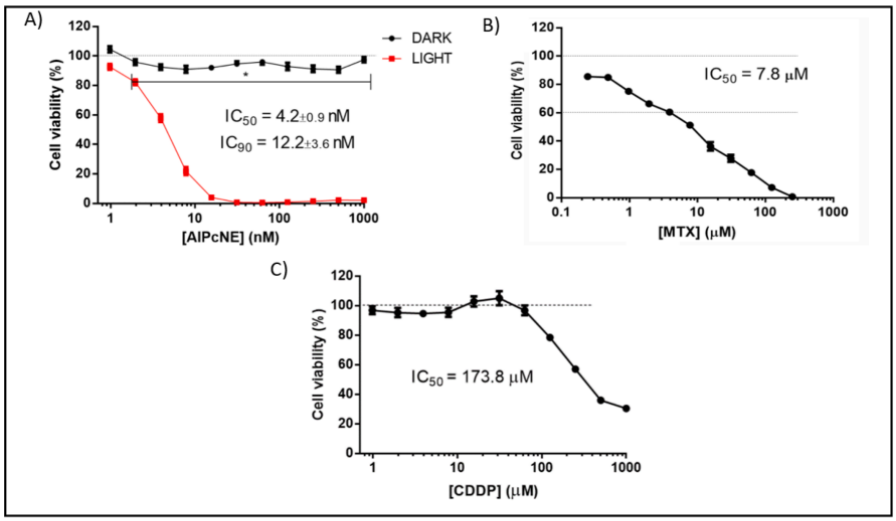

Fig. 1. Viability of B16F10 cells upon treatment with (A) AlPcNE, (B) mitoxantrone (MTX) and (C) cisplatin (CDDP) for 10 min, 2 h and 24 h respectively. Data expressed as mean ± standard error of the mean. * $p < 0.05$ for control group. Two-way ANOVA and Tukey's multiple comparison test.

aluminum-phthalocyanine in nanoemulsion (AlPcNE) in vitro. The results evidence that AlPcNE-mediated PDT induces both ICD and non-immunogenic cell death in a photosensitizer concentration-dependent manner.

2. Materials and methods

2.1. Photosensitizer and LED apparatus

The aluminum-phthalocyanine nanoemulsion (AlPcNE) was produced by spontaneous emulsification following Muehlmann et al. 2015 [17] protocols. A light-emitting diode (LED) array-based illumination system, kindly provided by Prof. Paulo Eduardo Narcizo de Souza, was used to irradiate cells.

2.2. Cell culture conditions

The murine melanoma cell line B16F10 was obtained from the Cell Bank of Rio de Janeiro (BCRJ, Rio de Janeiro, RJ, Brazil). Cells were grown in DMEM medium supplemented with 10% fetal bovine serum, penicillin (100 U/mL), and streptomycin (100 μg/mL) (Gibco Invitrogen, USA), at 37°C in 5% CO_2.

2.3. AlPcNE-mediated PDT protocol

The B16F10 cells were cultured in 96-well microplates and exposed for 15 min to different concentrations of AlPcNE. Then the cells were washed twice with PBS and kept in the dark or irradiated with LED light (660 nm at 25.9 J/cm^2 energy density).

2.4. Cell viability assay

Cell viability was measured by the MTT [3-(4,5-dimethylthiazol-2-yl)-2,5-diphenyltetrazolium bromide) assay. Briefly, 24 h after the PDT treatment, B16F10 cells (1×10^4 cells per well in 96-well plates) were incubated with MTT 0.5 mg/mL for 2 h at 37°C. Then, the supernatant was removed, and the dark blue crystal of formazan was dissolved with DMSO. The optical density at 570 nm of the resulting solutions was then measured with a spectrophotometer, and the results were expressed as percentage relative to negative control (non-treated cells). Positive and negative controls for ICD consisted of B16F10 cells treated with mitoxantrone for 4 h and cisplatin for 24 h, respectively[7,18]. Each treatment was performed in triplicates repeated in three independent experiments.

2.5. Quantification of cell death

Cell death was assessed 4 h after treatment by fluorescence microscopy analysis under acridine orange (AO) (1 μg/mL) and propidium iodide (PI) (20 μg/mL) staining[19]. Briefly, cells were incubated with AO/PI for 5 min and analyzed in a fluorescence microscope (EVOS Cell Imaging Systems, ThermoFisher). The counts were double-blindly performed by four different analysts.

2.6. HMGB1 release

The concentration of HMGB1 in the supernatants of the treated cells was assessed 24 h after treatment, according to the manufacturer's instructions (IBL international).

2.7. Detection of extracellular ATP

Extracellular ATP concentrations were measured in culture supernatants of treated cells with the adenosine 5'-triphosphate (ATP) Bioluminescent Assay Kit (Sigma Aldrich, USA), as recommended by the manufacturer. Bioluminescence was measured with a spectrophotometer (Spectramax M2, Molecular Devices, USA) in opaque plates.

2.8. Calreticulin exposure

CRT exposure was assessed by fluorescence microscopy (EVOS Cell Imaging Systems, ThermoFisher) following the manufacturer's instructions. Briefly, cells were harvested and washed with ice-cold PBS 4 h after the treatment, then incubated with BSA 2% (bovine albumin) for 30 min, washed, and incubated with an anti-calreticulin (Abcam) antibody for 1 h at 37°C. Thereafter, cells were washed with PBS, incubated with anti-IgG 488 (Abcam) antibody for 30 min at 37°C in the dark and

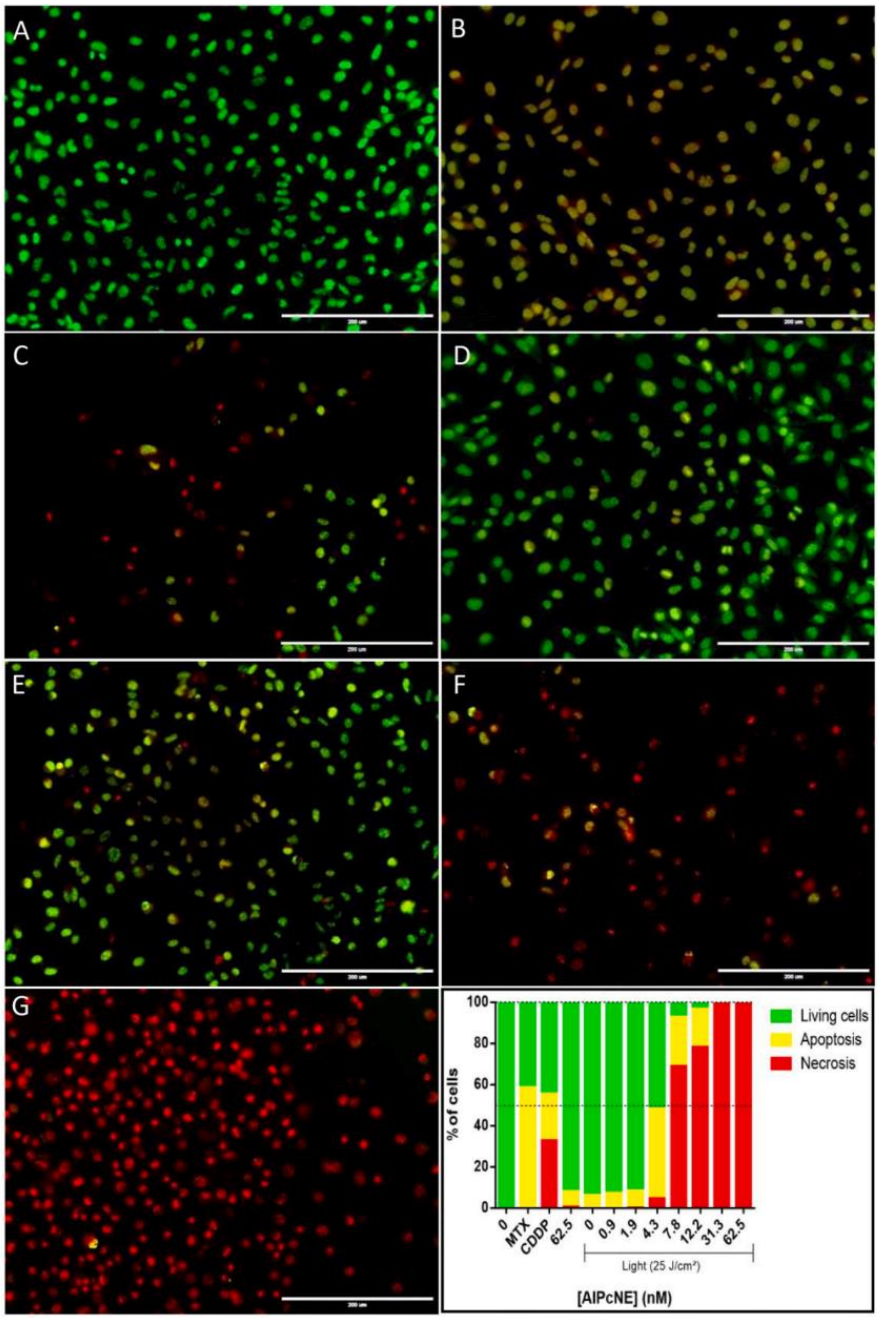

Fig. 2. Quantification of cell death by AO/PI labeling in B16F10 cells after application of different treatments: A. non-treated control; B. IC_{50} (7.8 μM) MTX; C. IC_{50} (173.8 μM) CDDP; D. IC_{20} (1.9 nM) AlPcNE; E. IC_{50} (4.3 nM) AlPcNE; F. IC_{70} (7.8 nM) AlPcNE; G. IC_{90} (12.2 nM) AlPcNE. Magnification 20X. Graph representing fluorescence intensity AO/PI by percent of B16F10 cells. Scale bar = 200 μm.

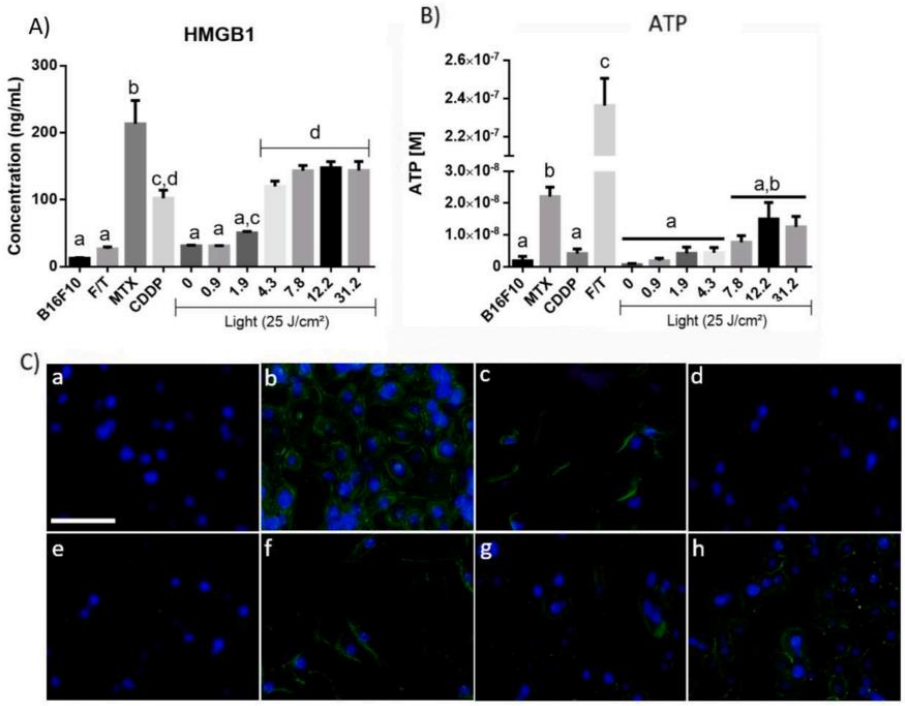

Fig. 3. Extracellular concentrations of (A) HMGB1 and (B) ATP. Freezing/thawing (F/T), mitoxantrone (MTX), cisplatin (CDDP). Equal letters correspond to groups with no statistical difference, $p < 0.05$. (C) Calreticulin labeling in B16F10 cells after application of different treatments. a. control; b. permeabilized; c. IC_{50} (7.8 μM) MTX; d. IC_{50} (173.8 μM) CDDP; e. IC_{20} (1.9 nM) AlPcNE; f. IC_{50} (4.3 nM) AlPcNE; g. IC_{70} (7.8 nM) AlPcNE; h. IC_{90} (12.2 nM) AlPcNE. In blue, DAPI and green, CRT. Scale bar = 50 μm.

then analyzed.

2.9. Animals

All experiments involving mice were approved by the Animal Ethics Committee at the University of Brasilia (UnBDOC n° 46/2019). Female, 6- to 8-week old C57Bl/6 mice (FS - University of Brasilia, Brasília, DF, BRAZIL) were maintained in a temperature-controlled environment with 12-h light–dark cycles and received food and water ad libitum.

2.10. Immunization-challenge in vivo studies

Briefly, 5×10^5 B16F10 cells were treated in vitro with mitoxantrone (MTX) IC_{50} (4 μM) for 4 h, cisplatin (CDDP) IC_{50} (150 μM) for 24 h, freezing and thawing (F/T) and four different PDT-AlPcNE protocols (mediated by AlPcNE at IC_{20}, IC_{50}, IC_{70}, IC_{90}). Then cells were detached with a scraper and pooled together according to their respective treatment group in 15 mL falcon tubes. The cells were centrifuged, the pellet was washed with PBS, and the cells were resuspended with PBS at a final concentration of 1×10^7 cells/mL. For the immunization of mice, 100 μL of the suspension, containing 1×10^6 cells, was s.c. injected into the left flank of mice. PBS was injected as a cell-negative control group. This procedure was repeated one week later. Seven days after the last injection, each mouse was challenged with a single s.c. injection of 1×10^6 viable B16F10 cells in the contralateral flank. Next, tumor occurrence was monitored every 2 days and tumor growth was measured. Mice were euthanized when tumor volume reached humane end-point according to the Animal Ethics Committee-approved protocol.

3. Results

3.1. AlPcNE-mediated PDT is effective against B16F10 melanoma cells

The in vitro viability of B16F10 cells treated with LED light alone or with AlPcNE in the dark was not significantly affected (Fig. 1). The PDT treatment with nanomolar concentrations of AlPcNE, however, significantly reduced the viability of cells (Fig. 1). At AlPcNE concentrations above 31 nM, there was a 100% reduction in cell viability.

3.2. PDT induces necrosis or apoptosis

At IC_{50} and lower AlPcNE concentrations, apoptosis was the main cell death mechanism elicited by PDT in B16F10 cells. At concentrations of AlPcNE higher than the IC_{50}, PDT induced mainly necrosis (Fig. 2). These data indicate that the type of cell death induced by AlPcNE-mediated PDT depends on the concentration of the photosensitizer. MTX induced mainly apoptosis in B16F10 cells.

3.3. Exposure of DAMPs

HMGB1 release. Extracellular HMGB1 levels in the supernatants of B16F10 cells were significantly increased after PDT treatment with IC_{50}, IC_{70} or IC_{90} AlPcNE (Fig. 3A). Moreover, treatments with IC_{50} MTX or IC_{50} CDDP induced the release of HMGB1.

Release of ATP. As expected, a significant release of ATP by B16F10 cells was detected after treatment with IC_{50} MTX, while cells treated with IC_{50} CDDP showed no difference in this parameter compared to the

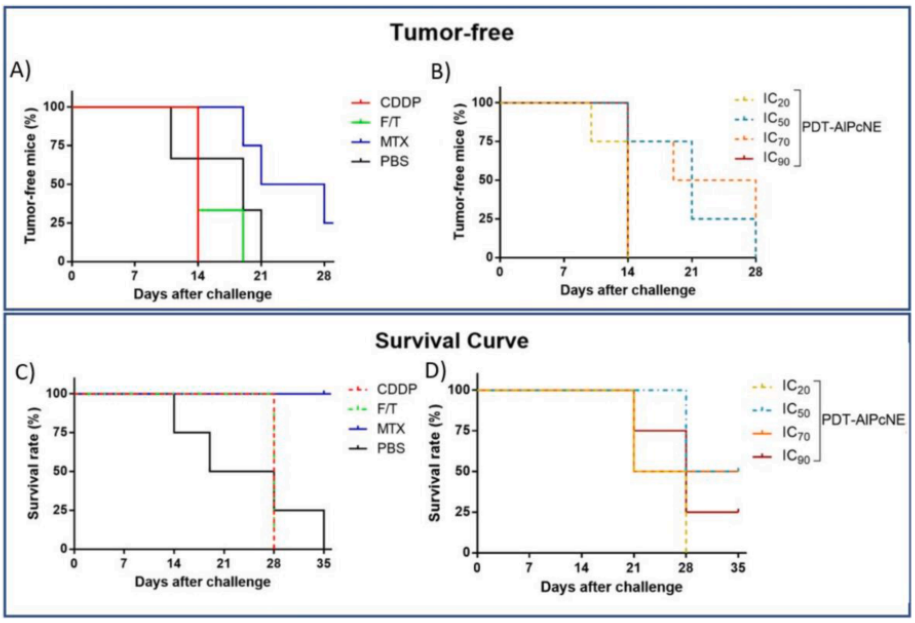

Fig. 4. In vivo impact of PDT-AlPcNE on the immune responses of B16F10 cells. Immunocompetent C57Bl / 6 mice (n = 4 per group) were inoculated s.c. on the left flank with B16F10 cells treated with different concentrations of AlPcNE (IC_{20}, IC_{50}, IC_{70} and IC_{90}) followed by light and with different control conditions (F/T); mitoxantrone (MTX); cisplatin (CDDP); and PBS (negative control)). Stage repeated seven days later. Another week later, all mice were again challenged with live B16F10 cells in opposite flank and the incidence of tumors was monitored. The percentage of tumor-free mice (A., B.) and the survival curve (C., D.) are indicated.

non-treated B16F10 cells (Fig. 3B). The PDT treatment induced a significant release of ATP only at concentrations of AlPcNE above IC_{70}. The freezing/thawing treatment also induced a release of ATP from B16F10 cells.

CRT exposure. PDT induced the exposure of CRT on the plasma membrane of the B16F10 cells. As expected, the ICD-positive control, MTX, induced the exposure of CRT, while the non-treated B16F10 cells did not present CRT on the cell surface (Fig. 3C).

3.4. B16F10 cells treated with PDT in vitro can exhibit in vivo immunogenicity

Mice injected with B16F10 cells treated with MTX exhibited significantly increased resistance to the development of tumor at a subsequent challenge with viable B16F10 cells, which is suggestive of an activation of the immune system against these cells (Fig. 4A). By contrast, the mice injected with cells treated with CDDP or cells subjected to F/T showed the fastest development of tumor at the challenge site, confirming that B16F10 cells treated with CDDP or F/T-induced necrosis are less immunogenic (Fig. 4A). It is noteworthy that there were significant differences in tumor growth profiles among the mice injected with B16F10 cells treated with different PDT protocols. On the one hand, in comparison to control, mice injected with cells treated with PDT mediated by IC_{50} and IC_{70} AlPcNE exhibited a delay in tumor development, which is even comparable to that induced by ICD-positive, MTX-treated cells (Fig. 4B). The increased resistance to tumor development was also reflected in the survival curves, as the mice injected with B16F10 cells treated with MTX or with PDT mediated by IC_{50} or IC_{70} AlPcNE showed higher survival rates than mice from the other groups (Fig. 4C-D). On the other hand, the injection of B16F10 cells treated with PDT mediated by IC_{20} and IC_{90} did not render the mice any more resistant to the challenge, as the tumor development was comparable to that observed in the CDDP group (Fig. 4C-D).

4. Discussion

Although PDT has been suggested to activate immune responses against tumors, diverging studies evidence that details underlying this phenomenon are still to be uncovered[10–12]. O'Shaughnessy et al.[11] showed that the use of PDT alone neither prevented the growth of lung metastases nor increased survival in an animal model of primary kidney tumor, which is known to be quite responsive to immunotherapies. Different PDT protocols can act differently on the immune system. Pucelik et al.[10] developed PDT protocols which led to a significant increase in the survival rate of BALB/c mice bearing CT26 tumors, but the response depended on the dose of light.

The results presented in this work suggest that the concentration of the photosensitizer can also affect the immunogenicity of in vitro PDT-treated cells. For AlPcNE, used here as the photosensitizing system, both IC_{50} and IC_{70} PDT-AlPcNE were quite effective in inducing ICD and consequently rendering these cells immunogenic in the in vivo model of immunization-challenge.

In a study by Turubanova et al.[14], GL261 and MCA205 tumor cells treated with photosens-PDT exhibited ICD hallmarks and acted as a therapeutic vaccine, preventing the regrowth of tumors. Garg et al.[20] also showed that expression of a cell surface CRT increased with PDT dose. In the present work, however, both the highest and the lowest AlPcNE concentrations failed to increase the immunogenicity of B16F10 cells in vivo, showing that a window of ICD-inducing photosensitizer concentration exists, rather than only a minimum threshold. At the lowest AlPcNE concentration, as expected, PDT failed to kill the cells and to induce the exposure of DAMPs, but at the highest AlPcNE concentration – IC_{90} – the predominant death mechanism elicited by PDT was necrosis, with DAMPs detected both in the supernatant and in the

cells. However, it has to be noted that the release of DAMPs is probably a result of plasma membrane permeabilization that occurs in necrotic cells, rather than the active process of DAMP exposure observed in ICD.

Tatsuno et al.[21] showed that cancer cells depleted of CRT, or HMGB1 or ATP treated with 8-MOP plus UVA irradiation in vitro do not vaccinate immunocompetent mice against live cancer cells of the same type. Liu et al.[22] showed that the removal of any of the DAMPs, such as ANXA1, ATP, CRT or HMGB1, in non-small cell lung cancers, abolished the immunogenicity of dead cells. Although some DAMPs are essential to induce ICD, the simple release of DAMPs is not enough to induce a robust immune response against the antigens of the succumbing cells. Hodge et al.[23], for instance, showed that although docetaxel promoted CRT exposure, the cells were not immunogenic in vivo. In the work by Tesniere et al.[18], both oxaliplatin and cisplatin were shown to induce the release of HMGB1 by colon cancer cells, but only oxaliplatin was able to elicit immunity against CT26 cells in mice in vivo. Obeid et al.[24] showed that some drugs, such as carboplatin, etoposide and mitomycin C, are capable of inducing the release of DAMPs, but cannot be considered bona fide ICD inducers. ICD exhibits hallmarks of apoptosis and a well-defined temporospatial pattern of DAMP exposure.

Therefore, it is not surprising that B16F10 cells treated with the IC_{90} PDT-AlPcNE released DAMPs but failed to increase the resistance of mice to a subsequent challenge with viable B16F10 cells. Thus, based on the present study, it is possible to suggest that the concentration of the photosensitizer in the target cells is an important parameter of the PDT protocol to be taken into account for eliciting an immune response against tumor cells.

5. Conclusion

Our results show that both immunogenic and nonimmunogenic cell death can be induced by the same in vitro PDT setting with different concentrations of photosensitizer. Although further studies are necessary to investigate this event in vivo, the present work suggests that clinical PDT protocols have to be fine-tuned to optimize their immune effects, rather than simply aiming at the direct elimination of tumor cells. Moreover, PDT can be viewed as an ICD-inducing approach with the potential to be used as a vaccination strategy, which could be applied alone or combined with chemotherapy, radiotherapy, surgery or immunotherapy approaches.

Declaration of Competing Interest

The authors have no conflicts of interest to declare.

Funding information

This study was funded by the Brazilian government agencies FAP-DF/Brazil (0193.001020/2015, and 0193.001626/2017), PRONEX FAP-DF, CNPq (0447628/2014-3, 193.001.200/2016) and Coordenação de Aperfeiçoamento de Pessoal de Nível Superior – Brasil (CAPES) – Finance Code 001.

References

[1] S.O. Gollnick, B. Owczarczak, P. Maier, Photodynamic therapy and anti-tumor immunity, Lasers Surg. Med. 38 (2006) 509–515.
[2] R.A. Akasov, N.V. Sholina, D.A. Khochenkov, A.V. Alova, P.V. Gorelkin, Photodynamic therapy of melanoma by blue-light photoactivation of flavin mononucleotide, Sci. Rep. 9 (2019) 1–11.
[3] M.J. Niedre, C.S. Yu, M.S. Patterson, B.C. Wilson, Singlet oxygen luminescence as an in vivo photodynamic therapy dose metric : validation in normal mouse skin with topical amino-levulinic acid, Br. J. Cancer 92 (2005) 298–304.
[4] E. Buytaert, M. Dewaele, P. Agostinis, Molecular effectors of multiple cell death pathways initiated by photodynamic therapy, Biochim. Biophys. Acta - Rev. Cancer 1776 (2007) 86–107.
[5] M.A. Sirotkina, L.A. Matveev, M.V. Shirmanova, V.Y. Zaitsev, N.L. Buyanova, Photodynamic therapy monitoring with optical coherence angiography, Sci. Rep. 7 (2017) 1–11.
[[6]] Q. Wang, et al., Immunogenic cell death in anticancer chemotherapy and its impact on clinical studies, Cancer Lett. 438 (2018) 17–23.
[7] M. Corrêa, et al., Photodynamic therapy mediated by aluminium-phthalocyanine nanoemulsion eliminates primary tumors and pulmonary metastases in a murine 4T1 breast adenocarcinoma model, J. Photochem. Photobiol. B Biol. 204 (2020) 1–11.
[8] Y. Shen, et al., Low-dose photodynamic therapy-induced increase in the metastatic potential of pancreatic tumor cells and its blockade by simvastatin, J. Photochem. Photobiol. B Biol. 207 (2020), 111889.
[9] Z. Zhu, et al., Photodynamic activity of Temoporfin nanoparticles induces a shift to the M1-like phenotype in M2-polarized macrophages, J. Photochem. Photobiol. B Biol. 185 (2018) 215–222.
[10] Pucelik, B. & Arnaut, L.G. Lipophilicity of bacteriochlorin-based photosensitizers as a determinant for PDT optimization through the modulation of the inflammatory mediators. 5–7 (2020).
[11] M.J. O'Shaughnessy, et al., Systemic antitumor immunity by PD-1/PD-L1 inhibition is potentiated by vascular-targeted photodynamic therapy of primary tumors, Clin. Cancer Res. 24 (2018) 592–599.
[12] R. Liang, et al., Oxygen-boosted immunogenic photodynamic therapy with gold nanocages@manganese dioxide to inhibit tumor growth and metastases, Biomaterials 177 (2018) 149–160.
[[13]] C. Donohoe, M.O. Senge, L.G. Arnaut, L.C. Gomes-da-Silva, Cell death in photodynamic therapy: from oxidative stress to anti-tumor immunity, Biochim. Biophys. Acta - Rev. Cancer 1872 (2019), 188308.
[14] V.D. Turubanova, et al., Immunogenic cell death induced by a new photodynamic therapy based on photosens and photodithazine, J. Immunother. Cancer 7 (2019) 1–13.
[15] L. Bezu, et al., Combinatorial strategies for the induction of immunogenic cell death, Front. Immunol. 6 (2015) 1–11.
[[16]] P. Vandenabeele, K. Vandecasteele, C. Bachert, O. Krysko, D.V. Krysko, Immunogenic apoptotic cell death and anticancer immunity. In apoptosis in cancer pathogenesis and anti-cancer therapy, Adv. Exp. Med. Biol. (2016) 133–149.
[[17]] L.A. Muehlmann, et al., Aluminium-phthalocyanine chloride nanoemulsions for anticancer photodynamic therapy : development and in vitro activity against monolayers and spheroids of human mammary adenocarcinoma MCF-7 cells, J. Nanobiotechnol. 13 (2015) 1–11.
[18] A. Tesniere, et al., Immunogenic death of colon cancer cells treated with oxaliplatin, Oncogene 29 (2010) 482–491.
[19] P.G. Sangaran, Z.A. Ibrahim, Z. Chik, Z. Mohamed, A. Ahmadiani, Lipopolysaccharide pre-conditioning attenuates pro-inflammatory responses and promotes cytoprotective effect in differentiated PC12 cell lines via pre-activation of toll-like receptor-4 signaling pathway leading to the inhibition of caspase-3 /nuclear Fa. Front. Cell. Neurosci. 14 (2021) 1–29.
[20] A.D. Garg, D.V. Krysko, P. Vandenabeele, P. Agostinis, Hypericin-based photodynamic therapy induces surface exposure of damage-associated molecular patterns like HSP70 and calreticulin, Cancer Immunol. Immunother. 61 (2012) 215–221.
[[21]] K. Tatsuno, et al., Extracorporeal photochemotherapy induces bona fide immunogenic cell death, Cell Death Dis. (2019).
[22] P. Liu, et al., Crizotinib-induced immunogenic cell death in non-small cell lung cancer, Nat. Commun. 10 (2019) 1–17.
[23] J.W. Hodge, et al., Chemotherapy-induced immunogenic modulation of tumor cells enhances killing by cytotoxic T lymphocytes and is distinct from immunogenic cell death, Int. J. cancer 133 (2014) 624–636.
[24] M. Obeid, et al., Calreticulin exposure dictates the immunogenicity of cancer cell death, Nat. Med. 13 (2007) 54–61.

CAPÍTULO 2: An Overview on Immunogenic Cell Death in Cancer Biology and Therapy

José Athayde Vasconcelos Morais[1,2], Mosar Corrêa Rodrigues[1,2], Rayane Ganassin[1,2], Giulia Rosa Tavares Oliveira[1,2], Fabiana Chagas Costa[1,2], Amanda Alencar Cabral Morais[2], Ariane Pandolfo Silveira[2], Victor Carlos Mello Silva[2], João Paulo Figueiró Longo[2] and Luis Alexandre Muehlmann[1,2]*

1. Laboratory of Nanoscience and Immunology, Faculty of Ceilandia, University of Brasilia, Brasilia/DF, 72220-900, Brazil.

2. Department of Genetics and Morphology, Institute of Biological Sciences, University of Brasilia, Brasilia 70910-900, Brazil.

Paper published in **Pharmaceutics**, 2022.

KEYWORDS: DAMPs; immune system; chemotherapy; photodynamic therapy; radiotherapy; immunotherapy

pharmaceutics

MDPI

Review

An Overview on Immunogenic Cell Death in Cancer Biology and Therapy

Mosar Corrêa Rodrigues [1,2,†], José Athayde Vasconcelos Morais [1,2,†], Rayane Ganassin [1,2], Giulia Rosa Tavares Oliveira [1,2], Fabiana Chagas Costa [1,2], Amanda Alencar Cabral Morais [2], Ariane Pandolfo Silveira [2], Victor Carlos Mello Silva [2], João Paulo Figueiró Longo [2] and Luis Alexandre Muehlmann [1,2,*]

[1] Faculty of Ceilandia, University of Brasilia, Brasilia 72220-275, Brazil; mosarcr@gmail.com (M.C.R.); joseavmorais@gmail.com (J.A.V.M.); rayaneganassin@hotmail.com (R.G.); giulia_rosa12@hotmail.com (G.R.T.O.); fchagas16@gmail.com (F.C.C.)

[2] Laboratory of Nanobiotechnology, Department of Genetics and Morphology, Institute of Biological Sciences, University of Brasilia, Brasilia 70910-900, Brazil; amandaalencarcabral@gmail.com (A.A.C.M.); pandolfo.ariane@gmail.com (A.P.S.); victor@spctm.com (V.C.M.S.); jplongo82@gmail.com (J.P.F.L.)

* Correspondence: luisalex@unb.br

† These authors contributed equally to this work.

Abstract: Immunogenic cell death (ICD) is a modality of regulated cell death that is sufficient to promote an adaptive immune response against antigens of the dying cell in an immunocompetent host. An important characteristic of ICD is the release and exposure of damage-associated molecular patterns, which are potent endogenous immune adjuvants. As the induction of ICD can be achieved with conventional cytotoxic agents, it represents a potential approach for the immunotherapy of cancer. Here, different aspects of ICD in cancer biology and treatment are reviewed.

Keywords: DAMPs; immune system; chemotherapy; photodynamic therapy; radiotherapy; immunotherapy

Citation: Rodrigues, M.C.; Morais, J.A.V.; Ganassin, R.; Oliveira, G.R.T.; Costa, F.C.; Morais, A.A.C.; Silveira, A.P.; Silva, V.C.M.; Longo, J.P.F.; Muehlmann, L.A. An Overview on Immunogenic Cell Death in Cancer Biology and Therapy. *Pharmaceutics* **2022**, *14*, 1564. https://doi.org/10.3390/pharmaceutics14081564

Academic Editor: Jun Dai

Received: 27 June 2022
Accepted: 25 July 2022
Published: 27 July 2022

1. Introduction

Both the innate and the adaptive branches of the immune system are involved in the elimination of malignant cells. Generally, for the successful elimination of tumors by immunity, the in situ presence of immunoadjuvants and antigens, as well as a non-immunosuppressor tumor microenvironment, are essential.

Tumor cells commonly express neoantigens, which are different from any other normal protein in the host, or tumor-associated antigens, which are expressed in an unusual tissue or in aberrantly high amounts [1,2]. As a result, one important feature of cancers is their ability to escape immunity, as the immune system is crucially involved in the defense against the development and progression of malignant cells [3].

In certain situations, the immunogenicity of tumors can be enhanced by increasing the local release and exposure of endogenous immunoadjuvants, such as damage-associated molecular patterns (DAMPs). The release of these molecules with a well-defined, immune-activating pattern is observed in a regulated cell death (RCD) modality known as immunogenic cell death (ICD). In this review we discuss how ICD can help to trigger or boost immune responses against cancer.

2. A Historical Overview on Cancer Immunotherapy

Activating or boosting adaptive immune responses against tumors has become a main pillar in the treatment of different cancers. Currently, immune-checkpoint inhibitors, chimeric antigen receptor (CAR) T cells, dendritic cell (DC)-based vaccines and immunostimulatory cytokines have been successfully used in clinical practice [4]. Different immune-checkpoint inhibitors approved by the FDA have significantly improved the treatment of

immunostimulatory cytokines have been successfully used in clinical practice [4]. Different immune-checkpoint inhibitors approved by the FDA have significantly improved the treatment of advanced-stage melanoma, non-small-cell lung carcinoma, kidney carcinoma, urothelial carcinoma, hepatocellular carcinoma, and others [4,5].

The first evidence that the host immune system could be therapeutically targeted to treat cancer was brought to light in the 19th century, when erysipelas was reported to have an influence on tumor progression. This erythematous infection of the skin was relatively common in post-surgery patients given the poor sanitary conditions of surgery at that time. In 1867, the German physician Wilhelm Busch reported that a malignant tumor disappeared after the patient had contracted this infection [6].

In 1883, the German surgeon Friedrich Fehleisen demonstrated that the etiologic agent of erysipelas was *Streptococcus pyogenes* [7]. In his experiments, Fehleisen produced erysipelas by inoculating patients with pure cultures of *S. pyogenes*. On one occasion, out of six patients with inoperable malignancies who reacted to this inoculum, three showed only a slight change in their tumors. The other three patients, however, exhibited significant changes in the evolution of the disease. The fibrosarcoma nodules of one patient thus treated were reported to have disappeared, while two other patients with breast carcinoma had tumor remission. Similar clinical experiments were performed by other surgeons at that time [8].

In 1891, the American surgeon William Bradley Coley published an article citing the work of Fehleisen and his own observations on the curative effect of erysipelas upon malignancies [9]. Coley injected patients with *S. pyogenes*, inducing erysipelas on purpose. Some of these patients, after having recovered from local inflammation and fever, exhibited reduced tumor size or were even cured of the malignancy. According to Coley, some promptly responded to this therapy upon the first injection, while others needed several doses before some clinical improvement could be observed. As there were cases of death after the injection, Coley decided to inactivate the bacteria with heat before injecting them, in a preparation which was named Coley's toxin. The use of this bacterial preparation gave good results in bone and soft-tissue sarcomas [10]. This was one of the first anticancer immunotherapies described in the scientific literature.

Despite the reported success, many were quite skeptical about the results described by Coley. As recognized later, his work was probably the first formal study on immunotherapy and presented a rationale for inducing immune responses against tumors, but the lack of knowledge on immune mechanisms at the time his first patients were treated was a huge barrier to the acceptance of this approach [10,11]. However, as immunology advanced, many oncologists began to support the use of Coley's toxin. In 1935, the prestigious surgeon Ernest Amory Codman asserted that the results described by Coley were solid scientific evidence [10,12]. Codman was particularly impressed with six cases registered by Coley of five-year cures of patients with Ewing's sarcoma injected with the toxin [12]. Codman suggested that the increased production of lymphocytes induced by Coley's toxin might explain the "occasional miracle which follows this treatment".

In 1909, the renowned German scientist and physician Paul Ehrlich suggested that the immune system played an important role in eliminating cancer cells, speculating that it might be involved in suppressing the development and progression of carcinomas [13]. Later, as the role of the immune system in distinguishing self from non-self became clear, Frank Macfarlane Burnet developed the concept of immunosurveillance [14,15].

As Burnet wrote [15], cancer cells grow free from the normal control exercised by the organism as a whole. Cancer is then the consequence of the breakdown in one or more aspects in this control mechanism that holds the multitude of cells of an organism working together as a single functioning unit [15]. One key part of this normal control was the immune system, which is normally able to identify and to mount an effective reaction against tumor-specific or -associated antigens, eventually eliminating most of the potential cancer cells before they become a clinically apparent tumor [15].

In a favorable immune context, tumor antigens are processed and presented by antigen presenting cells (APCs), triggering the activation of $CD4^+$ and $CD8^+$ T cells, ultimately

eliminating the tumor. However, malignant cells can suppress their own immunogenicity, thus avoiding being detected by the immune system. Cancer cells can, for instance, up-regulate the expression of programmed cell death ligand 1 (PD-L1) molecules, present defects in the antigen presentation machinery, recruit immunosuppressive cells, such as myeloid-derived suppressor cells (MDSC) and T regulatory (Treg) cells, and lead to direct or indirect secretion of TGF-β and IL-10 [5,16].

The development of an immunoevasive phenotype is the result of a long, complex and dynamic interaction of transformed host cells and the immune system in what is known as cancer immunoediting [16,17]. This process can be divided into three stages: elimination, equilibrium and escape. If elimination is successful, the immune system eradicates aberrant cells and prevents the continuation of carcinogenesis. This event represents the fulfillment of immunosurveillance and is highly dependent on the immunogenicity of the abnormal cells. If the elimination is not complete, however, an equilibrium stage may occur, i.e., although these cells persist, they are not able to freely proliferate, and do not generate clinically apparent tumors. Occasionally, some of these aberrant cells may develop more efficient immune evasion abilities, then becoming poorly immunogenic or non-immunogenic. These cells eventually escape the immune system and generate a growing tumor mass [17,18].

Therefore, changing the balance towards the host immune system could be used therapeutically against cancers. In the 20th century, many advances in immunology contributed to the development of modern immunotherapy [19]. Some of these advances are particularly noteworthy: (i) the identification and demonstration of the role of T lymphocytes in animal models [20]; (ii) the demonstration of the presence of dendritic cells in peripheral lymphoid organs [21]; and (iii) the identification of natural killer cells (NK cells) [22]. Many approaches to target the immune system as an anticancer strategy followed, such as the use of cytokines, vaccines, adoptive cell therapies and antibodies against immune checkpoints [11].

The most recent milestone in modern immunotherapy, the discovery of immune checkpoint inhibitors, led to the development and approval by the FDA of anti-PD-1/PD-L1 and anti-CTLA-4 antibodies, which proved to be effective against melanoma and other different tumors [23].

Currently, many studies show that it is possible to increase the immunogenicity of tumors by triggering specific cell death modalities in cancer cells. In that regard, it has been observed that specific cytotoxic treatments, such as anthracycline-based chemotherapy [24] radiotherapy [25] and photodynamic therapy (PDT) [26,27], can induce immunogenic cell death (ICD), which can render cancers more efficient at triggering or boosting tumor antigen-specific immune responses. As this event can lead to the elimination of the primary tumor, and of occasional antigen-sharing metastatic foci as well, the induction of ICD has been suggested as a potential immunotherapeutic approach.

3. Immunogenic Cell Death

As defined by the Nomenclature Committee on Cell Death, ICD is a modality of RCD [28,29]. This implies that ICD activation depends on signaling transduction programs, and can thus be triggered or modulated by drugs and genetic components [28].

ICD differs from other RCD types, such as necroptosis, ferroptosis and pyroptosis, not only by the conditions under which it is triggered, but also by the fact that it activates an adaptive immune response in immunocompetent syngeneic hosts against antigens expressed by the dying cell [28]. The cells undergoing ICD exhibit morphological and molecular hallmarks of apoptosis with a well-defined pattern of release and exposure of DAMPs [29]. Thus, cells at ICD exhibit the two conditions necessary for eliciting an adaptive immune response: antigenicity and adjuvanticity [28,29].

DAMPs form a group of different molecules that normally perform structural and metabolic functions in living cells unrelated to their immune functions during ICD [30]. However, when emitted with a specific temporospatial profile during ICD, DAMPs are able to trigger or boost antigen-specific immune responses [31,32]. The activation of pattern recognition receptors (PRR) by DAMPs results in the maturation of dendritic cells

(DCs) and the activation of $CD4^+$ and $CD8^+$ T cells [33], as represented in Figure 1. Different aspects of the activation of adaptive immune responses are fulfilled by the different DAMPs involved in ICD.

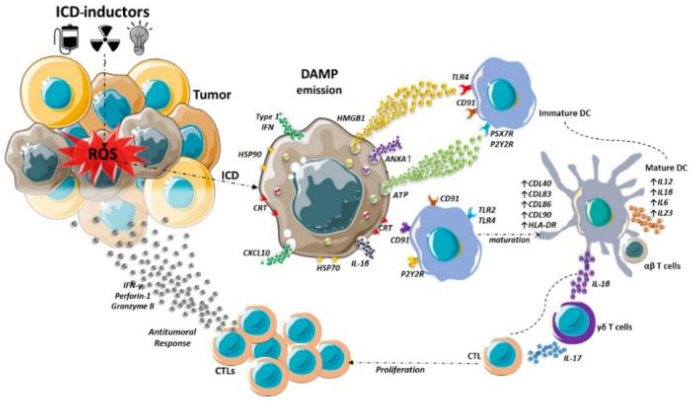

Figure 1. Engagement of adaptive immune response after immunogenic cell death in a tumor. Chemotherapy, radiotherapy, and photodynamic therapy can induce immunogenic cell death (ICD), which is a programmed cell death accompanied by the exposure of damage-associated molecular patterns (DAMPs). This can occur, for instance, as a consequence of oxidative stress in the endoplasmic reticulum. Some DAMPs, such as heat-shock protein (HSP)70, HSP90, and calreticulin are exposed on the plasma membrane, while others such as adenosine triphosphate (ATP), high mobility group box 1 protein (HMGB1), C-X-C motif chemokine ligand 10 (CXCL10) and annexin A1 (ANXA-1) are released to the extracellular medium. DAMPs then activate pattern recognition receptors of dendritic cells (DCs) and other antigen-presenting cells. This culminates in the maturation of the DCs and in the recruitment and activation of T cells. In this way, ICD can trigger or boost an adaptive antitumor immune response.

The time profile of the release and exposure, as well as the specific actions performed by the DAMPs, orchestrates the attraction, phagocytic activity and maturation of APCs in the tumor bed. The simple presence of a single DAMP or just a couple of them in the vicinity of tumor cells is generally not enough for the initiation or boosting of a cytotoxic, effective anticancer immune response. The absence of calreticulin or ANXA1, for example, is known to severely limit immune responses against tumor cells [34–36]. Moreover, the tumor microenvironment must permit immune cells to be activated and to perform their roles properly in order for DAMPs to exert their immunoadjuvant effects.

Specific conditions are known to induce ICD, such as chemotherapy [37–39], radiotherapy [40,41] and PDT [26,27,42–45]. Parameters such as the protocol of application and the drug used in these treatments are crucial to determine whether ICD is induced or not. In the case of chemotherapy, for instance, ICD can be induced by drugs such as mitoxantrone, oxaliplatin and cyclophosphamide, but not by cisplatin, etoposide and mitomycin C. In the case of PDT, the type and concentration of the photosensitizer, as well as the irradiation regimen, are key factors [26,27].

4. Endoplasmic Reticulum Stress

Different ICD-inducers act as stressors of the endoplasmic reticulum (ER) of target cells [31,33,46]. Indeed, the ER has been linked by many studies to programmed cell death [46–48]. Stressing conditions, such as oxidative stress and hyperthermia, can impair the folding of proteins. Unfolded proteins bind the luminal ER chaperone GRP78/BiP (Figure 2), triggering the activation of three ER transmembrane proteins: inositol-requiring enzyme 1α (IRE1α), protein kinase RNA-like endoplasmic reticulum kinase (PERK), and

activating transcription factor 6 (ATF6). The downstream cellular events following the activation of these ER sensors can either restore normal ER metabolism or induce cell death [48].

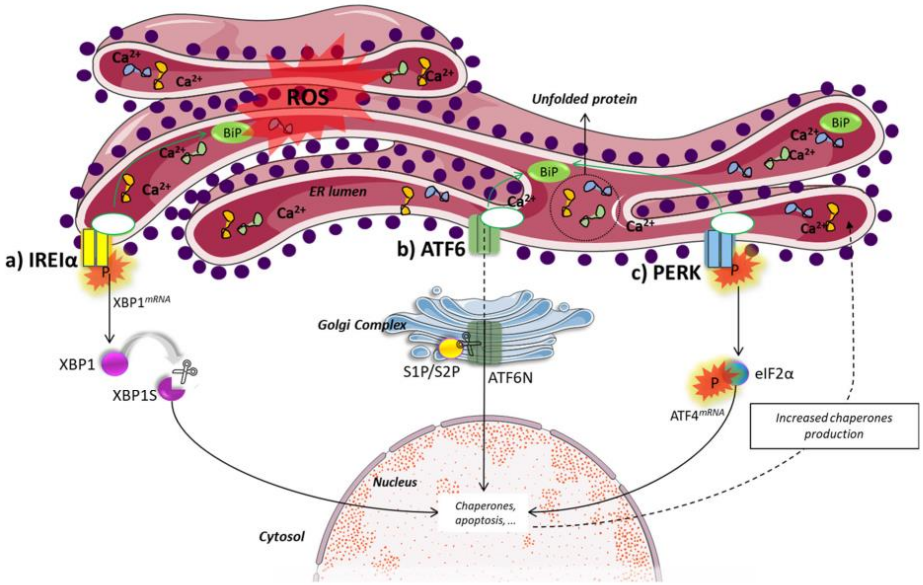

Figure 2. Activation of responses to protein malformation. These three pathways—IRE1α (**a**), ATF6 (**b**) and PERK (**c**)—are activated in unfolded protein response (UPR) to cope with disturbances in protein folding and to restore endoplasmic reticulum homeostasis after stress. The phosphorylation of eIF2α is a hallmark of immunogenic cell death. Legend: ROS: reactive oxygen species; BiP: Binding immunoglobulin protein; ER: endoplasmic reticulum; IRE1α: inositol-requiring enzyme 1α; XBP1: X box-binding protein 1 mRNA; XBP1S: spliced X box-binding protein 1 mRNA; ATF6: activating transcription factor 6; PERK: protein kinase RNA-like endoplasmic reticulum kinase; ATF4: activating transcription factor 4; S1P: site-1 protease; S2P: site-1 protease; eIF2α: eukaryotic initiation factor 2α.

The activated IRE1α dimerizes and is autophosphorylated, becoming able to catalyze the unconventional, cytosolic splicing of the mRNA for the transcription factor X box-binding protein 1 (uXBP1) to sXBP1, which is then translated. The XBP1 is a key protein in UPR, activating the transcription of different genes that can reinstate normal ER metabolism [49]. The PERK protein also dimerizes and auto-phosphorylates, activating its kinase domain to phosphorylate the eukaryotic initiation factor 2α (eIF2α) [50,51]. The phosphorylation of eIF2α is the key event in the integrated stress response (ISR), which is a part of the ER stress response, and is common to ICD induced by different cytotoxicants [34]. Thus, the presence of phosphorylated eIF2α is a hallmark of ICD and can be used as a biomarker of ISR in cell cultures and in biological samples [52].

Phosphorylated eIF2α triggers the selective translation of the activating transcription factor (AFT4), which activates the expression of genes involved in protein folding, amino acid metabolism and regulation of oxidative stress [53]. Also, ATF6 is translocated to the Golgi apparatus, where it is then cleaved to ATF6N, releasing its transcription factor moiety that activates the transcription of genes for chaperones, XBP1, C/enhancer binding protein-homologous protein (CHOP), and others [48,54].

The UPR is important for cells under stress to survive and restore homeostasis. The activation of this response is often observed in cancer cells, as the tumor is often a stressing environment, with acidic pH and hypoxia, for instance. Thus, the phosphorylation of eIF2α is

frequently observed in cancer cells and plays an important role in tumor growth, invasion, and angiogenesis [55]. In this situation, tumors can cope with the constant stress and progress.

However, if the UPR is unable to restore the ER protein folding capacity, then cell death is triggered. In this context, the pro-apoptotic factor CHOP plays a key role [55–57]. The PERK/eIF2α/ATF4 pathway activates the production of CHOP [53], which activates the expression of the BH3-only protein Bim. This leads to the activation of Bax/Bak and the release of cytochrome C to the cytosol, with the consequent induction of apoptosis [56,58]. It is worth mentioning that CHOP also acts on the Bcl2 protein (autophagy activation factor), inhibiting its action [59,60]. IRE1α and ATF6 will also activate CHOP via fragments of XBP1S or ATF6N, thereby triggering apoptosis [60,61].

An intense stress in the ER not only activates apoptosis but also promotes the exposure of ER chaperones, such as calreticulin and HSP70, and other DAMPs involved in ICD [62]. The main DAMPs are discussed in the next section.

5. Damage-Associated Molecular Patterns

Processes associated with ICD result in the emission of DAMPs, such as HSP70, HSP90, calreticulin, HMGB1, ATP, type I IFN, cancer cell-derived nucleic acids, ANXA1, and others [29,31,63]. The recognition of DAMPs by cells of the immune system triggers intracellular signaling pathways involved in responses to injury [33]. Frequently, many of these DAMPs perform specific functions in cells not related to immunity. Nevertheless, outside the cells, they can activate various immune cell receptors from the family of PRR. They are also capable of potentiating pro-inflammatory effects such as the maturation and activation of antigen-presenting cells, such as dendritic cells and macrophages, which ultimately activate T cells ($CD8^+$), creating an anti-tumor immunity [32].

The DAMPs are emitted by different mechanisms, such as the active exposure on plasma membrane (e.g., calreticulin, HSP70 and HSP90), released as end-stage degradation products (e.g., DNA and RNA), and secreted to the extracellular medium (e.g., ATP, HMGB1, uric acid, IL-1α and other pro-inflammatory cytokines) [33,64].

A well-studied DAMP is calreticulin, a soluble protein found mainly in the ER. Its main functions in this organelle are the buffering of Ca^{2+} [65], contributing to the homeostasis of this cation, and the lectin-like chaperone activity, essential to the folding of N-glycosylated proteins [66]. During ICD, it is exposed on the plasma membrane even before phosphatidylserine [67] and acts as an eat-me signal, inducing antigen-presenting cells to phagocytose the target cell [68]. Although calreticulin is essential to the immunogenicity of cells undergoing ICD, its presence alone on the cell surface is not enough for starting an immune response [36]. The presence of other DAMPs, therefore, is crucial for the immunogenicity of ICD. Other chaperones exposed on the plasma membrane in ICD are HSPs, which also act as eat-me signals for phagocytes [69,70].

In cancer cells undergoing ICD, type I interferons (IFN-Is) are released by mechanisms involving the detection of endogenous nucleic acids [28], i.e., dsRNA by TLR3 [71], or dsDNA by cyclic GMP-AMP synthase (cGAS) [72]. The release of this DAMP has been shown to be crucial for the success of the ICD-inducing anthracycline-based chemotherapy [71]. IFN-Is are potent immunostimulatory proteins with significant anticancer effects, and they have been used to treat chronic myeloid leukemia, acute lymphoblastic leukemia, multiple myeloma, melanoma, Kaposi's sarcoma, and renal cell and bladder carcinoma [73]. It is notable that the nucleic acids released by cancer cells at ICD are also taken up by DCs and other immune cells, triggering potent IFN-I responses [28].

ANXA1 is also among the crucial DAMPs in ICD. This protein is expressed in granules of different cells, such as neutrophils, eosinophils and monocytes, and is found in different organs and tissues, such as the lungs the bone marrow and intestine [74,75]. Like other members of the annexins superfamily, ANXA1 binds phospholipids and can thus affect eicosanoid production [74]. It has an important role in the regulation and resolution of inflammation. Although ANXA1 has been described as a negative regulator of innate immunity, with neutrophils being its main target [74], it is known to be passively released

by cells undergoing ICD, then activating the migration of APCs towards the dying cells, facilitating their engulfment and processing [34]. The importance of this DAMP in tumor immunology can be noted by the fact that the low expression of ANXA1 is often associated with poor DCs and T lymphocyte infiltration in the tumor bed and a higher ability of different human cancers to escape immunity [35].

Another DAMP released to the extracellular medium is ATP [43,76]. Extracellular ATP operates as a strong chemoattractant and promotes not only the recruitment of immune cells but also their maturation [77,78]. In addition to serving as one of the main sources of intracellular energy, ATP also acts in the extracellular signaling mechanisms [67]. ATP is secreted in response to the cytotoxic and cytostatic effects of some aggressive agents such as chemotherapy drugs [46]. ATP release occurs during the process of apoptosis, and different mechanisms can lead to the release of ATP from the intracellular to the extracellular environment, such as the caspase-dependent activation of Rho-associated, coiled-coil containing protein kinase 1 (ROCK1)-mediated, myosin II-dependent cellular blebbing, as well as the opening of pannexin 1 (PANX1) channels, which is also triggered by caspases and autophagy [79–81]. Of these three, opening pannexin 1 channels and autophagy appear to occur in ICD.

During the formation of apoptotic bodies, caspases 3 and/or 7 act in the cleavage in the C-terminal portion leading to the opening and activation of PANX 1, then releasing the ATP into the extracellular region [82]. In autophagy, the cytoplasmic constituents are degraded in double-membrane organelles, and the autophagosomes are subsequently fused with lysosomes, resulting in the degradation of the autophagocytic content by acid hydrolases and recycling towards energy metabolism or anabolic reactions, releasing the ATP for the extracellular portion [83]. ATP binds the purinergic receptors P2RY2 and P2RX7 of DCs, resulting in the influx of K^+ and Ca^{2+} ions, activating the inflammasome NLRP3, followed by activation of caspase-1, consequently stimulating the proteolytic maturation and secretion of interleukin 1 (IL-1) and interleukin 18 (IL-18), contributing to the immunogenic response [84].

HMGB1 is a non-histone nuclear protein that, once secreted, acts as an essential DAMP in the activation of DCs by ICD [76,85–87]. Its release occurs sometime after apoptosis [63,86]. It can also be released by cells of the innate immune system without the need for cell death in response to pathogens or secreted by cells in response to some damage in the late phase of apoptosis—necrosis [86,88,89]. HMGB1 activates toll-like receptors (TLR)4 and 2, and stimulates the production of pro-inflammatory factors by DCs [90], strongly contributing to the immunogenicity of ICD [33,91].

The exposure of calreticulin and the release of ANXA1, ATP and HMGB1 result in the attraction and maturation of DCs in the tumor microenvironment [91,92]. Once there, the DCs phagocytose the tumor cells and release pro-inflammatory mediators in the tumor, such as IL-1β, IL-18, IFN-γ, among others. Activated DCs also present the tumor antigens, culminating mainly in the activation of $CD8^+$ cytotoxic T lymphocytes, which are fundamental in the activation of the tumor retraction immune antitumor response [33,43]. The effects of the DAMPs discussed in this section are summarized in Table 1.

Table 1. Damage-associated molecular patterns involved in immunogenic cell death.

DAMP	Abbreviation	Effect on Immune Cells	References
Annexin A1	ANXA1	Expressed in different cells (neutrophils, eosinophils, and monocytes), ANXA1 has a role in the regulation and resolution of inflammation. It can act as a negative regulator of innate immunity, with neutrophils being its main target; it activates the migration of APCs towards the dying	[34,74]

		cells, facilitating their engulfment and processing.	
Adenosine triphosphate	ATP	ATP acts as a strong chemoattractant and promotes not only the recruitment of immune cells but also their maturation.	[73,75]
Calreticulin	CRT	Calreticulin acts as phagocytosis inducer. Its exposure and the release of ANXA1, ATP and HMGB1 result in the attraction and maturation of DCs in the tumor microenvironment.	[36,39]
Deoxyribonucleic acid	DNA	With its accumulation in the cytoplasm, DNA can stimulate innate immune responses.	[93]
High mobility group box 1 protein	HMGB1	Acts as an essential DAMP in the DCs activation, stimulating the production of pro-inflammatory factors, strongly contributing to the immunogenicity of ICD.	[29,94]
Heat-shock protein	HSP 70 HSP 90	HSP act as eat-me signals for phagocytes. They can induce DC maturation and promote target engulfment by APC cells.	[29]
Type I interferon	IFN-I	IFN-Is acts as potent immunostimulatory proteins and have a crucial role in ICD. It can modulate the maturation, differentiation, and migration of DC cells, increase primary antibody responses, and activate B and T cells directly or indirectly.	[29,71]
Ribonucleic acid	RNA	It recruits leukocyte and M1-type macrophages.	[95]
Uric acid	UA	Crystalline UA can produce inflammatory mediators through macrophage activation and the enhancement of T cells.	[96]

6. ICD and DAMPs in Cancer Therapy

The literature on ICD in cancer biology has been significantly expanded over the last years, providing new possibilities for cancer treatment. Firstly, the discovery that ICD can be induced by certain classical anticancer agents has made it clear that some treatment regimens should be designed not only to directly eliminate tumor cells, but also to optimize their capacity to induce immune responses against tumor antigens. Secondly, ICD inducers can be used in combination with immunotherapeutics, such as immune checkpoint inhibitors.

Recently, Ganassin et al. (2022) demonstrated that curcumin, a polyphenol obtained from turmeric, causes ER stress and ICD in colorectal adenocarcinoma CT26 cells. The authors observed that, when treated with curcumin, these cells exhibited an initial increase of intracellular Ca^{2+}, which was followed by the activation of XBP1, a protein involved in the UPR response. The ER stress initiated by curcumin was accompanied by the induction of ICD.

Regarding chemotherapeutics, different drugs have been found to induce ICD in preclinical studies [36]. Moreover, chemotherapeutics such as doxorubicin, mitoxantrone, idarubicin, cyclophosphamide, bortezomib and oxaliplatin have already been clinically tested as ICD inducers, mainly in combination with immunotherapeutics [39]. For instance, the combination of doxorubicin, an ICD inducer, with the PD-1-targeting immune-checkpoint blocker, nivolumab, resulted in 35% objective response rates (ORRs) in the treatment of metastatic triple negative breast cancer patients [39,97]. When nivolumab was combined with cisplatin, a non-ICD inducer chemotherapeutic, ORRs were lower

(23%) [97]. A number of other clinical studies are already under way to test this immunostimulatory combination using not only immune-checkpoint blockers, but also CAR-T cells, DC-based vaccines, immunostimulatory cytokines, and others [39].

Interesting results of the Phase II study published by Bota et al. (2018) also show that ICD-inducers can improve clinical outcomes in glioblastoma (WHO grade IV astrocytic glioma) immunotherapy [98]. The authors used an allogeneic/autologous therapeutic glioblastoma vaccine (ERC1671, Gliovac), which is a mixture of inactivated tumor cells and lysates of tumor cells derived from the treated patient and three other glioblastoma patients, combined with recombinant colony stimulating factor 2 (CSF2, best known as GM-CSF, used to activate immune responses). The patients received a short regimen of low-dose cyclophosphamide (50 mg/day for 4 days) prior to vaccination. Cyclophosphamide is an ICD-inducer, used in this case, according to the authors, for relaxing the immunosuppressive environment. Indeed, low-dose cyclophosphamide has been reported to suppress Treg cell response, helping to promote DC expansion and antitumor cytotoxic T cell-mediated response [99]. The protocol of treatment described by Bota et al. (2018) also included the treatment of these glioblastoma patients with bevacizumab, a monoclonal antibody specific to VEGF. The results showed increased survival for the patients thus treated (12 months vs. 7.5 months for patients receiving bevacizumab only). Although the authors did not discuss the occasional contribution of ICD to the outcomes, the benefit observed with this protocol makes it worth investigating the possible contribution of ICD in preclinical and clinical models, which could help to improve this combinatory therapy in the future.

Radiotherapy has been shown to induce ICD as well. In clinical practice, radiotherapy and chemoradiotherapy were shown to induce the exposure of the ICD-related DAMPs calreticulin, HSP70 and HMGB1 when applied either as a pre- or post-operative protocol of different cancers [100]. The results, however, are still contradictory. A possible cause for this can be the different experimental settings used and insufficient data regarding ICD hallmarks.

Lämmer et al. (2019) investigated the expression of cytosolic HSP70 in tumor tissue of 60 patients diagnosed with primary glioblastoma. As discussed before in this review, HSP70 is released during ICD, acting as a DAMP. In this study [101], the tumors were surgically resected and patients were then treated with radiotherapy and temozolomide chemotherapy. The progression-free survival and overall survival were significantly longer in patients exhibiting a higher expression of cytosolic HSP70. The authors hypothesized that this result may be due to the induction of ICD by the combination of radiotherapy and chemotherapy given to patients.

Rothammer et al. (2019) analyzed the concentration of HSP70 in the serum of 40 breast cancer patients, who received breast-conserving surgery and adjuvant radiotherapy [102]. The authors observed that patients with higher serum concentrations of HSP70 had an increased probability of developing contralateral recurrence or metastases within two years of receiving radiotherapy.

Protocols based on the combination of radiotherapy and immunotherapeutics have also been tested, and it remains unclear if patients benefit from radiotherapy-induced ICD, as the clinical data are contradictory. For instance, in the treatment of rectal cancer, the increase in HMGB1 was associated both with poorer [103] and with better [104] responses to chemoradiotherapy.

Hongo et al. (2015) studied 75 patients with lower rectal cancer who were treated with preoperative chemoradiotherapy, consisting of radiotherapy (1.8 Gy × 28 fractions) and chemotherapy with a 5-fluorouracil (FU) prodrug (300 mg/m^2/day) and leucovorin (75 mg/day). After chemoradiotherapy, tumors were surgically resected and analyzed for their expression of HMGB1. The patients with a higher expression of HMGB1 had a poorer response to chemoradiotherapy [103]. In the study by Huang et al. (2018), the presence of HMGB-1 in the cytosol, resulting from its translocation from the nucleus, was analyzed in the samples of locally advanced rectal cancer from 89 patients. The authors reported that patients whose cancer exhibited cytosolic HMGB-1 before neoadjuvant chemoradiotherapy had a better clinical outcome.

PDT has also been shown to induce ICD. This therapy is based on the pre-treatment of target cells with a photosensitizer, which is next photoactivated to generate reactive species and cause oxidative stress in situ [105]. As a consequence of the photoreactions thus induced, reactive species are produced, which can overwhelm the antioxidant defenses of the cell, generating oxidative stress and cell death [26]. This approach has been shown to induce ICD in specific conditions. The type and concentration of the photosensitizer [27,106], as well as the light dose [26], can significantly affect its ICD-inducing capacity. Moreover, oxygen supply in the target tissue can also affect PDT outcomes.

Doix et al. (2019) reported that the combination of a therapeutical vaccine based on DCs stimulated with PDT-killed cells and radiotherapy can delay the development of experimental squamous cell carcinoma in mice. Firstly, the authors showed that the non-porphyrinic photosensitizer OR141, at low doses, induced ICD in SCC7 squamous cell carcinoma cells in vitro. These PDT-killed SCC7 cells were then used to prime and stimulate the maturation of DCs in vitro, which were then employed as a therapeutic vaccine against xenografts of SCC7 cells developed in the flank of C3H mice. This DC vaccine was subcutaneously injected three times at one-week intervals near the tumor-draining lymph node. One week later, radiotherapy mediated by a Cesium-137 γ-ray irradiator was applied onto the tumors. Occasionally, a fourth injection of the DC vaccine was performed at the time of radiotherapy application (peri-radiotherapy). It was observed that the tumor growth was delayed only when the DC vaccine was applied during the peri-radiotherapy period.

Rodrigues et al. (2022) showed that PDT using the photosensitizer aluminum-phthalocyanine mainly induced necrosis at the highest photosensitizer concentration and light dose, while milder protocols of PDT were able to efficiently induce ICD in both colorectal CT26 and mammary 4T1 murine adenocarcinoma cells [26]. In vitro, the milder PDT protocol consisted of 12.2 nM aluminum-phthalocyanine for colorectal adenocarcinoma CT26 cells and 9.0 nM aluminum-phthalocyanine for breast adenocarcinoma 4T1 cells, both irradiated with 25 J/cm^2 red light dose. The exposure or release of calreticulin, HSP70, HSP90 and HMGB-1 close to that promoted by this PDT protocol was comparable to that observed with mitoxantrone treatment. Increasing the photosensitizer concentration and light dose resulted in a reduction on the release of these DAMPs. This shows that the PDT regimen has to be fine-tuned to induce ICD.

As commented previously, there are several ICD inducers described in the literature. Among them are classical approaches, such as chemotherapy, PDT and radiotherapy. These classical therapies are usually aimed at tumor destruction, mainly by inducing direct cytotoxicity to target tumor cells, regardless of the death mechanism underlying this effect. This cytotoxicity induced in a noncontrolled fashion can fail to trigger immune activation. Immune-targeted cytotoxic cancer treatments have to thus be designed to induce ICD, representing an adaptation in former protocols in order to increase the immunogenicity of cancer treatments.

Several ICD inducers are used in well-recognized therapies. Thus, we understand that the translation of this knowledge to clinical protocols can be easier if compared to the implementation of new anticancer drugs which are currently under development. As previously discussed, the literature shows evidence of abscopal effects in radiotherapy and PDT protocols, for example, that could be due to ICD. However, due to the complexity of cancer cells and tumor tissues, it is probable that personalized approaches are necessary to the successful use of immune-activating strategies in the clinic. Another barrier to the development of clinical protocols for ICD induction is the lack of standardization in ICD studies, as evidenced in this section. Thus, the use of widely recognized, bona-fide parameters that demonstrate that an immunogenic response is being induced is essential for translating research into clinical protocols [107]. This can be supported by guidelines proposed in the literature [29].

7. Delivery of DAMPs and ICD-Inducers to Tumor Tissues

As commented previously, ICD is triggered by the combined release of a specific set-up of DAMPs that includes calreticulin, HMGB-1, and ATP, among others. These

molecules are exposed to the external cell membrane, and/or released to the external media in dying cells. All of these events are part of a cyclic process which is finely regulated during this specific sub-type of apoptosis. In terms of cell biology, as previously mentioned, several therapeutic procedures can trigger this event and have been investigated in both pre-clinical and clinical applications [88].

However, due to the variety of these different types of stimuli, the exposure or release of DAMPs can vary among the therapeutic strategies. Moreover, it is possible that, for clinical applications, the control of DAMPs exposure and release can be different among patients and tumor stages due to internal sub-tumoral tissue organizations and the different phenotypes of cancer cells. This situation makes the clinical translation difficult, delaying this therapy for patients.

To reduce this potential drawback, some authors have discussed alternative strategies to burst the DAMPs present inside tumor tissues (Figure 3), thus ensuring the presence of these molecular triggers for ICD induction. In terms of efficacy, the simple delivery strategy of DAMPs to target tumor tissues may not be efficient because ICD induction depends both on the release of chemotactic agents and on the presence of recognition molecules, such as calreticulin, on the cell membrane surface. Moreover, as discussed earlier, calreticulin exposure is a key factor for specific cell recognition.

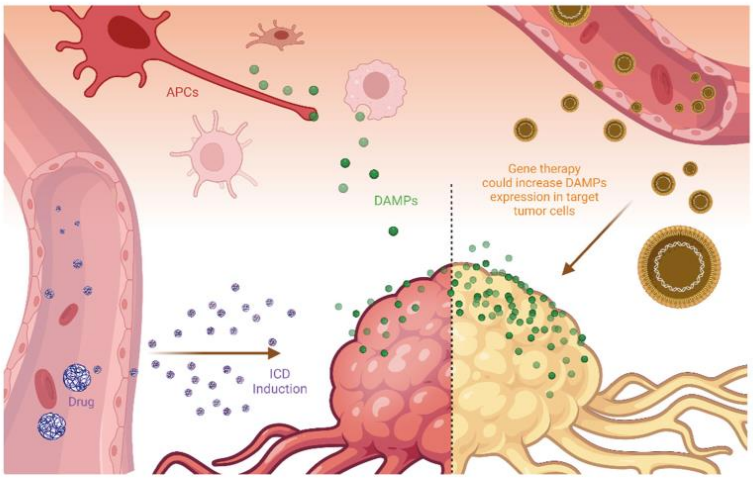

Figure 3. The induction of immunogenic cell death (ICD), the exposure of damage-associated molecular patterns (DAMPs), and the activation of antigen-presenting cells (APC) can be enhanced by delivery strategies based on nanotechnology.

Alternatively, some authors proposed the use of gene therapy to deliver DNA sequences that could increase DAMPs expression in target tumor cells. The rationale for this strategy is supported by the fact that some tumor types have a reduced expression of DAMPs, such as calreticulin. For instance, Garg et al. (2015) described a pre-clinical tumor model that reduces the constitutive calreticulin expression, thus reducing the effectiveness of immunogenic protocols [104]. The authors defined this tumor model as resistant to immunization against cancer cells. In terms of microevolution, it makes sense, as calreticulin is a molecule that activates tumor cell phagocytosis by APC. In this situation, selected tumor clones could reduce the expression of DAMPs, thus impairing ICD activation.

Due to the challenge of tumor targeting, nanoparticles or nanocarriers could be used to concentrate ICD inducers and DAMP molecules close to tumor tissues [26,27,108]. This is the classical argument for using nanotechnology for tumor therapy. Within this approach, nanocarriers are passively or actively delivered to the tumor regions and release the carried

ICD activators to induce cell death and initiate the immune recognition and then the immune surveillance against malignant cells. This approach is somewhat different from the direct delivery of DAMPS to tumor tissues, but has been used successfully [108].

In the ICD approach widely proposed in the literature, conventional drugs, such as doxorubicin or mitoxantrone, for example, will lead tumor cells to succumb to ICD and release DAMPS. The preclinical results are promising; however, there are some concerns about the translation possibilities for this strategy, especially for the passive delivery of nanocarriers for tumor tissues. The main problems are the structural differences between preclinical induced tumor tissues and natural tumors that are developed in clinical conditions [109]. The argument is that passive targeting is not reproduced in clinical conditions. Despite all this discussion, there is some evidence that, at least in part, nanocarriers can increase the delivery of drugs and immunoadjuvant molecules to tumor tissues.

In the work by Zhou et al. (2022), murine melanoma (B16F10) cells were subjected to different treatments, such as hypoxia, cisplatin, radiotherapy, photodynamic therapy, and hypochlorous acid (HOCl). The cell-delivered secretions (CDS) of melanoma cells treated with HOCl activated dendritic cells and macrophages and produced the best antitumor immune response when compared to the other treatments. Aiming to increase the effectiveness of the treatment, the HOCl-CDS produced in vitro was then associated to nanofibers of a scaffold hydrogel containing melittin and RADA24 peptides. This nanosystem was then injected into the subcutaneous melanoma in vivo (C57BL/6 mice). The results indicated that the obtained hydrogel induced cell death, cytotoxicity in T lymphocytes, and increased the antitumor effect of the immune checkpoint inhibitors.

Another example of a successful use of nanocarriers for increasing the immunogenicity of tumors was published by Sethuraman et al. (2020) [105]. In this work, the authors describe a liposome nanocarrier with a DNA plasmid encoding calreticulin. They observed that this strategy increased the expression of calreticulin in target tumor cells, reducing tumor growth due to immune activation. Interestingly, when they combined this liposomal formulation with the application of focused ultrasound treatment, the results were better. This improvement is probably related to the temperature increase provided by the ultrasound. In higher temperatures, some amount of cell death could be triggered, which in combination with calreticulin superexpression could increase the immune activation.

The authors did not evaluate the modality of cell death induced by the treatment. However, it shows the potential of DAMPs delivery for immune system activation. As a potent phagocytosis inducer, calreticulin is a key factor for alternative types of immune activation. As noted previously, this protein was included as a molecular signature for the ICD, but its presence in external spaces may also promote tumor recognition by APC, thus contributing to immunological surveillance [106].

In this section, we presented potential uses of drug delivery strategies to optimize ICD induction. First, nanoparticles could deliver DAMPs directly to target tissues; second, nanocarriers could deliver ICD inducers; and third, nanoparticles could be used during gene therapy to increase the expression of DAMPS in the target tumor tissues. There is certainly no ideal strategy, but an effective therapy could be based on the combination of different approaches, and eventually on other strategies to optimize ICD induction in immunotherapies.

8. Conclusions

Although the induction of ICD has not been rationally used as a clinical treatment modality, it has potential for being exploited as an immunotherapy tool. The recent advances in immunotherapy have opened new fronts and possibilities in the fight against melanoma, for instance, with prolonged survival and durable responses in many patients. Studies on the immune evasion strategies deployed by tumors, as well as on the mechanisms underlying the activation of immune cells against abnormal host cells, can help to develop new weapons against cancer. The current knowledge allows us to suggest that the induction of ICD combined with other immunotherapeutic strategies, such as immune checkpoint blockade, can be explored to treat cancer. However, barriers such as the lack

of standardization of ICD detection in clinical patients, as well as the need for more personalized protocols based on the detailed characterization of the tumor cells, have to be overcome to translate experimental protocols into the clinic.

Funding: This work was funded by the Brazilian agencies FAP-DF/Brazil (00193.00001053/2021-24), CNPq (403536/2021-9) and Coordenação de Aperfeiçoamento de Pessoal de Nível Superior—Brasil (CAPES)—Finance Code 001.

Institutional Review Board Statement: Not applicable.

Informed Consent Statement: Not applicable.

Data Availability Statement: Not applicable.

Conflicts of Interest: The authors declare no conflict of interest.

References

1. Jiang, T.; Shi, T.; Zhang, H.; Hu, J.; Song, Y.; Wei, J.; Ren, S.; Zhou, C. Tumor neoantigens: From basic research to clinical applications. *J. Hematol. Oncol.* **2019**, *12*, 93. https://doi.org/10.1186/s13045-019-0787-5.
2. Yamamoto, T.N.; Kishton, R.J.; Restifo, N.P. Developing neoantigen-targeted T cell–based treatments for solid tumors. *Nat. Med.* **2019**, *25*, 1488–1499. https://doi.org/10.1038/s41591-019-0596-y.
3. Weinberg, R.A. *The Biology of Cancer*, 2nd ed.; Garland Science, Taylor & Francis Group, LLC: New York, NY, USA, 2013.
4. Hegde, P.S.; Chen, D.S. Top 10 Challenges in Cancer Immunotherapy. *Immunity* **2020**, *52*, 17–35. https://doi.org/10.1016/j.immuni.2019.12.011.
5. O'Donnell, J.S.; Teng, M.W.L.; Smyth, M.J. Cancer immunoediting and resistance to T cell-based immunotherapy. *Nat. Rev. Clin. Oncol.* **2019**, *16*, 151–167. https://doi.org/10.1038/s41571-018-0142-8.
6. Busch, W. Aus der Sitzung der medicinischen Section vom 13 November 1867. *Berl. Klin. Wochenschr.* **1868**, *5*, 137.
7. Fehleisen, F. *Die Aetiologie des Erysipels*; Theodor Fischer: Berlin, Germany, 1883.
8. Bruns, P. Die Heilwirkung des Erysipels auf Geschwülste. *Beitr Klin Chir*, 1887. Available online: https://books.google.com.br/books?id=0Gw1AQAAMAAJ&printsec=frontcover&source=gbs_ge_summary_r&cad=0#v=onepage&q&f=false (accessed on 5 May 2022).
9. Coley, W.B., II. Contribution to the Knowledge of Sarcoma. *Ann. Surg.* **1891**, *14*, 199–220. https://doi.org/10.1097/00000658-189112000-00015.
10. McCarthy, E.F. The toxins of William B. Coley and the treatment of bone and soft-tissue sarcomas. *Iowa Orthop. J.* **2006**, *26*, 154–158 Available online: https://www.ncbi.nlm.nih.gov/pmc/articles/PMC1888599/ (accessed on 6 May 2022).
11. Oiseth, S.J.; Aziz, M.S. Cancer immunotherapy: A brief review of the history, possibilities, and challenges ahead. *J. Cancer Metastasis Treat.* **2017**, *3*, 250. https://doi.org/10.20517/2394-4722.2017.41.
12. Codman, E. Symposium on the Treatment of Primary Malignant Bone Tumors: The Memorial Hospital Conference on the Treatment of Bone Sarcoma. *Am. J. Surg.* **1935**, *27*, 3–6. https://doi.org/10.1016/s0002-9610(35)90819-4.
13. Ehrlich, P. "Über den Jetzigen Stand der Karzinomforschung" Beiträge zur Experimentellen. Pathologie und Chemotherapie. 1909. Available online: https://curiosity.lib.harvard.edu/contagion/catalog/36-990061083080203941 (accessed on 5 May 2022).
14. Dunn, G.P.; Old, L.J.; Schreiber, R.D. The Immunobiology of Cancer Immunosurveillance and Immunoediting. *Immunity* **2004**, *21*, 137–148. https://doi.org/10.1016/j.immuni.2004.07.017.
15. Burnet, M. Cancer—A biological approach. I. The processes of control. *Br. Med. J.* **1957**, *1*, 779–786. https://doi.org/10.1136/bmj.1.5022.779.
16. Schreiber, R.D.; Old, L.J.; Smyth, M.J. Cancer Immunoediting: Integrating Immunity's Roles in Cancer Suppression and Promotion. *Science* **2011**, *331*, 1565–1570. https://doi.org/10.1126/science.1203486.
17. Pernot, S.; Terme, M.; Voron, T.; Colussi, O.; Marcheteau, E.; Tartour, E.; Taieb, J. Colorectal cancer and immunity: What we know and perspectives. *World J. Gastroenterol.* **2014**, *20*, 3738–3750.
18. Sanchez-Castañón, M.; Er, T.; Bujanda, L.; Herreros-Villanueva, M. Immunotherapy in colorectal cancer: What have we learned so far? *Clin. Chim. Acta* **2016**, *460*, 78–87.
19. Dobosz, P.; Dzieciątkowski, T. The Intriguing History of Cancer Immunotherapy. *Front. Immunol.* **2019**, *10*, 2965. https://doi.org/10.3389/fimmu.2019.02965.
20. Miller, J.F.A.P.; Mitchell, G.F.; Weiss, N.S. Cellular Basis of the Immunological Defects in Thymectomized Mice. *Nature* **1967**, *214*, 992–997.
21. Steinman, R.M.; Cohn, Z.A. Identification of a novel cell type in peripheral lymphoid organs of mice: I. morphology, quantitation, tissue distribution. *J. Exp. Med.* **1973**, *137*, 1142–1162. https://doi.org/10.1084/jem.137.5.1142.
22. Kiessling, R.; Klein, E.; Wigzell, H. "Natural" killer cells in the mouse. I. Cytotoxic cells with specificity for mouse Moloney leukemia cells. Specificity and distribution according to genotype. *Eur. J. Immunol.* **1975**, *5*, 112–117. https://doi.org/10.1002/eji.1830050208.
23. Yousefi, H.; Yuan, J.; Keshavarz-Fathi, M.; Murphy, J.F.; Rezaei, N. Immunotherapy of cancers comes of age. *Expert Rev. Clin. Immunol.* **2017**, *13*, 1001–1015. https://doi.org/10.1080/1744666x.2017.1366315.

24. Casares, N.; Pequignot, M.O.; Tesniere, A.; Ghiringhelli, F.; Roux, S.; Chaput, N.; Schmitt, E.; Hamai, A.; Hervas-Stubbs, S.; Obeid, M.; et al. Caspase-dependent immunogenicity of doxorubicin-induced tumor cell death. *J. Exp. Med.* **2005**, *202*, 1691–1701. https://doi.org/10.1084/jem.20050915.
25. Krombach, J.; Hennel, R.; Brix, N.; Orth, M.; Schoetz, U.; Ernst, A.; Schuster, J.; Zuchtriegel, G.; Reichel, C.A.; Bierschenk, S.; et al. Priming anti-tumor immunity by radiotherapy: Dying tumor cell-derived DAMPs trigger endothelial cell activation and recruitment of myeloid cells. *OncoImmunology* **2018**, *8*, e1523097. https://doi.org/10.1080/2162402x.2018.1523097.
26. Rodrigues, M.C.; Júnior, W.T.D.S.; Mundim, T.; Vale, C.L.C.; de Oliveira, J.V.; Ganassin, R.; Pacheco, T.J.A.; Morais, J.A.V.; Longo, J.P.F.; Azevedo, R.B.; et al. Induction of Immunogenic Cell Death by Photodynamic Therapy Mediated by Aluminum-Phthalocyanine in Nanoemulsion. *Pharmaceutics* **2022**, *14*, 196. https://doi.org/10.3390/pharmaceutics14010196.
27. Morais, J.A.V.; Almeida, L.R.; Rodrigues, M.C.; Azevedo, R.B.; Muehlmann, L.A. The induction of immunogenic cell death by photodynamic therapy in B16F10 cells in vitro is effected by the concentration of the photosensitizer. *Photodiagnosis Photodyn. Ther.* **2021**, *35*, 102392.
28. Galluzzi, L.; Vitale, I.; Aaronson, S.A.; Abrams, J.M.; Adam, D.; Agostinis, P.; Alnemri, E.S.; Altucci, L.; Amelio, I.; Andrews, D.W.; et al. Molecular mechanisms of cell death: Recommendations of the Nomenclature Committee on Cell Death 2018. *Cell Death Differ.* **2018**, *25*, 486–541. https://doi.org/10.1038/s41418-017-0012-4.
29. Galluzzi, L.; Vitale, I.; Warren, S.; Adjemian, S.; Agostinis, P.; Martinez, A.B.; Chan, T.A.; Coukos, G.; Demaria, S.; Deutsch, E.; et al. Consensus guidelines for the definition, detection and interpretation of immunogenic cell death. *J. Immunother. Cancer* **2020**, *8*, e000337. https://doi.org/10.1136/jitc-2019-000337.
30. Minton, K. DAMP-driven metabolic adaptation. *Nat. Rev. Immunol.* **2019**, *20*, 1. https://doi.org/10.1038/s41577-019-0258-9.
31. Collett, G.P.; Redman, C.W.; Sargent, I.L.; Vatish, M. Endoplasmic reticulum stress stimulates the release of extracellular vesicles carrying danger-associated molecular pattern (DAMP) molecules. *Oncotarget* **2018**, *9*, 6707–6717. https://doi.org/10.18632/oncotarget.24158.
32. Gong, T.; Liu, L.; Jiang, W.; Zhou, R. DAMP-sensing receptors in sterile inflammation and inflammatory diseases. *Nat. Rev. Immunol.* **2019**, *20*, 95–112. https://doi.org/10.1038/s41577-019-0215-7.
33. Serrano-del Valle, A.; Anel, A.; Naval, J.; Marzo, I. Immunogenic cell death and immunotherapy of multiple myeloma. *Front. Cell Dev. Biol.* **2019**, *7*, 50.
34. Kroemer, G.; Galassi, C.; Zitvogel, L.; Galluzzi, L. Immunogenic cell stress and death. *Nat. Immunol.* **2022**, *23*, 487–500. https://doi.org/10.1038/s41590-022-01132-2.
35. Baracco, E.E.; Stoll, G.; Van Endert, P.; Zitvogel, L.; Vacchelli, E.; Kroemer, G. Contribution of annexin A1 to anticancer immunosurveillance. *OncoImmunology* **2019**, *8*, e1647760. https://doi.org/10.1080/2162402x.2019.1647760.
36. Obeid, M.; Tesniere, A.; Ghiringhelli, F.; Fimia, G.M.; Apetoh, L.; Perfettini, J.-L.; Castedo, M.; Mignot, G.; Panaretakis, T.; Casares, N.; et al. Calreticulin exposure dictates the immunogenicity of cancer cell death. *Nat. Med.* **2006**, *13*, 54–61. https://doi.org/10.1038/nm1523.
37. Chattopadhyay, S.; Liu, Y.-H.; Fang, Z.-S.; Lin, C.-L.; Lin, J.-C.; Yao, B.-Y.; Hu, C.-M.J. Synthetic Immunogenic Cell Death Mediated by Intracellular Delivery of STING Agonist Nanoshells Enhances Anticancer Chemo-immunotherapy. *Nano Lett.* **2020**, *20*, 2246–2256. https://doi.org/10.1021/acs.nanolett.9b04094.
38. Jafari, S.; Lavasanifar, A.; Hejazi, M.S.; Maleki-Dizaji, N.; Mesgari, M.; Molavi, O. STAT3 inhibitory stattic enhances immunogenic cell death induced by chemotherapy in cancer cells. *DARU J. Pharm. Sci.* **2020**, *28*, 159–169. https://doi.org/10.1007/s40199-020-00326-z.
39. Vanmeerbeek, I.; Sprooten, J.; De Ruysscher, D.; Tejpar, S.; Vandenberghe, P.; Fucikova, J.; Spisek, R.; Zitvogel, L.; Kroemer, G.; Galluzzi, L.; et al. Trial watch: Chemotherapy-induced immunogenic cell death in immuno-oncology. *OncoImmunology* **2020**, *9*, 1703449. https://doi.org/10.1080/2162402x.2019.1703449.
40. Doix, B.; Trempolec, N.; Riant, O.; Feron, O. Low Photosensitizer Dose and Early Radiotherapy Enhance Antitumor Immune Response of Photodynamic Therapy-Based Dendritic Cell Vaccination. *Front. Oncol.* **2019**, *9*, 811. https://doi.org/10.3389/fonc.2019.00811.
41. Rapoport, B.L.; Anderson, R. Realizing the Clinical Potential of Immunogenic Cell Death in Cancer Chemotherapy and Radiotherapy. *Int. J. Mol. Sci.* **2019**, *20*, 959. https://doi.org/10.3390/ijms20040959.
42. Li, W.; Yang, J.; Luo, L.; Jiang, M.; Qin, B.; Yin, H.; Zhu, C.; Yuan, X.; Zhang, J.; Luo, Z.; et al. Targeting photodynamic and photothermal therapy to the endoplasmic reticulum enhances immunogenic cancer cell death. *Nat. Commun.* **2019**, *10*, 3349. https://doi.org/10.1038/s41467-019-11269-8.
43. Turubanova, V.D.; Balalaeva, I.V.; Mishchenko, T.A.; Catanzaro, E.; Alzeibak, R.; Peskova, N.N.; Efimova, I.; Bachert, C.; Mitroshina, E.V.; Krysko, O.; et al. Immunogenic cell death induced by a new photodynamic therapy based on photosens and photodithazine. *J. Immunother. Cancer* **2019**, *7*, 350. https://doi.org/10.1186/s40425-019-0826-3.
44. He, H.; Liu, L.; Liang, R.; Zhou, H.; Pan, H.; Zhang, S.; Cai, L. Tumor-targeted nanoplatform for in situ oxygenation-boosted immunogenic phototherapy of colorectal cancer. *Acta Biomater.* **2020**, *104*, 188–197. https://doi.org/10.1016/j.actbio.2020.01.012.
45. Deng, H.; Zhou, Z.; Yang, W.; Lin, L.-S.; Wang, S.; Niu, G.; Song, J.; Chen, X. Endoplasmic Reticulum Targeting to Amplify Immunogenic Cell Death for Cancer Immunotherapy. *Nano Lett.* **2020**, *20*, 1928–1933. https://doi.org/10.1021/acs.nanolett.9b05210.

46. Ganassin, R.; Oliveira, G.R.T.; da Rocha, M.C.O.; Morais, J.A.V.; Rodrigues, M.C.; Motta, F.N.; Azevedo, R.B.; Muehlmann, L.A. Curcumin induces immunogenic cell death in murine colorectal carcinoma CT26 cells. *Pharmacol. Res.-Mod. Chin. Med.* **2022**, *2*, 100046. https://doi.org/10.1016/j.prmcm.2022.100046.
47. Dulloo, I.; Atakpa-Adaji, P.; Yeh, Y.-C.; Levet, C.; Muliyil, S.; Lu, F.; Taylor, C.W.; Freeman, M. iRhom pseudoproteases regulate ER stress-induced cell death through IP3 receptors and BCL-2. *Nat. Commun.* **2022**, *13*, 1257. https://doi.org/10.1038/s41467-022-28930-4.
48. Iurlaro, R.; Muñoz-Pinedo, C. Cell death induced by endoplasmic reticulum stress. *FEBS J.* **2015**, *283*, 2640–2652. https://doi.org/10.1111/febs.13598.
49. Acosta-Alvear, D.; Zhou, Y.; Blais, A.; Tsikitis, M.; Lents, N.H.; Arias, C.; Lennon, C.J.; Kluger, Y.; Dynlacht, B.D. XBP1 Controls Diverse Cell Type- and Condition-Specific Transcriptional Regulatory Networks. *Mol. Cell* **2007**, *27*, 53–66. https://doi.org/10.1016/j.molcel.2007.06.011.
50. Wang, Q.; Sun, A.-Z.; Chen, S.-T.; Chen, L.-S.; Guo, F.-Q. SPL6 represses signalling outputs of ER stress in control of panicle cell death in rice. *Nat. Plants* **2018**, *4*, 280–288. https://doi.org/10.1038/s41477-018-0131-z.
51. Shibusawa, R.; Yamada, E.; Okada, S.; Nakajima, Y.; Bastie, C.C.; Maeshima, A.; Kaira, K.; Yamada, M. Dapagliflozin rescues endoplasmic reticulum stress-mediated cell death. *Sci. Rep.* **2019**, *9*, 9887. https://doi.org/10.1038/s41598-019-46402-6.
52. Bezu, L.; Sauvat, A.; Humeau, J.; Leduc, M.; Kepp, O.; Kroemer, G. eIF2α phosphorylation: A hallmark of immunogenic cell death. *OncoImmunology* **2018**, *7*, e1431089. https://doi.org/10.1080/2162402x.2018.1431089.
53. Anspach, L.; Tsaryk, R.; Seidmann, L.; Unger, R.E.; Jayasinghe, C.; Simiantonaki, N.; Kirkpatrick, C.J.; Pröls, F. Function and mutual interaction of BiP-, PERK-, and IRE1α-dependent signalling pathways in vascular tumours. *J. Pathol.* **2020**, *251*, 123–134.
54. Yoshida, H.; Okada, T.; Haze, K.; Yanagi, H.; Yura, T.; Negishi, M.; Mori, K. ATF6 Activated by Proteolysis Binds in the Presence of NF-Y (CBF) Directly to the *cis* -Acting Element Responsible for the Mammalian Unfolded Protein Response. *Mol. Cell. Biol.* **2000**, *20*, 6755–6767. https://doi.org/10.1128/mcb.20.18.6755-6767.2000.
55. Rozpedek, W.; Pytel, D.; Mucha, B.; Leszczynska, H.; Diehl, J.A.; Majsterek, I. The Role of the PERK/eIF2α/ATF4/CHOP Signaling Pathway in Tumor Progression During Endoplasmic Reticulum Stress. *Curr. Mol. Med.* **2016**, *16*, 533–544.
56. Klymenko, O.; Huehn, M.; Wilhelm, J.; Wasnick, R.; Shalashova, I.; Ruppert, C.; Henneke, I.; Hezel, S.; Guenther, K.; Mahavadi, P.; et al. Regulation and role of the ER stress transcription factor CHOP in alveolar epithelial type-II cells. *Klin. Wochenschr.* **2019**, *97*, 973–990. https://doi.org/10.1007/s00109-019-01787-9.
57. Yang, H.; Niemeijer, M.; van de Water, B.; Beltman, J.B. ATF6 Is a Critical Determinant of CHOP Dynamics during the Unfolded Protein Response. *iScience* **2020**, *23*, 100860. https://doi.org/10.1016/j.isci.2020.100860.
58. Sheng, X.; Nenseth, H.Z.; Qu, S.; Kuzu, O.F.; Frahnow, T.; Simon, L.; Greene, S.; Zeng, Q.; Fazli, L.; Rennie, P.S.; et al. IRE1α-XBP1s pathway promotes prostate cancer by activating c-MYC signaling. *Nat. Commun.* **2019**, *10*, 323. https://doi.org/10.1038/s41467-018-08152-3.
59. Zhou, W.; Fang, H.; Wu, Q.; Wang, X.; Liu, R.; Li, F.; Xiao, J.; Yuan, L.; Zhou, Z.; Ma, J.; et al. Ilamycin E, a natural product of marine actinomycete, inhibits triple-negative breast cancer partially through ER stress-CHOP-Bcl-2. *Int. J. Biol. Sci.* **2019**, *15*, 1723–1732. https://doi.org/10.7150/ijbs.35284.
60. Singh, R.; Letai, A.; Sarosiek, K. Regulation of apoptosis in health and disease: The balancing act of BCL-2 family proteins. *Nat. Rev. Mol. Cell Biol.* **2019**, *20*, 175–193. https://doi.org/10.1038/s41580-018-0089-8.
61. Cubillos-Ruiz, J.R.; Bettigole, S.E.; Glimcher, L.H. Tumorigenic and Immunosuppressive Effects of Endoplasmic Reticulum Stress in Cancer. *Cell* **2017**, *168*, 692–706.
62. Wang, Q.; Ju, X.; Wang, J.; Fan, Y.; Ren, M.; Zhang, H. Immunogenic cell death in anticancer chemotherapy and its impact on clinical studies. *Cancer Lett.* **2018**, *438*, 17–23. https://doi.org/10.1016/j.canlet.2018.08.028.
63. Coleman, L.G.; Maile, R.; Jones, S.W.; Cairns, B.A.; Crews, F.T. HMGB1/IL-1β complexes in plasma microvesicles modulate immune responses to burn injury. *PLoS ONE* **2018**, *13*, e0195335.
64. Mishchenko, T.; Mitroshina, E.; Balalaeva, I.; Krysko, O.; Vedunova, M.; Krysko, D.V. An emerging role for nanomaterials in increasing immunogenicity of cancer cell death. *Biochim. Biophys. Acta* **2019**, *1871*, 99–108. https://doi.org/10.1016/j.bbcan.2018.11.004.
65. Michalak, M.; Groenendyk, J.; Szabo, E.; Gold, L.I.; Opas, M. Calreticulin, a multi-process calcium-buffering chaperone of the endoplasmic reticulum. *Biochem. J.* **2009**, *417*, 651–666. https://doi.org/10.1042/bj20081847.
66. Spiro, R.G.; Zhu, Q.; Bhoyroo, V.; Söling, H.-D. Definition of the Lectin-like Properties of the Molecular Chaperone, Calreticulin, and Demonstration of Its Copurification with Endomannosidase from Rat Liver Golgi. *J. Biol. Chem.* **1996**, *271*, 11588–11594. https://doi.org/10.1074/jbc.271.19.11588.
67. Ahmed, A.; Tait, S.W. Targeting immunogenic cell death in cancer. *Mol. Oncol.* **2020**, *14*, 2994–3006. https://doi.org/10.1002/1878-0261.12851.
68. Schcolnik-Cabrera, A.; Oldak, B.; Juárez, M.; Cruz-Rivera, M.; Flisser, A.; Mendlovic, F. Calreticulin in phagocytosis and cancer: Opposite roles in immune response outcomes. *Apoptosis* **2019**, *24*, 245–255. https://doi.org/10.1007/s10495-019-01532-0.
69. Calvet, C.Y.; Famin, D.; André, F.M.; Mir, L.M. Electrochemotherapy with bleomycin induces hallmarks of immunogenic cell death in murine colon cancer cells. *OncoImmunology* **2014**, *3*, e28131. https://doi.org/10.4161/onci.28131.
70. Pitt, J.M.; Kroemer, G.; Zitvogel, L. Immunogenic and Non-immunogenic Cell Death in the Tumor Microenvironment. *Adv. Exp. Med. Biol.* **2017**, *1036*, 65–79. https://doi.org/10.1007/978-3-319-67577-0_5.

71. Sistigu, A.; Yamazaki, T.; Vacchelli, E.; Chaba, K.; Enot, D.P.; Adam, J.; Vitale, I.; Goubar, A.; Baracco, E.E.; Remédios, C.; et al. Cancer cell–autonomous contribution of type I interferon signaling to the efficacy of chemotherapy. *Nat. Med.* **2014**, *20*, 1301–1309. https://doi.org/10.1038/nm.3708.
72. MacKenzie, K.J.; Carroll, P.; Martin, C.-A.; Murina, O.; Fluteau, A.; Simpson, D.J.; Olova, N.; Sutcliffe, H.; Rainger, J.K.; Leitch, A.; et al. cGAS surveillance of micronuclei links genome instability to innate immunity. *Nature* **2017**, *548*, 461–465. https://doi.org/10.1038/nature23449.
73. Kumar, A.; Khani, A.T.; Swaminathan, S. Type I interferons: One stone to concurrently kill two birds, viral infections and cancers. *Curr. Res. Virol. Sci.* **2021**, *2*, 100014. https://doi.org/10.1016/j.crviro.2021.100014.
74. Bruschi, M.; Petretto, A.; Vaglio, A.; Santucci, L.; Candiano, G.; Ghiggeri, G.M. Annexin A1 and Autoimmunity: From Basic Science to Clinical Applications. *Int. J. Mol. Sci.* **2018**, *19*, 1348. https://doi.org/10.3390/ijms19051348.
75. Gavins, F.N.E.; Hickey, M.J. Annexin A1 and the regulation of innate and adaptive immunity. *Front. Immunol.* **2012**, *3*, 354. https://doi.org/10.3389/fimmu.2012.00354.
76. Hernández, I.B.B.; Angelier, M.L.; D'Ondes, T.D.B.D.B.; Di Di Maggio, A.; Yu, Y.; Oliveira, S. The Potential of Nanobody-Targeted Photodynamic Therapy to Trigger Immune Responses. *Cancers* **2020**, *12*, 978. https://doi.org/10.3390/cancers12040978.
77. Tripathi, D.; Tanaka, K. A crosstalk between extracellular ATP and jasmonate signaling pathways for plant defense. *Plant Signal. Behav.* **2018**, *13*, e1432229. https://doi.org/10.1080/15592324.2018.1432229.
78. Rodríguez-Nuevo, A.; Zorzano, A. The sensing of mitochondrial DAMPs by non-immune cells. *Cell Stress* **2019**, *3*, 195–207. https://doi.org/10.15698/cst2019.06.190.
79. Martins, I.; Wang, Y.; Michaud, M.; Ma, Y.; Sukkurwala, A.Q.; Shen, S.; Kepp, O.; Metivier, D.; Galluzzi, L.; Perfettini, J.-L.; et al. Molecular mechanisms of ATP secretion during immunogenic cell death. *Cell Death Differ.* **2013**, *21*, 79–91. https://doi.org/10.1038/cdd.2013.75.
80. Di Virgilio, F.; Sarti, A.C.; Falzoni, S.; De Marchi, E.; Adinolfi, E. Extracellular ATP and P2 purinergic signalling in the tumour microenvironment. *Nat. Rev. Cancer* **2018**, *18*, 601–618.
81. Deng, Z.; He, Z.; Maksaev, G.; Bitter, R.M.; Rau, M.; Fitzpatrick, J.A.J.; Yuan, P. Cryo-EM structures of the ATP release channel pannexin 1. *Nat. Struct. Mol. Biol.* **2020**, *27*, 373–381. https://doi.org/10.1038/s41594-020-0401-0.
82. Redza-Dutordoir, M.; Averill-Bates, D.A. Activation of apoptosis signalling pathways by reactive oxygen species. *Biochim. Biophys. Acta-Mol. Cell Res.* **2016**, *1863*, 2977–2992. https://doi.org/10.1016/j.bbamcr.2016.09.012.
83. Borges Da Silva, H.; Beura, L.K.; Wang, H.; Hanse, E.A.; Gore, R.; Scott, M.C.; Walsh, D.A.; Block, K.E.; Fonseca, R.; Yan, Y.; et al. The purinergic receptor P2RX7 directs metabolic fitness of long-lived memory CD8+ T cells. *Nature* **2018**, *559*, 264–268.
84. Amores-Iniesta, J.; Barberà-Cremades, M.; Martínez, C.M.; Pons, J.A.; Revilla-Nuin, B.; Martínez-Alarcón, L.; Di Virgilio, F.; Parrilla, P.; Baroja-Mazo, A.; Pelegrín, P. Extracellular ATP Activates the NLRP3 Inflammasome and Is an Early Danger Signal of Skin Allograft Rejection. *Cell Rep.* **2017**, *21*, 3414–3426. https://doi.org/10.1016/j.celrep.2017.11.079.
85. Andersson, U.; Yang, H.; Harris, H. High-mobility group box 1 protein (HMGB1) operates as an alarmin outside as well as inside cells. In *Seminars in Immunology*; Academic Press: New York, NY, USA, 2018.
86. Tanaka, M.; Kataoka, H.; Yano, S.; Sawada, T.; Akashi, H.; Inoue, M.; Suzuki, S.; Inagaki, Y.; Hayashi, N.; Nishie, H.; et al. Immunogenic cell death due to a new photodynamic therapy (PDT) with glycoconjugated chlorin (G-chlorin). *Oncotarget* **2016**, *7*, 47242–47251. https://doi.org/10.18632/oncotarget.9725.
87. Wang, Y.-J.; Fletcher, R.; Yu, J.; Zhang, L. Immunogenic effects of chemotherapy-induced tumor cell death. *Gene Funct. Dis.* **2018**, *5*, 194–203. https://doi.org/10.1016/j.gendis.2018.05.003.
88. Liu, P.; Zhao, L.; Loos, F.; Iribarren, K.; Lachkar, S.; Zhou, H.; da Silva, L.C.G.; Chen, G.; Bezu, L.; Boncompain, G.; et al. Identification of pharmacological agents that induce HMGB1 release. *Sci. Rep.* **2017**, *7*, 14915. https://doi.org/10.1038/s41598-017-14848-1.
89. Rufo, N.; Garg, A.; Agostinis, P. The Unfolded Protein Response in Immunogenic Cell Death and Cancer Immunotherapy. *Trends Cancer* **2017**, *3*, 643–658. https://doi.org/10.1016/j.trecan.2017.07.002.
90. Jin, Y.; Guan, Z.; Wang, X.; Wang, Z.; Zeng, R.; Xu, L.; Cao, P. ALA-PDT promotes HPV-positive cervical cancer cells apoptosis and DCs maturation via miR-34a regulated HMGB1 exosomes secretion. *Photodiagnosis Photodyn. Ther.* **2018**, *24*, 27–35. https://doi.org/10.1016/j.pdpdt.2018.08.006.
91. Antón, M.; Alén, F.; Gómez de Heras, R.; Serrano, A.; Pavón, F.J.; Leza, J.C.; García-Bueno, B.; Rodríguez de Fonseca, F.; Orio, L. Oleoylethanolamide prevents neuroimmune HMGB1/TLR4/NF-kB danger signaling in rat frontal cortex and depressive-like behavior induced by ethanol binge administration. *Addict. Biol.* **2017**, *22*, 724–741.
92. Radogna, F.; Dicato, M.; Diederich, M. Natural modulators of the hallmarks of immunogenic cell death. *Biochem. Pharmacol.* **2019**, *162*, 55–70. https://doi.org/10.1016/j.bcp.2018.12.016.
93. Nastasi, C.; Mannarino, L.; D'Incalci, M. DNA Damage Response and Immune Defense. *Int. J. Mol. Sci.* **2020**, *21*, 7504. https://doi.org/10.3390/ijms21207504.
94. Venereau, E.; Casalgrandi, M.; Schiraldi, M.; Antoine, D.J.; Cattaneo, A.; De Marchis, F.; Liu, J.; Antonelli, A.; Preti, A.; Raeli, L.; et al. Mutually exclusive redox forms of HMGB1 promote cell recruitment or proinflammatory cytokine release. *J. Gen. Physiol.* **2012**, *140*, i6. https://doi.org/10.1085/jgp1404oia6.
95. Preissner, K.T.; Fischer, S.; Deindl, E. Extracellular RNA as a Versatile DAMP and Alarm Signal That Influences Leukocyte Recruitment in Inflammation and Infection. *Front. Cell Dev. Biol.* **2020**, *8*, 619221. https://doi.org/10.3389/fcell.2020.619221.

96. Wang, Y.; Ma, X.; Su, C.; Peng, B.; Du, J.; Jia, H.; Luo, M.; Fang, C.; Wei, Y. Uric acid enhances the antitumor immunity of dendritic cell-based vaccine. *Sci. Rep.* **2015**, *5*, 16427. https://doi.org/10.1038/srep16427.
97. Voorwerk, L.; Slagter, M.; Horlings, H.M.; Sikorska, K.; Van De Vijver, K.K.; De Maaker, M.; Nederlof, I.; Kluin, R.J.C.; Warren, S.; Ong, S.; et al. Immune induction strategies in metastatic triple-negative breast cancer to enhance the sensitivity to PD-1 blockade: The TONIC trial. *Nat. Med.* **2019**, *25*, 920–928. https://doi.org/10.1038/s41591-019-0432-4.
98. Bota, D.A.; Chung, J.; Dandekar, M.; Carrillo, J.A.; Kong, X.-T.; Fu, B.D.; Hsu, F.P.; Schönthal, A.H.; Hofman, F.M.; Chen, T.C.; et al. Phase II study of ERC1671 plus bevacizumab versus bevacizumab plus placebo in recurrent glioblastoma: Interim results and correlations with $CD4^+$ T-lymphocyte counts. *CNS Oncol.* **2018**, *7*, CNS22. https://doi.org/10.2217/cns-2018-0009.
99. Le, D.T.; Jaffee, E.M. Regulatory T-cell Modulation Using Cyclophosphamide in Vaccine Approaches: A Current Perspective. *Cancer Res.* **2012**, *72*, 3439–3444. https://doi.org/10.1158/0008-5472.can-11-3912.
100. Vaes, R.; Hendriks, L.; Vooijs, M.; De Ruysscher, D. Biomarkers of Radiotherapy-Induced Immunogenic Cell Death. *Cells* **2021**, *10*, 930. https://doi.org/10.3390/cells10040930.
101. Lämmer, F.; Delbridge, C.; Würstle, S.; Neff, F.; Meyer, B.; Schlegel, J.; Kessel, K.A.; Schmid, T.E.; Schilling, D.; Combs, S.E. Cytosolic Hsp70 as a biomarker to predict clinical outcome in patients with glioblastoma. *PLoS ONE* **2019**, *14*, e0221502. https://doi.org/10.1371/journal.pone.0221502.
102. Rothammer, A.; Sage, E.K.; Werner, C.; Combs, S.E.; Multhoff, G. Increased heat shock protein 70 (Hsp70) serum levels and low NK cell counts after radiotherapy—Potential markers for predicting breast cancer recurrence? *Radiat. Oncol.* **2019**, *14*, 78 https://doi.org/10.1186/s13014-019-1286-0.
103. Hongo, K.; Kazama, S.; Tsuno, N.H.; Ishihara, S.; Sunami, E.; Kitayama, J.; Watanabe, T. Immunohistochemical detection of high-mobility group box 1 correlates with resistance of preoperative chemoradiotherapy for lower rectal cancer: A retrospective study. *World J. Surg. Oncol.* **2015**, *13*, 7. https://doi.org/10.1186/1477-7819-13-7.
104. Huang, C.-Y.; Chiang, S.-F.; Ke, T.-W.; Chen, T.-W.; Lan, Y.-C.; You, Y.-S.; Shiau, A.-C.; Chen, W.T.-L.; Chao, K.S.C. Cytosolic high-mobility group box protein 1 (HMGB1) and/or PD-1+ TILs in the tumor microenvironment may be contributing prognostic biomarkers for patients with locally advanced rectal cancer who have undergone neoadjuvant chemoradiotherapy. *Cancer Immunol. Immunother.* **2018**, *67*, 551–562. https://doi.org/10.1007/s00262-017-2109-5.
105. Muehlmann, L.; Ma, B.; Longo, J.P.; Santos, M.; Azevedo, R. Aluminum–phthalocyanine chloride associated to poly(methyl vinyl ether-co-maleic anhydride) nanoparticles as a new third-generation photosensitizer for anticancer photodynamic therapy. *Int. J. Nanomed.* **2014**, *9*, 1199–1213. https://doi.org/10.2147/ijn.s57420.
106. Garg, A.D.; Agostinis, P. ER stress, autophagy and immunogenic cell death in photodynamic therapy-induced anti-cancer immune responses. *Photochem. Photobiol. Sci.* **2014**, *13*, 474–487. https://doi.org/10.1039/c3pp50333j.
107. Fucikova, J.; Kepp, O.; Kasikova, L.; Petroni, G.; Yamazaki, T.; Liu, P.; Zhao, L.; Spisek, R.; Kroemer, G.; Galluzzi, L. Detection of immunogenic cell death and its relevance for cancer therapy. *Cell Death Dis.* **2020**, *11*, 1013. https://doi.org/10.1038/s41419-020-03221-2.
108. Sun, Y.; Feng, X.; Wan, C.; Lovell, J.F.; Jin, H.; Ding, J. Role of nanoparticle-mediated immunogenic cell death in cancer immunotherapy. *Asian J. Pharm. Sci.* **2020**, *16*, 129–132. https://doi.org/10.1016/j.ajps.2020.05.004.
109. Longo, J.P.F.; Muehlmann, L.A. Nanomedicine beyond tumor passive targeting: What next? *Nanomedicine* **2020**, *15*, 1819–1822. https://doi.org/10.2217/nnm-2020-0208.

CAPÍTULO 3: Direct and Abscopal Antitumor Responses Elicited by ALPCNE-Mediated PDT in a Murine Melanoma Model

ABSTRACT

Melanoma, the most aggressive form of skin cancer, presents a major clinical challenge due to tendency to metastasize and the recalcitrance to traditional therapies. Despite advances in surgery, chemotherapy, and radiotherapy, the outlook for advanced melanoma remains bleak, reinforcing the urgent need for more effective treatments. Photodynamic therapy (PDT) has emerged as a promising alternative, leading to targeted tumor destruction with minimal harm to surrounding tissues. In this study, the direct and abscopal antitumor effects of PDT in a bilateral murine melanoma model were evaluated. Although only one of the two tumors was treated, effects were observed in both. Our findings revealed significant changes in systemic inflammation and alterations in $CD4^+$ and $CD8^+$ T cell populations in treated groups, as evidenced by blood analyses and flow cytometry. High-throughput RNA sequencing (RNA-seq) further unveiled shifts in gene expression profiles in both treated and untreated tumors. This research sheds light on the novel antitumor and abscopal effects of AlPcNE-mediated PDT in melanoma, highlighting the potential of different PDT protocols to modulate immune responses and to achieve more effective and targeted cancer treatments.

KEYWORDS: photodynamic therapy; melanoma; immune system modulation; RNAseq.

1. INTRODUCTION

Melanoma, a highly aggressive form of skin cancer, represents a significant clinical challenge due to the high metastatic potential and recalcitrance to conventional treatments[1,2]. Despite advancements in surgical techniques, chemotherapy, and radiotherapy, the prognosis for advanced melanoma remains poor[1–4]. This fact spurs an intense search for novel therapeutic approaches that can more effectively combat this disease. Immunotherapy has emerged as a promising strategy, leveraging the immune system to target and eliminate tumor cells[3–5]. However, not all patients respond to it, and the efficacy of immunotherapy alone is often limited by the immunosuppressive tumor microenvironment and by the heterogeneous nature of melanoma, highlighting the need for complementary therapeutic strategies[3].

Photodynamic therapy (PDT) draws the attention as an alternative, particularly for localized treatment with minimal damage the surrounding healthy tissues[6]. PDT involves the generation of reactive oxygen species (ROS) following the activation of a photosensitizer by a specific light wavelength, leading to the direct cytotoxicity through apoptosis, necrosis, vascular damage, and the induction of an antitumor immune response via immunomodulatory mechanisms[7]. The ability of PDT to target primary tumors and to induce systemic antitumor immunity capable of addressing secondary tumors or metastases is a critical aspect of the therapeutic potential and gains prominence in various studies[8].

Despite its potential, the antitumor efficacy and induction of a robust immune response by PDT can be influenced by several factors, including the chemical nature and amount of photosensitizer, the light dose, and the treatment regimen[9–11]. In this context, chloride aluminum-phthalocyanine (AlPc) and its nanoemulsified form, AlPcNE, have emerged as potent photosensitizers for PDT. AlPcNE, in particular, presents high activity in aqueous media, making it a promising candidate for more effective PDT applications[12–14]. PDT mediated by AlPcNE has demonstrated efficacy against several types of tumors in preclinical studies[15–17] and also against bacteria[18] and fungi[19]. However, the antitumor potential in the treatment of melanoma and a possible effect in the activation of the immune system remains to be investigated.

This study assessed the antitumor efficacy and the immune-modulating effects of AlPcNE-mediated PDT in a murine model of melanoma (B16F10). The direct effects on treated tumors and the systemic, abscopal effects on distant, untreated tumors, immune cells modulation and gene expression profiles were investigated.

We aimed to gain insights into the interplay between PDT and the immune system, which could contribute to more effective and targeted melanoma treatments and improved outcomes for patients battling this kind of cancer.

2. MATERIALS AND METHOD

2.1. Cell culture

The murine melanoma cell line B16F10 was purchased from the Rio de Janeiro Cell Bank (BCRJ, Brazil). Cells were cultured in Dulbecco's Modified Eagle Medium containing 10% fetal bovine serum and 1% penicillin/streptomycin at 37 °C in a 5% CO_2 atmosphere.

2.2. Animals

All experiments involving mice were approved by the Animal Ethics Committee from the University of Brasilia (UnBDOC n◦ 46/2019) (ANNEX 1). Female, 18 ± 2 g, 6- to 8-week-old C57Bl/6 mice (Faculty of Medicine - Federal University of Goiás, Goiania, GO, Brazil) were maintained in a temperature-controlled environment with 12-h light–dark cycles and received food and water *ad libitum*.

2.3. Tumor model

To assess the direct and abscopal PDT effects, a bilateral tumor model was used. Mice were injected s.c. with 5×10^5 B16F10 cells in the right flank (primary tumor). Two days later, 2×10^5 tumor cells were implanted in the left flank (secondary tumor). Tumor size was monitored by caliper measurement every two days. Tumor volume was calculated as follows: tumor volume (mm^3) = width (mm)×width (mm)×length (mm)/2.

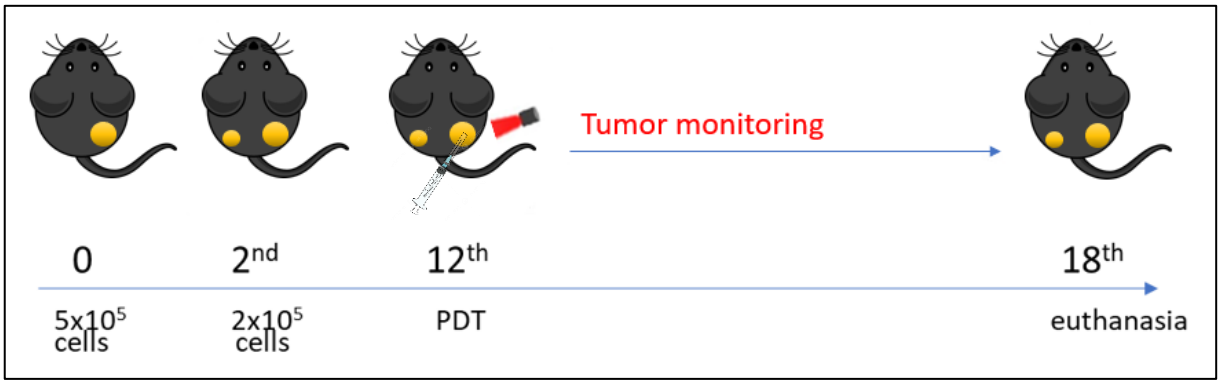

Figure 1. Treatment scheme for AlPcNE-mediated PDT in the mice animal model.

2.4. Photodynamic therapy Protocols

The AlPcNE was produced by spontaneous emulsification following the Muehlmann et al. (2015)[12] protocol. A light-emitting diode (LED) array-based illumination system, kindly provided by Prof. Paulo Eduardo Narcizo de Souza, was used to irradiate the animals. Mice were randomly assigned to be treated only on the primary tumor with either: PBS, 1) low energy density [25 J/cm²] with low AlPcNE concentration [10 nM] (LL_LPS); 2) low energy density [25 J/cm²] with high concentration of AlPcNE [40 nM] (LL_HPS); 3) high energy density [112 J/cm²] with low AlPcNE concentration [10 nM] (HL_LPS); and 4) high energy density [112 J/cm²] with high concentration of AlPcNE [40 nM] (HL_HPS). As control, mice were intratumor injected with PBS on day 12. For the PDT treatment, mice were intratumor injected with different AlPcNE concentrations on day 12. At 30 min post-injection in the right tumors, these were LED-irradiated. Mice were euthanized on day 18.

2.5. Hematological parameters analysis

On the day of euthanasia, the animals were anesthetized by 120 mg/kg ketamine and 16 mg/kg xylazine. Blood samples were then collected by cardiac puncture in EDTA Vacutte® microtubes after. The hematological parameters number of WBC (white blood cells), RBC (red blood cells), HGB (hemoglobin), HCT (hematocrit), PLT (platelets), MCV (mean corpuscular volume), MCH (mean corpuscular hemoglobin), and MCHC (mean corpuscular hemoglobin concentration) were evaluated by the automated hematology counter for veterinary use Horiba ABX Micros ESV 60 (São Paulo, Brazil).

2.6. Histology Analysis

On day 18, mice were euthanized and dissected to collect the irradiated and nonirradiated tumors. All tissues were fixed in 10% formalin for 24 h, and subsequently transferred to 70, 80, 90 and 100% ethanol. The material was subjected to three paraffin baths in an oven at 58 °C and included in paraffin blocks. Histological sections of 3 to 4 μm thick were fixed on glass slides for microscopy, and samples were stained in hematoxylin and eosin (HE).

2.7. Flow cytometry analysis

The single-cell suspension of mice splenocytes was prepared by mechanical digestion followed by filtering through a 40-mm cell strainer (SPL Life Sciences, Pocheon, Korea). Cells samples were resuspended in erythrolysis buffer for 10 min, washed with PBS, centrifuged, and counted. Cells were transferred to polypropylene tubes in 100 μl PBS $^{+}$ 2% FBS for labeling for 1 hour on ice, protected from light, with the Invitrogen APC anti-mouse CD3ε, PE/Cyanine7 anti-mouse CD4 and PE anti-mouse CD8b antibodies. The FITC anti-mouse CD45 and PerCP Cy5.5 anti-mouse CD45RA antibodies were used for activated T cells Panel 1. The FITC anti-mouse CD25 and PerCP Cy5.5 anti-mouse CD62L antibodies were used for regulatory T cells panel 2. After additional washes with PBS containing 2% FBS, the cells were resuspended, acquired by FACSVerse (BD Biosciences, San Jose, California, USA) and analyzed by FlowJo software X (BD Biosciences). Cells labeled with individual antibodies were used for compensation.

2.8. Gene Expression Evaluation

The total RNA was isolated from the frozen homogenized independent samples of melanoma primary and secondary allografts ($n = 3$ per group) using the RNeasy Mini kit (Qiagen, Hilden, Germany), according to the manufacturer instructions. Samples were quantified by the RNA-specific fluorimetric method using the Qubit™ RNA High Sensitivity kit (Invitrogen™), following the manufacturer's recommendations. Sequencing was carried out by the company GenOne Biotech using the Illumina platform (Illumina, Inc., CA, USA). According to the company's requirements, only samples with pure (OD 260/280>2.0) and intact

(with RIN>6.3) total RNA were sent for sequencing. Samples should consist of at least 2 ug of lyophilized RNA.

2.9. Statistical analysis

All the statistical differences were recorded using GraphPad Prism version 6.01 for Windows (California, USA). Statistical analyses were assessed by one-way or two-way ANOVA tests, with post-hoc Tukey's multiple comparisons tests. Values are presented as mean ± standard error of the mean. Significance was set at $p < 0.05$.

3. RESULTS AND DISCUSSION

3.1. The PDT Protocols, Except LL_LPS, Reduced the Growth of the Irradiated Tumor

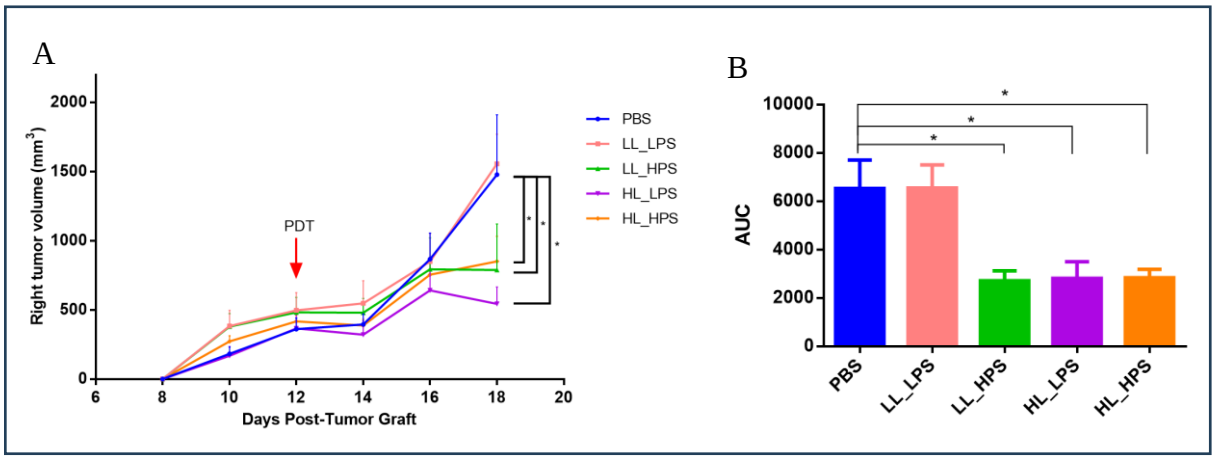

*Figure 2. Direct effect of PDT in primary site tumors. Primary subcutaneous B16F10 tumor bearing mice were treated with four different PDT protocols: low LED with low PS (LL_LPS) laser irradiation at 25 J/cm2 and AlPcNE (10 nM); low LED with high PS (LL_HPS), laser irradiation at 25 J/cm2 and AlPcNE (40 nM); high LED with low PS (HL_LPS), laser irradiation at 112 J/cm2 and AlPcNE (10 nM); and high LED with high PS (HL_HPS), laser irradiation at 112 J/cm2 and AlPcNE (40 nM). (A) Tumor volumes (mm³) for irradiated and PBS right tumors are shown. (B) Area under curve (AUC, mm³.day) analysis on day 18 post-tumor engraftment. Data are mean ± standard deviation. Statistical significance of the tumor volume was determined using a two-way ANOVA, followed by a Tukey's multiple comparisons test (n = 5, *p < 0.01).*

To verify the *in situ* effect of AlPcNE-PDT on melanoma grafts, four different PDT protocols were applied. As shown in Figure 2A-B, in a bilateral B16F10 model AlPcNE-PDT was administered locally only to the primary tumor, which was monitored for 18 days.

The LL_HPS, HL_LPS, and HL_HPS protocols significantly reduced the primary site tumors growth. In contrast, no direct effect was observed with the LL_LPS protocol, as the tumors continued to grow similarly to the control group. This can be due to the lower oxidation of cell components in the tumors treated with the LL_LPS protocol, as it involved lower concentrations of both AlPcNE and light energy.

3.2. Histological analyses of the primary site tumors

Typical features of melanoma tissue were verified in all the samples. Notably, atypical cells were present, characterized by pleomorphic nuclei. Areas of multifocal necrosis were evident, displaying regions of cellular death and nuclear depletion, indicative of an aggressive and rapidly proliferating tumor microenvironment. Additionally, the analysis confirmed the

presence of pigment characteristic of melanoma cells, reasserting the melanocytic origin of the tumor. Importantly, tumors in the PBS group exhibited a higher frequency of cells in mitosis compared to the treated groups, suggesting increased cellular proliferation.

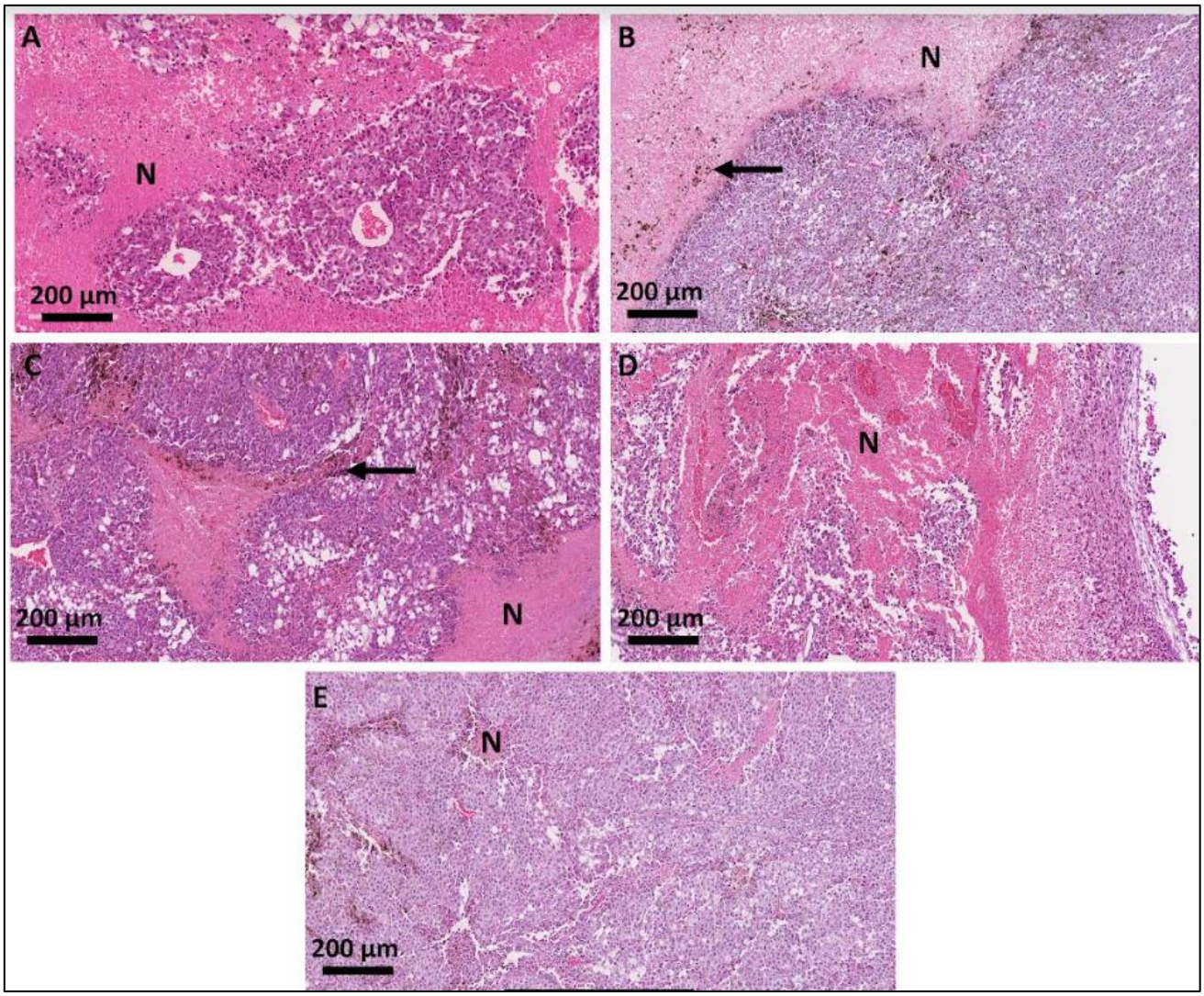

Figure 3. Photomicrographies of histopathological sections of the mice primary site tumors (A) PBS; (B) LL_LPS; (C) LL_HPS; (D) HL_LPS; (E) HL_HPS groups. N represents necrosis areas. Scale bar - 200 µm. Stained using H&E (hematoxylin and eosin).

3.3. The growth of the non-treated tumors of HL_HPS group is significantly reduced after PDT

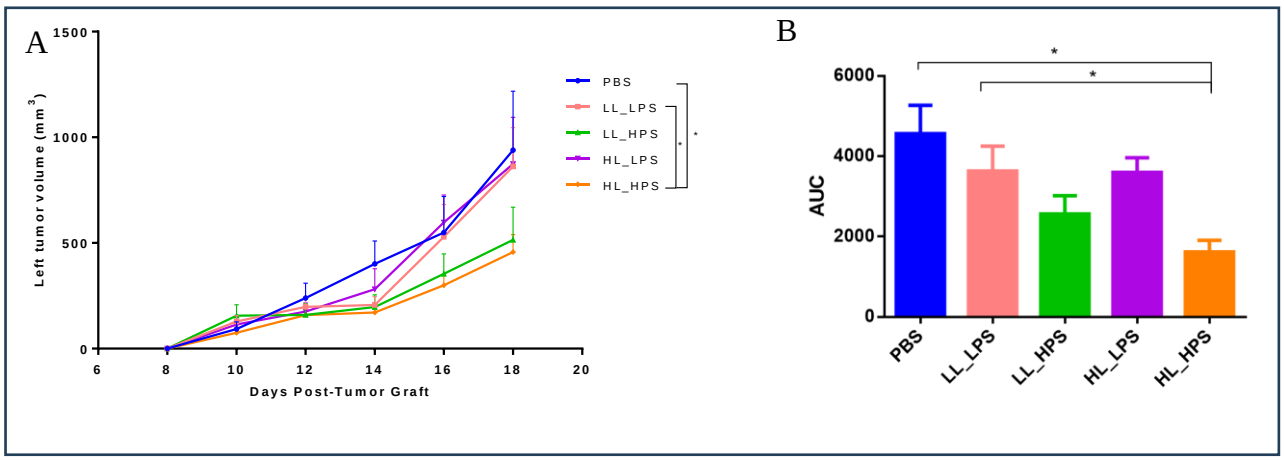

*Figure 4. Abscopal effect of non-irradiated left tumors. A) Volume growth (mm³) of the secondary site tumors are shown. (B) AUC (mm³.day) on day 18 post-tumor engraftment. Data are mean ± standard deviation. Statistical significance of the tumor volume was determined using a two-way ANOVA, followed by a Tukey's multiple comparisons test (n = 5, *p < 0.01).*

The abscopal effect of the four different AlPcNE-PDT protocols on melanoma grafts was also verified. The secondary site tumor was left untreated. Only the HL_HPS PDT protocol group presented significant growth reduction of the secondary site tumor when compared to the other groups (Fig. 4 A-B), suggesting the induction of systemic antitumor responses against B16F10 cells.

Even though the groups LL_HPS and HL_LPS PDT protocols directly reduced the primary site tumors volume, no induction of a systemic antitumor activity was detected. Abscopal antitumor activity was not promoted by the application of the LL_LPS protocol as well.

3.4. Histological analyses of the secondary site tumors

The histological analysis of the secondary site tumors revealed typical features of melanoma, like the primary tumor. Atypical cells, characterized by pleomorphic nuclei typical of melanoma, were observed. Unlike the primary tumor, the secondary site tumors displayed multiple small areas of necrosis, rather than large, focal areas. The presence of the pigment characteristic of melanoma cells was also noted.

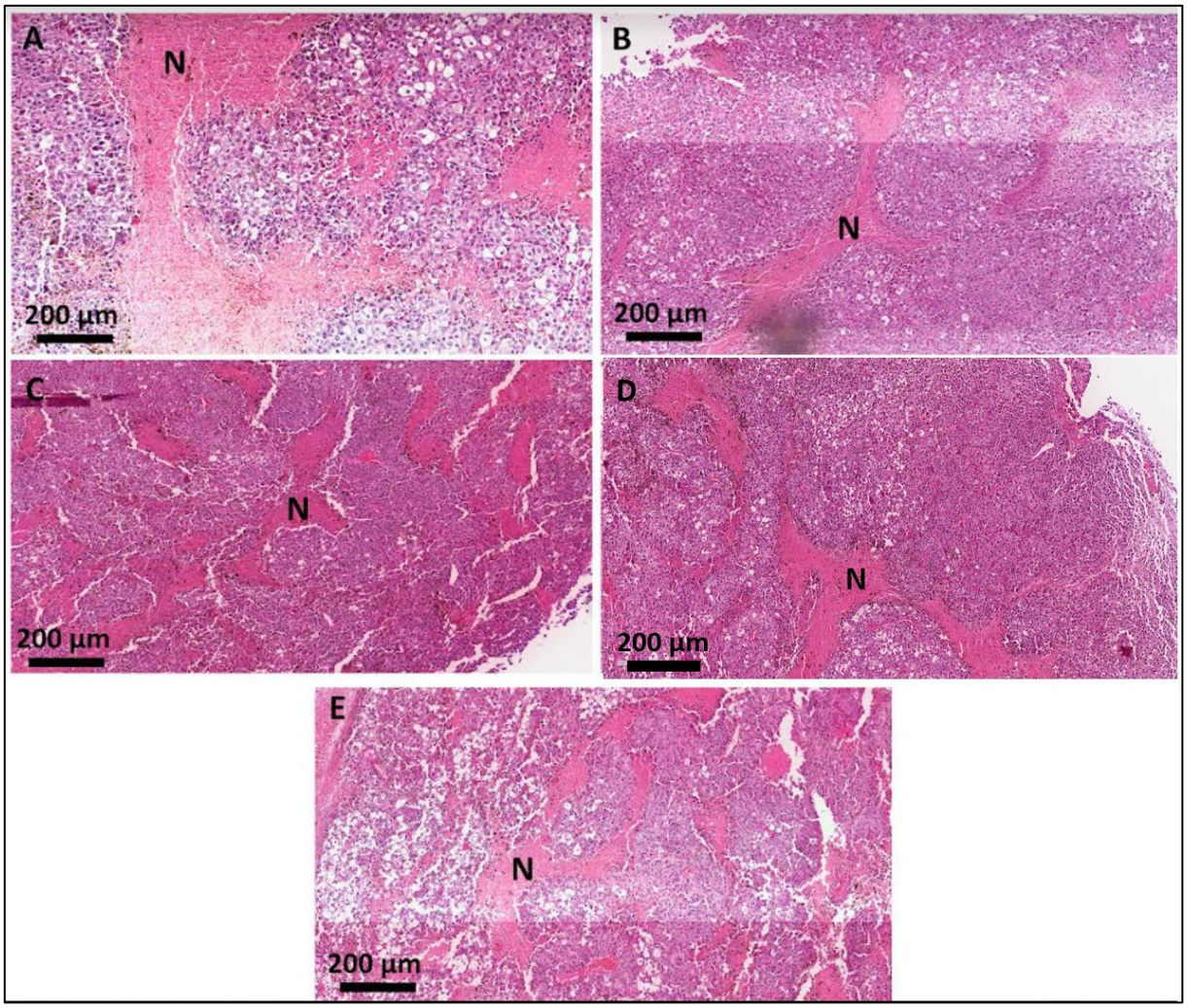

Figure 5. Photomicrographies of histopathological sections of the mice secondary tumor sites (A) PBS; (B) LL_LPS; (C) LL_HPS; (D) HL_LPS; (E) HL_HPS groups. N represents necrosis areas. Scale bar - 200 µm. Stained using H&E (hematoxylin and eosin).

3.5. Hematological analysis

To investigate how AlPcNE-PDT protocols influenced hematological parameters in mice with B16F10 grafts, blood samples were collected on the day of euthanasia and evaluated. All the AlPcNE-PDT protocols led to a decrease in the number of circulating leukocytes and lymphocytes compared to the untreated group (Table 1). The HL_HPS groups were associated with lower platelet levels. The LL_LPS and HL_HPS protocols showed a reduction in the number of circulating HCT. The levels of neutrophils, monocytes, eosinophils, and basophils remained unaffected by AlPcNE-PDT (Figure 6).

	PBS	LL_LPS	LL_HPS	HL_LPS	HL_HPS
Erythrogram					
RBC (×10³ /µL)	6.6 ± 1.1	4.0 ± 1.7	5.6 ± 1.5	4.4 ± 2.6	3.4 ± 1.3
HGB (g/dL)	10.9 ± 1.6	7.0 ± 2.7	9.1 ± 2.3	7.1 ± 4.1	5.8 ± 2.2
HCT (%)	31.3 ± 4.7	19.8 ± 8.1a	27.0 ± 7.6	20.8 ± 11.9	17.6 ± 7.1a
MCV (fL)	47.3 ± 2.0	50.2 ± 4.3	48.0 ± 1.0	48.5 ± 8.1	52.1 ± 2.8
MCH (pg)	16.5 ± 0.4	17.7 ± 1.0	16.4 ± 0.2	16.3 ± 0.4	17.2 ± 0.2
MCHC (g/dL)	35.0 ± 0.1	35.4 ± 1.4	34.0 ± 1.0	34.4 ± 4.7	33.1 ± 2.0
RDW-CV (%)	16.1 ± 3.8	19.6 ± 6.7	19.9 ± 5.4	24.6 ± 7.7	23.0 ± 5.6
RDW-SD (fL)	34.4 ± 10.3	44.4 ± 18.8	42.9 ± 13.3	54.7 ± 22.8a	54.3 ± 15.6a
Leukogram					
WBC (×10³ /µL)	10.8 ± 2.7	4.9 ± 1.3a	5.1 ± 1.5a	5.0 ± 0.2a	4.4 ± 1.7a
NEU (×10³ /µL)	3.2 ± 0.9	1.9 ± 0.7a	1.4 ± 0.7a	1.2 ± 0.4a	1.4 ± 0.6a
LYM (×10³ /µL)	6.2 ± 1.3	2.5 ± 1.0a	3.1 ± 0.7a	3.0 ± 0.8a	2.7 ± 1.4a
MON (×10³ /µL)	1.4 ± 0.7	0.5 ± 0.1a	0.4 ± 0.5	0.6 ± 0.4	0.3 ± 0.2a
EOS (×10³ /µL)	0.1 ± 0.0	0.0 ± 0.0	0.2 ± 0.2	0.1 ± 0.1	0.1 ± 0.0
BAS (×10³ /µL)	0.0 ± 0.0	0.0 ± 0.0	0.0 ± 0.0	0.0 ± 0.0	0.0 ± 0.0
NEU (%)	29.7 ± 3.7	39.5 ± 11.3	25.2 ± 7.7	24.2 ± 7.8	31.1 ± 9.4
LYM (%)	59.2 ± 7.0	49.6 ± 9.8	65.4 ± 14.3	60.6 ± 15.9	60.4 ± 13.1
MON (%)	10.2 ± 5.3	10.0 ± 2.4	7.1 ± 6.1	12.3 ± 7.8	6.7 ± 3.4
EOS (%)	0.9 ± 0.3	0.9 ± 0.8	2.4 ± 2.6	2.9 ± 1.6	1.9 ± 0.7
BAS (%)	0.0 ± 0.0	0.0 ± 0.0	0.0 ± 0.0	0.0 ± 0.0	0.0 ± 0.0
Platelet parameters					
PLT (×10³ /µL)	682.6 ± 107.0a	509.8 ± 187.9	476.8 ± 293.4	624.0 ± 308.0	530.8 ± 59.2a
MPV (fL)	5.5 ± 0.5	6.2 ± 1.0	5.4 ± 0.2	5.8 ± 0.2	6.6 ± 0.5
PDW	15.8 ± 0.4	15.9 ± 0.4	15.8 ± 0.2	16.0 ± 0.6	16.3 ± 0.4
PCT (%)	0.4 ± 0.1	0.3 ± 0.1	0.3 ± 0.2	0.4 ± 0.2	0.4 ± 0.1

Table 1. Results of erythrogram, leukogram and platelet count of female C57bl6 on day 18 after treatment with PDT or PBS. RBC - Red Blood Cells; HGB - Hemoglobin; HCT - Hematocrit; MCV - Mean Corpuscular Volume; MCH – Mean Corpuscular Hemoglobin; MCHC - Mean Corpuscular Hemoglobin Concentration; RDW-CV - Red Cell Distribution Width - Coefficient of Variation; RDW-SD Red Cell Distribution Width - Standard Deviation; WBC - Total White Blood Cells Count; NEU – Neutrophils; LYM – Lymphocytes; MON – Monocytes; EOS – Eosinophils; BAS – Basophils; PLT – Platelets; MPV- Mean Platelet Volume; PDW - Platelet Distribution Width; PCT – Plateletcrit; g/dL - grams per deciliter; fL - fentoliters; pg - picograms. Data correspond to mean ± standard deviation (SD). a = Significant difference compared to PBS group, detected by Tukey's multiple comparisons test, $p < 0.01$.

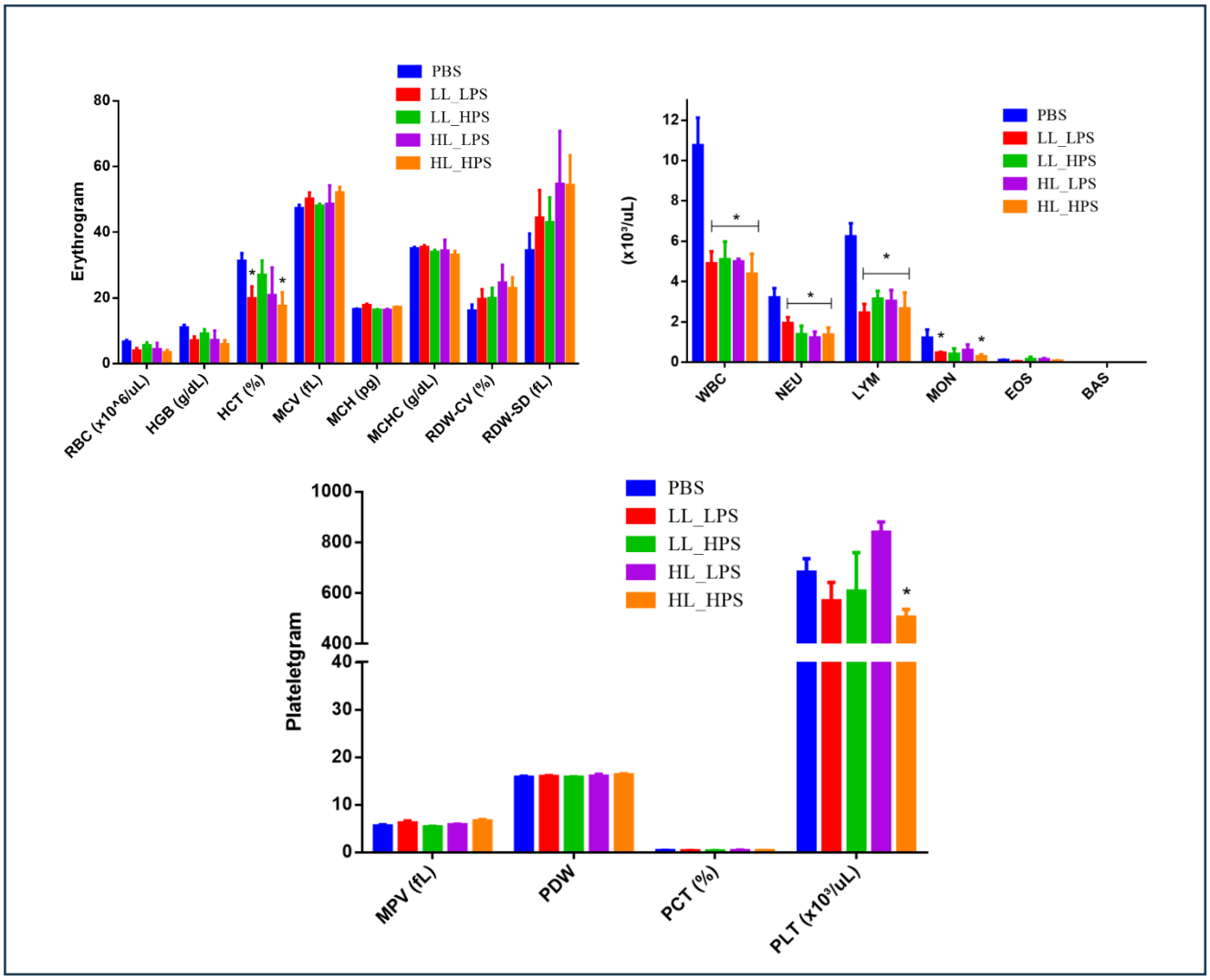

*Figure 6. Hemogram of female C57Bl6 on day 18 after treatment with PDT or PBS. A) Leukogram results. B) Erythrogram results. C) Platelet count results. RBC - Red Blood Cells; HGB - Hemoglobin; HCT - Hematocrit; MCV - Mean Corpuscular Volume; MCH – Mean Corpuscular Hemoglobin; MCHC - Mean Corpuscular Hemoglobin Concentration; RDW-CV - Red Cell Distribution Width - Coefficient of Variation; RDW-SD Red Cell Distribution Width - Standard Deviation; WBC - Total White Blood Cells Count; NEU – Neutrophils; LYM – Lymphocytes; MON – Monocytes; EOS – Eosinophils; BAS – Basophils; PLT – Platelets; MPV- Mean Platelet Volume; PDW - Platelet Distribution Width; PCT – Plateletcrit; g/dL - grams per deciliter; fL - fentoliters; pg - picograms. Data correspond to mean ± standard deviation (SD). * = Significant difference compared to PBS group, detected by Tukey's multiple comparisons test, $p < 0.01$.*

3.6. Flow cytometry analyses

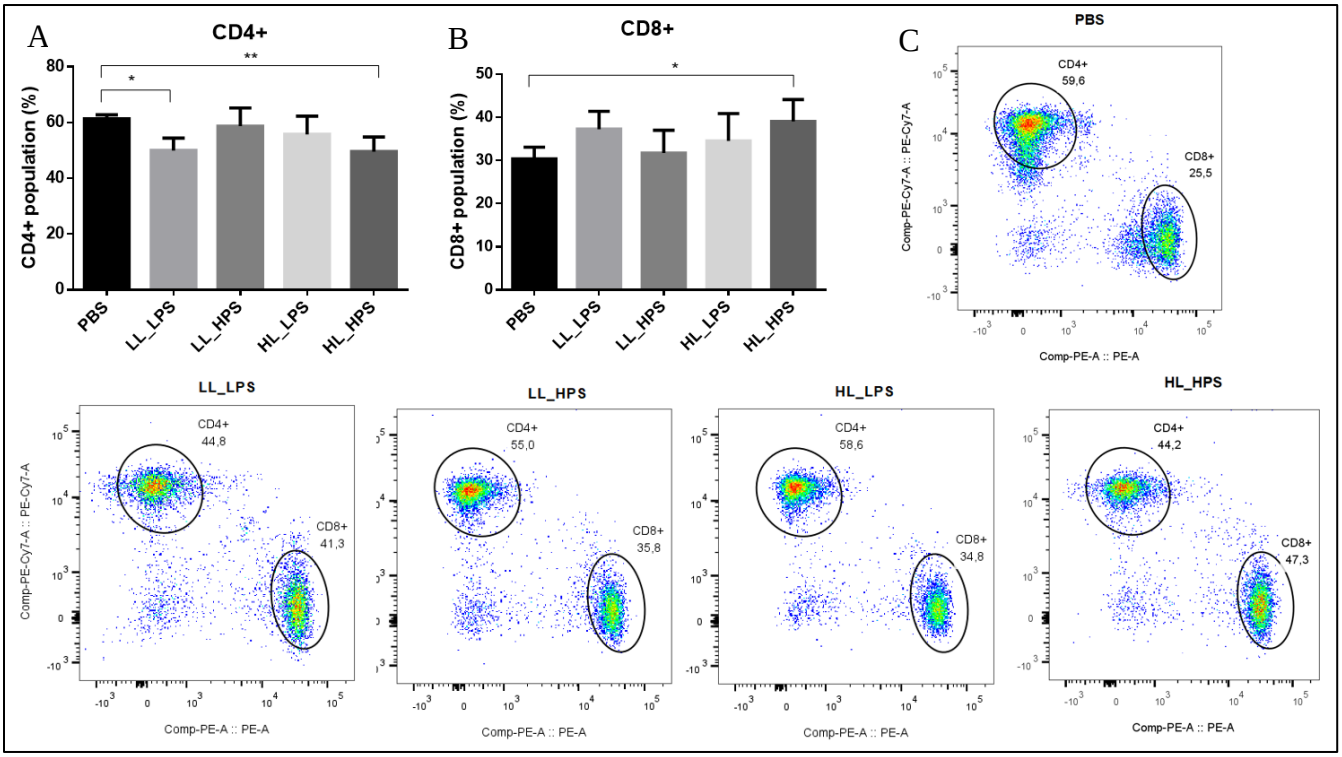

*Figure 7. Flow cytometry analyses of the mice spleens T cells populations. A) Percentage of CD4+ T cells; B) Percentage of CD8+T cells. C) CD4+ and CD8+ T cells. (n=6). One-way ANOVA followed by Tukey's post-hoc test was performed for statistical analysis; *p<0.05, **p<0.01. Data are presented as the mean ± SD.*

To evaluate the T cells population in mice spleens, the frequency of $CD4^+$ T and $CD8^+$ T cells was analyzed by flow cytometry. In mice from groups LL_LPS and HL_HPS, the population of $CD4^+$ T cells decreased compared to the control groups (Figure 3A). Additionally, the splenic $CD8^+$ T cell population in HL_HPS-treated mice increased compared to the controls (Figure 3B). These findings suggest that treatment with HL_HPS may promote antitumor immunity through both $CD4^+$ and $CD8^+$ T cells. There were no statistically significant differences in the CD4+ and CD8+ T cell populations between groups LL_HPS and HL_LPS compared to the control.

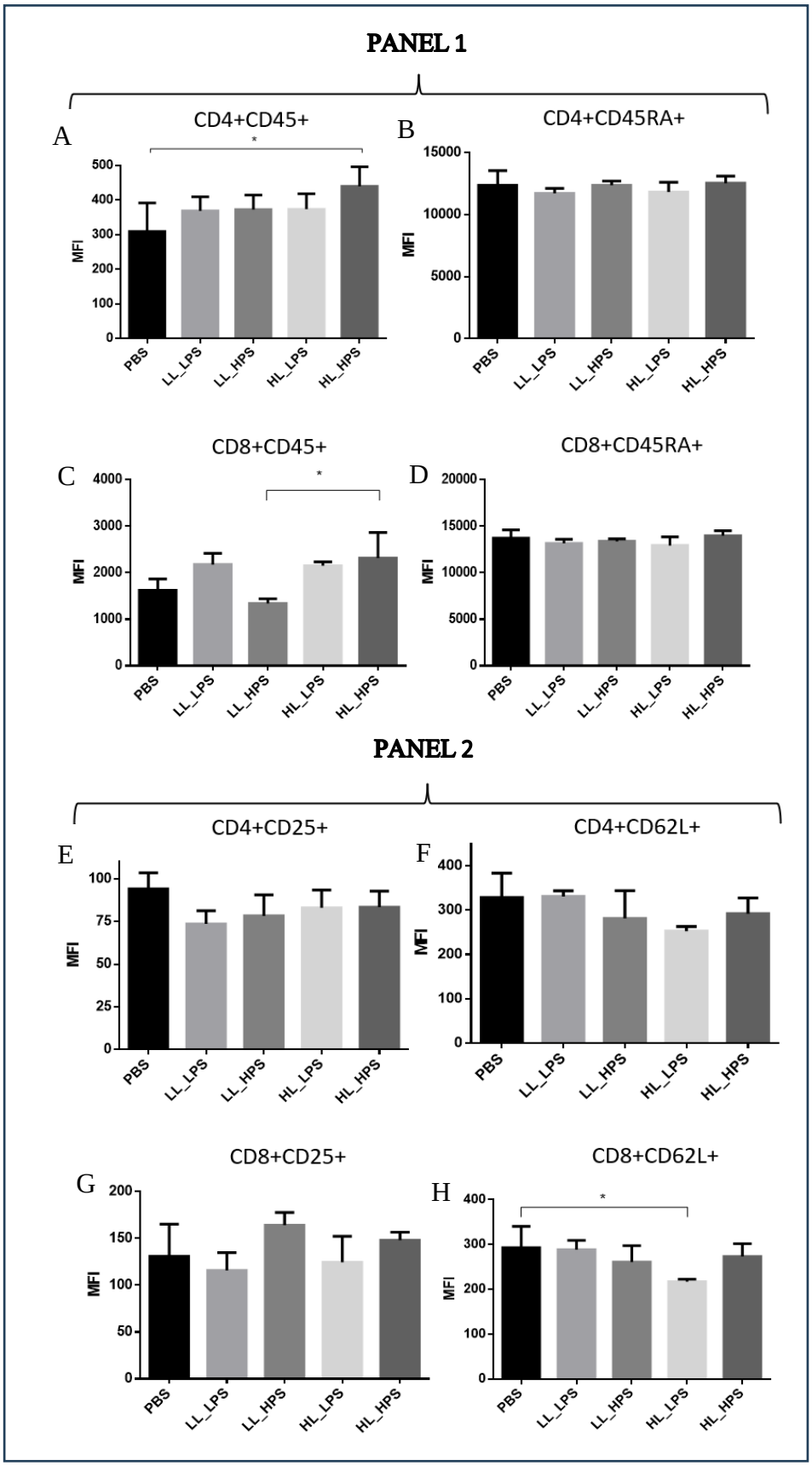

*Figure 8. Flow cytometry analyses of the mice splenic CD4+ and CD8+ T populations. PANEL 1: markers for CD45$^+$ and CD45RA$^+$ T cells. MFI of A) CD4$^+$CD45$^+$; B) CD4$^+$CD45RA$^+$; C) CD8$^+$CD45$^+$; D) CD8$^+$CD45RA$^+$. PANEL 2: E) CD4$^+$CD25$^+$; F) CD4$^+$CD62L$^+$; G) CD8$^+$CD25$^+$; H) CD8$^+$CD62L$^+$; MFI: mean fluorescence intensity. (n=3). One-way ANOVA followed by Tukey's post-hoc test was performed for statistical analysis; *p<0.05. Data are presented as the mean ±*

To explore the subpopulation of splenic $CD4^+$ and $CD8^+$ T cells, markers for $CD45^+$ and $CD45RA^+$ (Panel 1) and $CD25^+$ and $CD62L^+$ cells (Panel 2) were used.

Significant differences were revealed in the mean fluorescence intensity (MFI) of $CD4^+CD45^+$ cells among the experimental groups. Specifically, the HL_HPS protocols significantly increased the percentage of $CD4^+CD45^+$ cells compared to control. No statistically significant differences of $CD4^+CD45^+$ cells were observed between LL_LPS, LL_HPS, and HL_LPS groups and PBS (Figure 8A). These results suggest that the HL_HPS treatment may induce higher differentiation of $CD4^+CD45^+$ T cells compared to the control group, while the LL_LPS, LL_HPS, and HL_LPS protocols did not.

The LL_HPS group exhibited less $CD8^+CD45^+$ cells compared to the HL_HPS group. No statistically significant differences of $CD8^+CD45^+$ cells frequencies were observed for the LL_LPS and HL_LPS protocols compared to the control group (Figure 8C).

Collectively, these findings indicate that the HL_HPS protocol can promote a T cell-specific immune response.

3.7. The HL_HPS protocol induced distinct expression profiles for immune response genes in primary and secondary sites tumors

The reduction in the growth of the non-treated tumor, together with the distinct immunological responses elicited by the HL_HPS_PDT protocol was the most significant finding in this study. Consequently, we concentrated on the transcriptomic analysis via RNA-Seq of primary and secondary sites tumors in irradiated animals from the HL_HPS condition, in comparison tumors from the PBS group. This approach aimed to elucidate and correlate the underlying antitumor mechanisms involved.

For RNA sequencing, three independent samples from both primary and secondary sites tumors of the PBS and HL_HPS groups were collected. These samples met the required criteria for total RNA concentration, quality and purity stipulated by the service provider. Gene expression levels were estimated by transcripts abundance, with values normalized to FPKM (Fragments Per Kilobase of transcript per Million mapped reads), accounting for sequencing depth and gene length effects on the fragment counts.

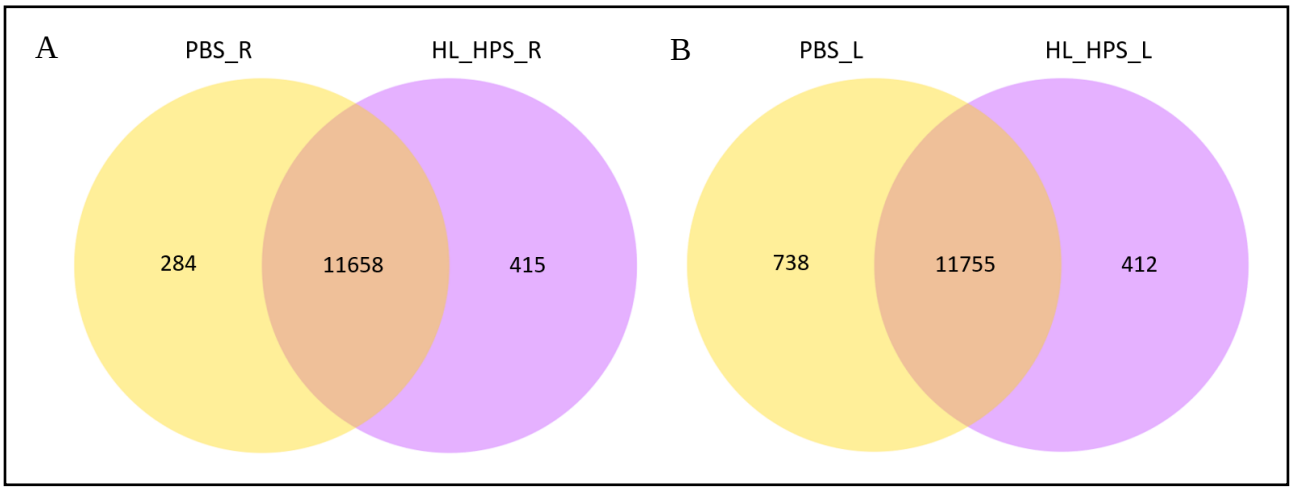

Figure 9. Venn diagram of the numbers and distribution of unique and co-expressed genes for the PBS and HL_HPS treatment conditions. A) Right tumors. B) Left tumors

The number of unique and co-expressed genes within each PDT and PBS protocol was illustrated using a Venn diagram. In the right tumor samples, 11,658 genes were co-expressed, with 284 and 415 unique genes in the PBS and HL_HPS group, respectively. In contrast, the left tumors presented 11,755 genes co-expressed across the two groups, with 738 and 412 unique genes in the PBS and HL_HPS group, respectively.

Profound alterations in gene expression profiles were observed between irradiated and control animals (Fig. 10). Additionally, there was a noticeable similarity in gene expression profiles between the right and left tumors in the PBS group, whereas the right and left tumors in the HL_HPS group exhibited predominantly different profiles.

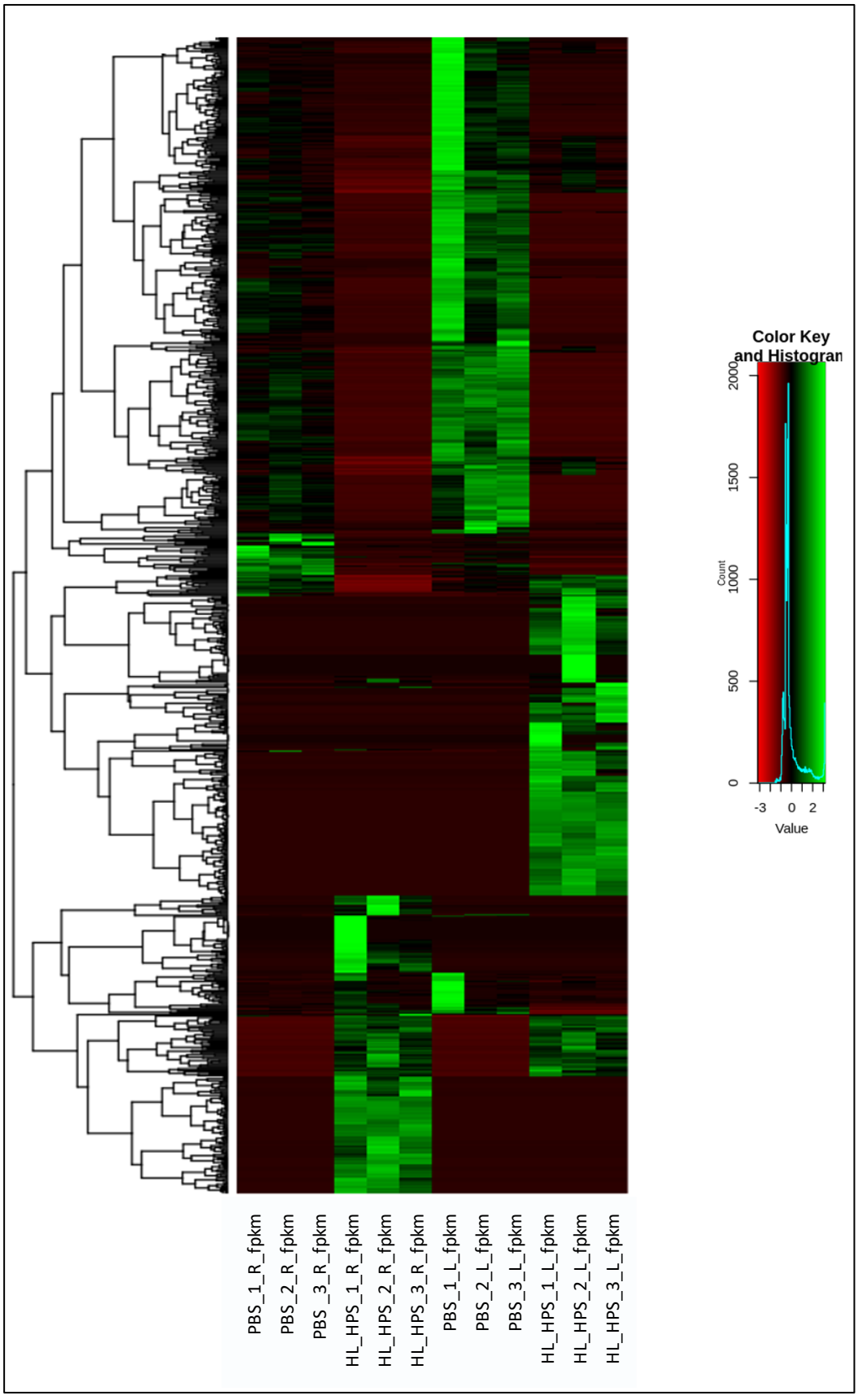

Figure 10. Heatmap of differentially expressed genes between the right and left tumor samples in PBS and HL_HPS groups. The heatmap displays the Z-score normalized differential expression across three replicates. R indicates right tumor, and L indicates left tumor.

Genes with significantly different expression levels under various conditions ($|\log2(\text{FoldChange})| \geq 1$ and $\text{padj} \leq 0.05$) were identified. A log2FC > 0 indicates higher gene expression in the experimental condition compared to the control condition, whereas a log2FC < 0 indicates lower expression in the experimental condition compared to the control. A log2FC = 0 indicates no difference in gene expression between the two conditions.

The global distribution of differentially expressed genes in the HL_HPS-PDT protocol for the primary and secondary sites tumors compared to the PBS control group, as well as between primary and secondary tumors within the same group, was inferred by volcano plots (Figure 11).

Comparing the PBS_R *vs* HL_HPS_R samples, a total of 693 differentially expressed genes were identified, with 273 upregulated and 420 downregulated transcripts in HL_HPS_R. The PBS_L *vs* HL_HPS_L samples comparison revealed 1,208 differentially expressed genes, including 835 upregulated and 373 downregulated in HL_HPS_L. The comparison the PBS_R *vs* PBS_L samples identified 1,052 differentially expressed genes, with 100 upregulated and 952 downregulated in PBS_L. The HL_HPS_R *vs.* HL_HPS_L samples comparison revealed 121 differentially expressed genes, including 60 upregulated and 61 downregulated sequences in HL_HPS_L.

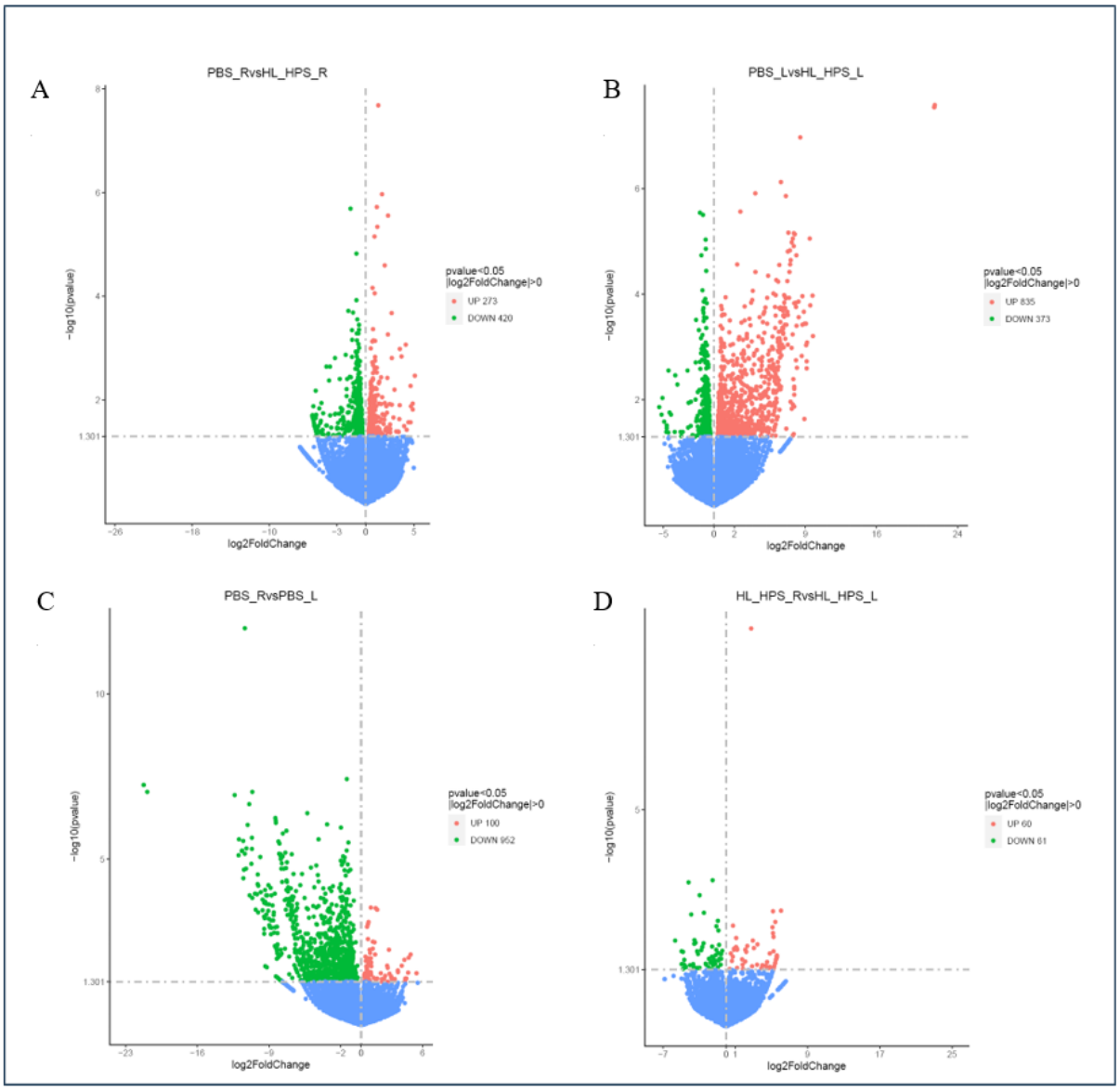

Figure 11. Volcano plot of differential expression of genes from RNA-seq comparing the A) PBS_R vs HL_HPS_R; B) PBS_L vs HL_HPS_L; C) PBS_R vs PBS_L; D) HL_HPS_R vs HL_HPS_L. Each dot indicates one gene. Red dots represent upregulated genes, while green dots represent downregulated genes.

The evaluation of the gene ontology of DEG in the PBS_R vs. HL_HPS_R samples comparison identified several genes related to the immune response most of them being downregulated (Fig. 12, A). Conversely, in the PBS_L *vs.* HL_HPS_L samples analysis, differentially expressed immune response-related genes were predominantly upregulated (Fig. 12, B).

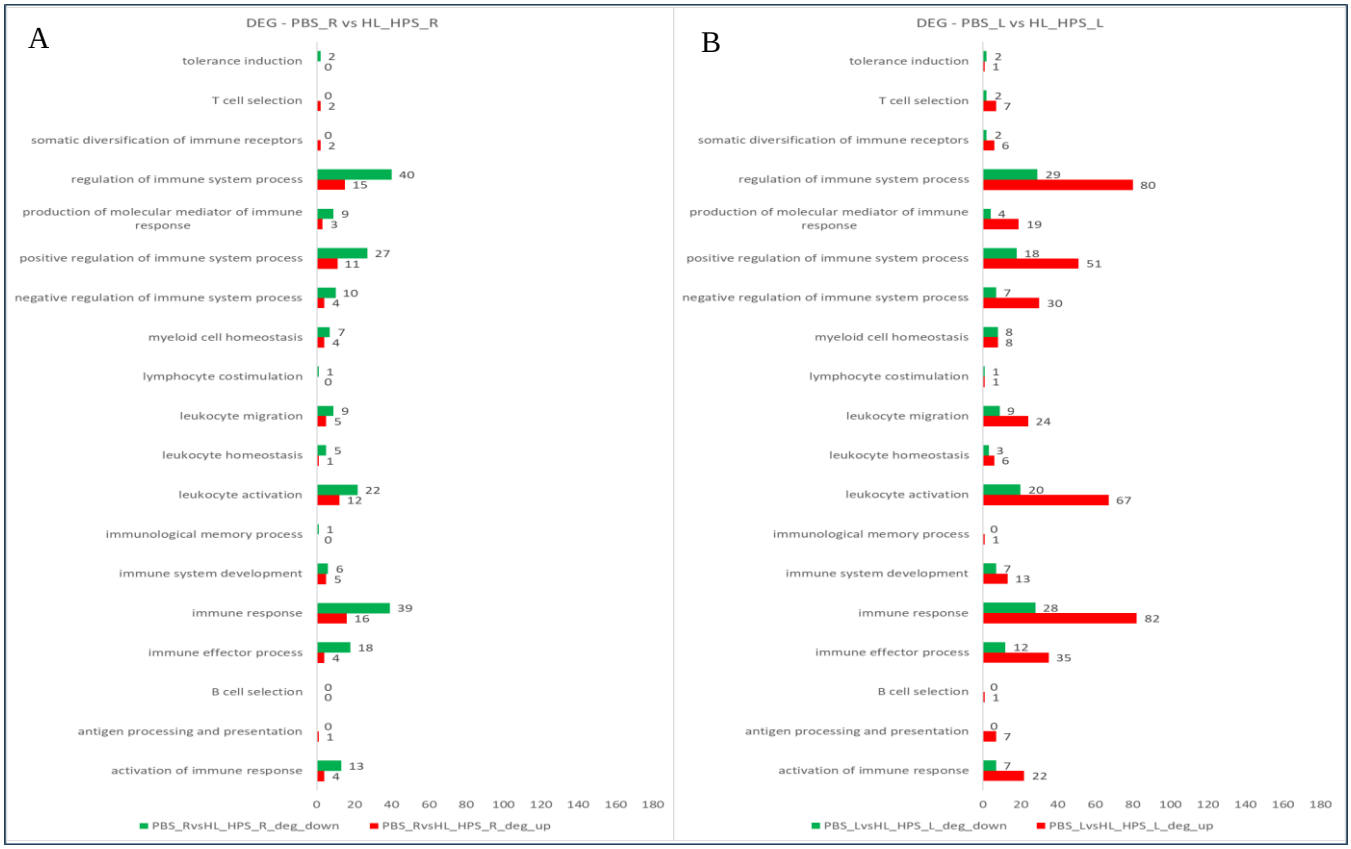

Figure 12. Number of upregulated (red) and downregulated (green) genes based on Gene Ontology (GO) in Immune System Processes (GO:0002376). (A) Comparison between PBS_R vs HL_HPS_R. (B) PBS_L vs HL_HPS_L.

Table 2 highlights the DEGs for the comparisons PBS_R *vs*. HL_HPS_R and PBS_L *vs*. HL_HPS_L based on the GO category for Immune System Processes (GO:0002376). This analysis revealed that the HL_HPS_R tumor exhibited 28 upregulated genes and 60 downregulated genes associated with immune system processes, while in the HL_HPS_L tumor, 122 genes were upregulated, and 49 were downregulated.

	DEGs_UP	DEGs_DOWN
PBS_R*vs*HL_HPS_R	Asxl1, Brpf1, Cacnb4, Cd3d, Chid1, Cmtm7, Cnpy3, Crtam, Cxcl11, Gli3, Gpr17, H2-Eb2, Herc6, Kat7, Kit, Klrk1, Mef2c, Nuggc, Prss56, Rbm15, Shld3, Slc25a38, Socs1, Sox6, Spp1, Stxbp4, Tab1, Traf4.	Ackr3, Acvr1b, Ahr, Arg1, C6, Ccnd3, Cd36, Cdc42ep2, Cdkn1a, Cebpg, Ctla2a, Defb1, Dusp10, Ecm1, Egr3, Emp2, Ephb3, Fosl2, Fzd9, Gprc5b, Gramd4, Grem1, Hcfc2, Hexim1, Il36g, Ivl, Jun, Jund, Kcnj8, Lrp1, Mavs, Meis1, Mitf, Mospd2, Nfkb2, Nos2, Nr4a3, Pde4b, Plec, Prkd2, Ptk6, Pura, Pvr, Rarg, Sfn, Sh2b2, Six1, Sox9, Tbkbp1, Thra, Tmem45b, Tnfaip3, Tnfsf14, Tnfsf9, Trpm4, Ttbk1, Vegfa, Xkr8, Zbtb7a, Zbtb7b.
PBS_L*vs*HL_HPS_L	Adgre1, Adgrf4, Adtrp, Alcam, Angpt1, Aqp3, Bank1, Bcl11a, Bcl11b, Bcl2a1d, Blnk, Bmi1, Bmp4, Bpifc, Ccl28, Ccn3, Cd180, Cd209b, Cd55, Ciita, Coch, Crhr1, Ctsc, Ctse, Cx3cl1, Cx3cr1, Cxadr, Cxcl10, Cxcr6, Cyld, Dapk2, Dapl1, Ddx3x, Defb1, Dhx15, Dnase1l3, Dock11, Edn2, Egr3, Emp2, Endou, Erap1, Evpl, Ext1, F2rl1, F830016B08Rik, Fgfr3, Fgl2, Foxn1, Foxp1, Fzd5, Gata3, Gbp10, Gbp6, Herc6, Igf1, Ighm, Il1rap, Irf4, Itgal, Itgax, Itgb8, Ivl, Kat7, Kif5b, Lacc1, Lair1, Lcp2, Lef1, Ly6d, Marchf7, Mecom, Mef2c, Mill1, Mysm1, Nedd9, Nfkbiz, Notch1, Padi4, Pag1, Pdgfd, Pik3ap1, Pla2g2f, Pparg, Ppl, Prdm1, Prkcb, Prlr, Psg17, Ptger4, Ptprc, Pycard, Rasgrp1, Rbm15, Rel, Ret, Rnf115, S100a14, Selp, Serpinb9, Sfn, Sfrp1, Shld3, Sirpb1a, Sirt1, Skil, Slamf8, Slc40a1, Socs6, Sp1, Sp3, Spn, Tbx1, Tcea1, Trim29, Usp14, Usp9x, Vav3, Wdfy4, Wnt5a, Ythdf2, Zbtb6.	Aire, Ccr10, Cdc42ep2, Cebpg, Cxcl1, Cybc1, Cyren, Ephb4, F7, Fkbp1b, Fzd9, Gata2, Gdf15, Gpr137, Gprc5b, Hexim1, Hs1bp3, Il15, Il17d, Irf3, Jmjd6, Kcnj8, Kcnn4, Kmt5c, Mark4, Men1, Mitf, Mospd2, Nemp1, Nfkb2, Nr4a3, Orai1, Ppbp, Prdm16, Prelid1, Prkd2, Rac3, Rara, Rarg, Rbm14, Slc37a4, Sppl2b, Tal1, Tbkbp1, Trim68, Tusc2, Vegfa, Xkr8, Zbtb7b.

Table 2. List of DEGs upregulated and downregulated in HL_HPS_R in PBS_RvsHL_HPS_R and HL_HPS_L in PBS_LvsHL_HPS_L based on Gene Ontology (GO) in Immune System Processes (GO:0002376). (|log2(FoldChange)| ≥ 1 and padj ≤ 0.05).

It was possible to identify genes that are upregulated both in the HL_HPS_R and HL_HPS_L tumors compared to the same tumors in PBS group, such as Herc6, Kat7, Mef2c, Rbm15, and Shld3 (Table 2). On the other hand, the genes that were downregulated both in HL_HPS_R and HL_HPS_L tumors compared to the same tumors in the control group were: Cdc42ep2, Cebpg, Fzd9, Gprc5b, Hexim1, Kcnj8, Mitf, Nfkb2, Nr4a3, Prkd2, Rarg, Tbkbp1, Vegfa, Xkr8, and Zbtb7b (Table 2).

The comparison of DEGs between the primary and secondary sites tumors in each treatment indicated that, in the PBS group, most immune response-related genes were downregulated in the secondary site tumor compared to the primary one (Fig. 13A). In contrast, the primary and secondary site tumors in the HL_HPS group did not exhibit significant differential expression of immune-related genes (Fig. 13B).

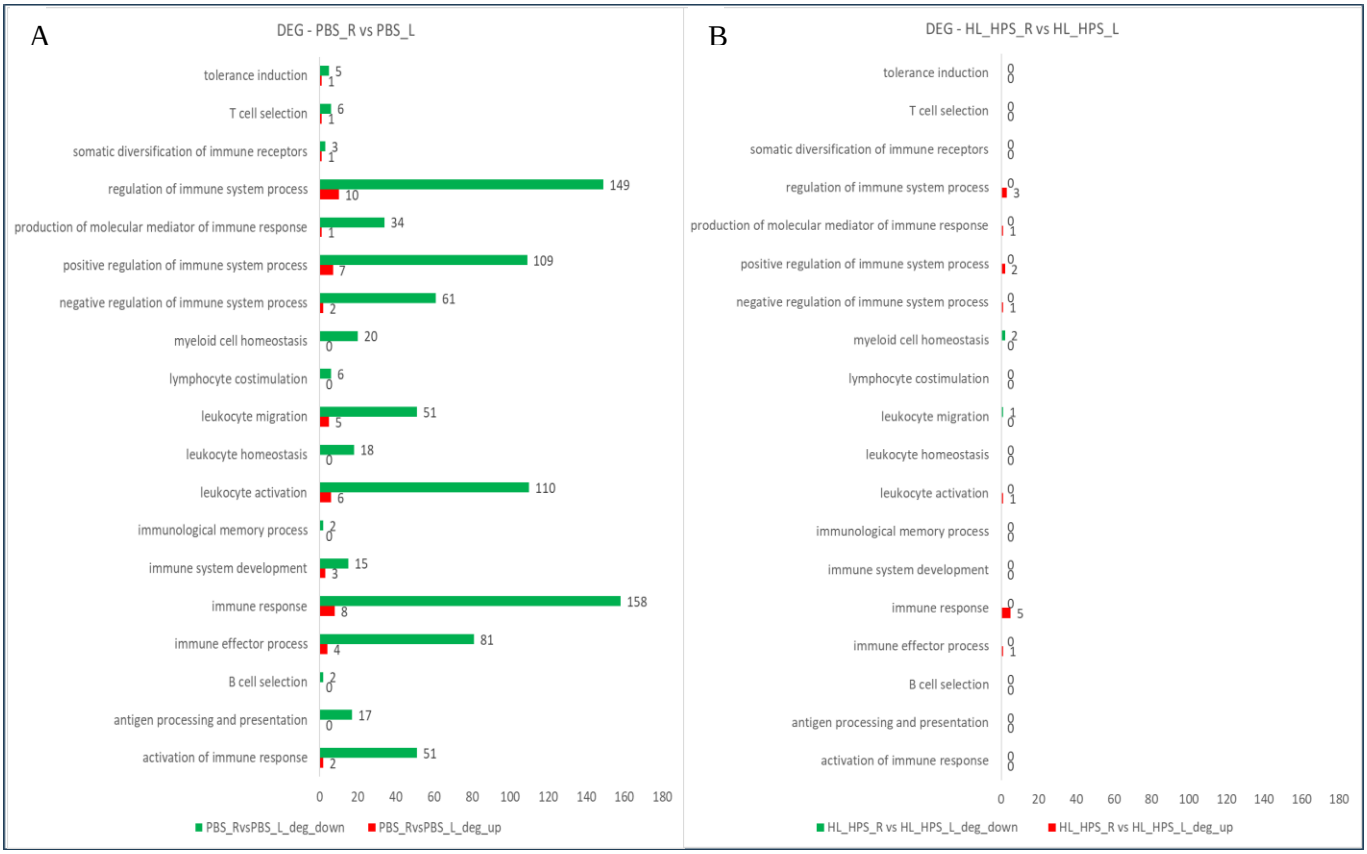

Figure 13. Number of upregulated (red) and downregulated (green) DEGs based on Gene Ontology (GO) in Immune System Processes (GO:0002376). (A) Comparison between PBS_R vs PBS_L. (B) HL_HPS_R vs HL_HPS_L.

Table 3 presents the DEGs identified in the comparison between tumors within the same group, PBS_R *vs.* PBS_L and HL_HPS_R *vs.* HL_HPS_L. This analysis revealed 12 upregulated and 206 downregulated genes associated with Immunological Processes in PBS_L. Conversely, in the HL_HPS_L group, only 7 genes related to immunological processes were upregulated and 3 were downregulated.

	DEGs_UP	DEGs_DOWN
PBS_R*vs*PBS_L	Aire, Cdh17, Evl, Gpr137, Kcnj8, Kcnn4, Kmt5c, Ppbp, Prss56, Prxl2a, Rara, Vegfb	Acp5, Adgre1, Adgrf4, Adipoq, Adtrp, Aim2, Alox5, Ang, Angpt1, Anxa3, Aqp3, Bcl11b, Bcl2a1d, Blnk, Bmp4, Bpifc, Bst1, Btk, C1qb, C1qc, C3ar1, C6, Camk1d, Ccl21a, Ccl6, Ccl7, Ccl8, Ccl9, Ccn3, Ccr2, Ccr5, Cd209b, Cd209d, Cd244a, Cd24a, Cd36, Cd37, Cd55, Cd84, Cd86, Cebpa, Cfh, Clec2d, Clec2g, Clec4a1, Clec4a2, Clec4a3, Cmklr1, Coch, Coro1a, Crhr1, Csf1r, Csf2rb, Csf2rb2, Ctsc, Ctse, Ctss, Cxcl12, Cxcl14, Cxcl16, Cybb, Cysltr1, Dapk1, Dapk2, Dapl1, Defb1, Dock2, Dpp4, Dtx4, Ear2, Edn2, Ednrb, Egr1, Egr3, Emp2, Ephb3, Evpl, F2rl1, Fcer1g, Fcgr2b, Fcgr3, Fcgr4, Fgfr3, Fgl2, Fgr, Foxn1, Gas6, Gata3, Gbp2b, Gm5431, Gpr55, H2-T24, Hck, Hspb1, Ifi204, Ifi205, Ifi207, Ifi209, Igf1, Ighm, Ikzf1, Il1rl2, Il4ra, Il6ra, Inpp5d, Irf5, Itgal, Itgam, Itgb2, Ivl, Kitl, Lair1, Laptm5, Lcp2, Lef1, Lfng, Lilrb4a, Lilrb4b, Lmo2, Lpxn, Ly6d, Ly86, Lyn, Lyve1, Mafb, Marchf1, Mill1, Mpeg1, Mrgprb1, Myo1f, Myo1g, Mysm1, Naip6, Ncf1, Nckap1l, Nedd9, Nfam1, Notch1, P2ry14, Padi4, Pag1, Pck1, Pdgfd, Pik3ap1, Pirb, Pla2g2f, Plcl2, Pld4, Plscr2, Pou2f2, Pparg, Ppl, Prdm1, Prkcb, Prkch, Prlr, Psg17, Ptafr, Ptger4, Ptprc, Ptpre, Ptpro, Rac2, Rasgrp1, Rftn1, Rnase4, S100a14, S1pr1, Sash3, Selp, Sema4a, Sfn, Sfrp1, Sirpb1c, Slamf7, Slc11a1, Slc7a2, Slfn1, Slfn2, Spink5, Svep1, Tbx1, Themis2, Tifab, Tlr13, Tlr8, Tlr9, Tmem229b, Tmem98, Tnfaip8l2, Tnfrsf13b, Tnfrsf1b, Tnfrsf21, Tnip3, Trem2, Trim29, Trpm2, Tyrobp, Vav1, Vcam1, Vsig4, Vsir, Wdfy4, Wfdc17, Wnt10b, Zeb1,
HL_HPS_R*vs*HL_HPS_L	Egr3, Endou, Il36g, Il36rn, Klk5, Ptk6, Sox9	Dpep1, Hba-a1, Hba-a2

Table 3. List of DEGs upregulated and downregulated in PBS_L in PBS_RvsPBS_L and HL_HPS_L in HL_HPS_RvsHL_HPS_L based on Gene Ontology (GO) in Immune System Processes (GO:0002376). (|log2(FoldChange)| ≥ 1 and padj ≤ 0.05).

Overall, The HL_HPS-PDT protocol elicited substantial changes in the gene expression profiles of both primary and secondary site tumors, in comparison to the corresponding tumors of the PBS group. These alterations underscore the impact of HL_HPS-PDT on the molecular landscape of the tumors, highlighting its potential as an effective modulator of tumor genes expression.

4. DISCUSSION

In recent years, photodynamic therapy (PDT) has garnered increasing attention due to the broad range of anticancer mechanisms [9,13,14,20]. The impact of PDT on the immune system is becoming an area of intense study[21,22]. The results of this study highlight the efficacy of PDT in treating grafted melanoma in mice, emphasizing significant effects on both the primary site and distant tumors (abscopal effect), providing insights into tumor and immune response mechanisms. To test the direct and abscopal effects mediated by AlPcNE-PDT, a bilateral melanoma graft model (B16F10) in mice was established, with PDT applied to only one of the tumors.

The LL_HPS, HL_LPS, and HL_HPS PDT protocols showed a significant reduction in the volume of the primary site tumor. This effect can be attributed to the antitumor capabilities of PDT through the production of reactive oxygen species (ROS), leading to necrosis and apoptosis of tumor cells. Pan et al. (2021)[23] demonstrated that PDT can inhibit the proliferation of malignant melanoma cells by increasing intracellular ROS levels and activating the mitochondrial apoptotic pathway.

Notably, the HL_HPS condition not only reduced the volume of the primary site tumor but also induced an abscopal effect, evidenced by the reduction in the volume of the secondary site, non-irradiated tumor grafted on the opposite side. This phenomenon suggests the activation of a systemic immune response capable of attacking tumors distant from the primary treatment site. This abscopal effect is particularly significant as it indicates a therapeutic potential for treating metastases in locations not directly exposed to PDT. A similar effect was found in other studies, such as Gurung et al. (2023)[24], which showed that PDT with Ce6 as a photosensitizer was able to induce potent local and systemic antitumor immune responses in a murine model of malignant melanoma, further enhanced by the combination with PD-1/PDL-1 inhibitors.

The variation in efficacy among treatments can be attributed to differences in the concentration of the photosensitizer, as well as to the different light dosages. According to Morais et al. (2021)[9], different PS concentrations in PDT can induce different biological responses, including various types of cell death and the release of DAMPs, thereby influencing the induction of immunogenic cell death. This supports our study finding that mice treated with different PS concentrations and light dosages exhibited varying direct and abscopal antitumor outcomes.

The observed hematological changes highlight the impact of different photodynamic therapy (PDT) protocols on systemic physiology. The PBS control group shows an WBC count

of 10.8 ± 2.7×10^3/μL, which is within the normal range for C57BL/6 mice (typically around 6.0−10.0×10^3/μL) as reported in studies like White et al. (2016)[25]. The elevated WBC levels in the PBS group could indicate a systemic inflammatory response to the grafted tumor. Corroborating the chronic inflammatory responses seen in tumor-bearing hosts[26]. Conversely, the LL_LPS, LL_HPS and HL_LPS, groups showed significantly lower WBC counts, particularly the HL_HPS group with 4.4 ± 1.3×10^3/μL, suggesting a reduction in systemic inflammation in response to the treatment.

Lymphocyte (LYM) counts also varied, with the PBS group showing elevated levels (6.2 ± 1.3×10^3/μL), which aligns with chronic immune responses described for tumors (Zhou et al., 2015). Treated groups showed reduced LYM counts, with HL_HPS exhibiting 2.7 ± 1.4×10^3/μL, suggesting a dampening of the immune response or a shift towards immune regulation. According to Was et al. (2020)[27], this reduction may indicate an active mobilization of leukocytes from the blood to the tumor site.

Additionally, the reduction of WBC and LYM counts in treated groups suggests that PDT may mitigate systemic inflammation, which could contribute to the antitumor efficacy by reducing pro-tumorigenic inflammatory environments. This can be explained by the modulation of the immune response, promoting the activation of dendritic cells and the presentation of tumor antigens, which may lead to a more effective and targeted immune response, resulting in the reduction of WBC and LYM levels[28]. Other studies also report that PDT can decrease inflammatory markers in animal models and patients[29].

Studies have demonstrated that the presence of tumors can trigger a chronic immune response, characterized by the increased presence of leukocytes and lymphocytes in peripheral blood. This response reflects the immune system attempt to combat the tumor presence, although it is often insufficient to contain tumor growth[30,31]. On the other hand, this inflammation can create a pro-tumor environment that favors cancer cells survival and invasion, increased angiogenesis, and recruitment of immunosuppressive cells, allowing tumor cells to escape immune destruction[30]. Studies have shown that inflammatory cytokines such as TNF-α, IL-6, and IL-1β can activate cellular signaling pathways that promote tumor survival and growth[32]. The understanding these hematological impacts is crucial for optimizing PDT regimens therapeutic benefits while minimizing adverse effects.

The present study found that AlPcNE-PDT induced a systemic increase in the population of cytotoxic $CD8^+$ T cells and a reduction in the population of $CD4^+$ T cells in HL_HPS group. The reduction in $CD4^+$ T cells may reflect an impact on immune regulation,

while the increase in $CD8^+$ T cells suggest cytotoxic activation against tumor cells. It is well known that subpopulations of $CD4^+$ T cells, such as regulatory T cells (Tregs), promote immunosuppression, while helper T cells (Th) support $CD8^+$ T cells by providing activating cytokines[33]. Our study suggests that, despite the reduction in the systemic population of $CD4^+$ T cells, most of these cells in the HL_HPS group correspond to the differentiated $CD4^+CD45^+$ form, an important marker of antigen receptor signal transduction and lymphocyte development, indicating a potential long-term immune response[34]. $CD8^+$ T cells, which have effector cytotoxic functions, are known to slow down distal tumor growth[35,36].

Several studies have demonstrated that PDT stimulates the immune system in various ways, including the release of tumor-associated antigens (TAAs) and immunostimulatory molecules from tumors, which can activate and trigger an anticancer immune response[37,38]. While PDT has been shown to activate both humoral immunity and cell-mediated adaptive immunity, $CD8^+$ T cells are primarily responsible for the immunological effects of PDT[37,38]. Our findings demonstrated that the systemic population of $CD8^+$ T cells was enhanced by AlPcNE-PDT in the HL_HPS condition. However, systemic T cells were depleted in the other irradiated groups and were unable to evoke an anticancer immune response. This could explain the non-occurrence of an abscopal effect with PDT, in groups other than HL_HPS.

Despite the direct antitumor effect observed in the LL_HPS and HL_LPS groups, antitumor immunity appears to be insufficient to eradicate the melanoma. This is possibly due to the low proliferation and activation of $CD8^+$ T cells, in face of the tumors aggressiveness. According to previous studies, in tumoral microenvironment, barriers can develop to prevent immune cells from migrating and penetrating the non-irradiated tumor[36,39].

Encouraged by the immunogenic capabilities of HL_HPS-PDT, we hypothesized that the antitumor immunity generated resulted from the modulation of the expression of genes involved in immune system processes. RNA-Seq data revealed distinct patterns of gene expression in response to the treatment. In the HL_HPS condition, the primary site tumor exhibited more downregulated genes related to immunological processes, while the secondary site tumor presented prevalence of upregulated genes in the same category. This suggests that the mechanism of tumor growth inhibition were different in the two tumors.

The genes Herc6, Kat7, Mef2c, Rbm15, and Shld3 were found to be upregulated in both the right and left tumors of the treated groups, suggesting a coordinated response in tumor inhibition. Mao and colleagues (2018)[40] and Sala-Gaston et al. (2020)[41] proposed that HERC proteins may have dual roles in cancer, acting as oncogenes or tumor suppressors depending on

the tumor type, although there is a lack of studies specifically on HERC6. Swanson and collaborators (1998)[42] demonstrated that all members of the MEF2 family (A-D) are expressed in B cell lines and all, except MEF2C, are expressed in T cell lines. This suggests that MEF2C expression is related to B cell development and function. Newman and collegues (2017)[43] highlighted the essential role of Kat7 in the development, fitness, and survival of T cells, particularly in maintaining the acetylation of the histone 3 lysine 14 (H3K14ac), an essential epigenetic mark for the development of a normal immune system. Gao and collaborators (2021)[44] identified KAT7 as a tumor suppressor protein in colorectal cancer and non-small cell lung cancer, while Dong et al. (2023)[45] showed that Rbm15 is associated with pancreatic cancer progression by promoting tumor proliferation, migration, and metastasis. Nonetheless, the role of Rbm15 on melanoma cells remains understudied. Lastly, Shld3 is involved in DNA regulation and repair[46].

The high expression of CD3D correlates with immune cells infiltration and to the response to immunotherapy in patients with head and neck squamous cell carcinoma[47] and colon adenocarcinoma[48]. Upregulatino of CXCL10 in the HL_HPS_R tumor and upregulation of CXCL11 in the HL_HPS_L tumor seem relevant since they act as key immunological chemoattractant during inflammatory responses[49]. The positive modulation of these genes can potentially enhance the efficacy of the immune response against melanoma tumor cells.

Calabrese and co-workers (2009)[50] showed that the inactivation of SOCS1 disabled the p53-dependent senescence in response to oncogenic STAT5A and radiation-induced apoptosis in T cells, corroborating the results of inhibition of tumor growth and the upregulation of this gene in HL_HPS_R and indicating that SOCS1 could be a key gene in inhibiting tumor growth.

Another significant gene found as a DEG of the primary site tumor in the HL_HPS group is CRTAM. CRTAM is a protein-coding gene expressed on the surface of activated NK T cells and $CD8^+$ T lymphocytes. It enhances the infiltration in the tumor of immune cells, particularly $CD8^+$ T cells. Moreover, CRTAM may promote the proliferation of activated T cells and the secretion of interferon (IFN)-γ, thereby enhancing the anti-tumor effectiveness of T cells[51].

Huang and colleagues (2020)[52] found a strong positive correlation between the gene expression of CXCL10 gene expression and the infiltration in the tumor of immune cells (B cells, $CD8^+$ T cells, $CD4^+$ T cells, macrophages, neutrophils, dendritic cells).

Several genes associated with memory, activation, and survival of CD8 T cells, such as REL and FOXP1, were found to be upregulated in the secondary site HL_HPS tumor in accordance to Feldman et al. (2018)[53] in melanoma mice model.

These results above suggest a differential modulation of immune responses, potentially reflecting a systemic immune activation.

Among the downregulated genes known to play an important role in melanoma progression, are CXCL1, which exerts melanoma growth-stimulating activity, and MITF a crucial oncogenic transcription factor to maintain tumor survival, increase proliferation, and promote differentiation[54–56]. These downregulated genes are involved in the signaling pathway and in the activation of the immune system. They also reduce immunosuppression and decrease tumor cells survival and proliferation. The genes CXCL1 and MITF were downregulated in both tumors of the HL_HPS group. This downregulation could create an environment less favorable to tumor growth and more permissive to the action of immune cells, resulting in a more effective AlPcNE-PDT response and the potential increase in abscopal effects.

Comparison between primary and secondary site tumors in the control group revealed a higher number of downregulated genes in the secondary one, indicating an immunosuppressive or adaptive response. In contrast, the absence of significantly DEGs between primary and secondary sites tumors in the AlPcNE-PDT HL_HPS-treated group suggests a homogenization of the immune response, likely due to the dissemination of systemic immune signals induced by AlPcNE-PDT.

The noteworthy results in the HL_HPS group can be attributed to the ability of AlPcNE-PDT to modulate the expression profile of genes involved in the immune system process. This modulation led to an increase in the systemic population of CD8 T cells and the identification of an abscopal effect in the non-irradiated tumor.

5. CONCLUSION

Our findings suggest for the first time that AlPcNE-PDT can induce potent local and systemic antitumor immune responses. The antitumor effects of AlPcNE-PDT were achieved through direct action and by modulation of the gene expression profile of both primary and secondary sites tumors, leading to the observed abscopal effects. To our knowledge, this is also the first evaluation of AlPcNE-PDT impact on both direct and abscopal effects.

This study confirmed the efficacy of PDT in reducing tumor volume and inducing systemic immune responses, particularly highlighted by in the HL_HPS-PDT group, which presented an abscopal effect. Hematological changes and alterations in the T cell population indicated a complex interaction between PDT and the immune system, suggesting new avenues for optimizing combination therapies. RNA-Seq analysis reinforces the idea that PDT can modulate gene expression related to the immune system in a localized and systemic manner. To strengthen our conclusions, it would be beneficial to conduct additional studies to validate the RNA-Seq results, using techniques such as RT-PCR, and to investigate the molecular mechanisms underlying the abscopal effect.

In summary, this study demonstrated that PDT with AlPcNE can induce local and systemic antitumor immune responses, representing a potentially robust approach to enhance melanoma treatment outcomes. The identification of modulated genes by the therapy, in both primary and secondary sites tumors, suggests new therapeutic targets and strategies to enhance the abscopal effects and reduce the adverse effects. These discoveries represent a significant advancement in the field of photodynamic therapy and may positively impact melanoma and other cancer treatments.

REFERÊNCIAS BIBLIOGRÁFICAS

1. Hayward NK, Wilmott JS, Waddell N, et al. Whole-genome landscapes of major melanoma subtypes. Nature. 2017;545(7653):175-180. doi:10.1038/nature22071

2. Schadendorf D, van Akkooi ACJ, Berking C, et al. Melanoma. Lancet. 2018;392(10151):971-984. doi:10.1016/S0140-6736(18)31559-9

3. Teh JLF, Aplin AE. Playing the melanoma endgame. Clin Cancer Res. 2018;24(19):1-7. doi:10.1158/1078-0432.CCR-18-0989

4. Weiss SA, Wolchok JD, Sznol M. Immunotherapy of Melanoma: Facts and Hopes. Clin Cancer Res. 2019;25(17):5191-5201. doi:10.1158/1078-0432.CCR-18-1550

5. Chin L, Garraway LA, Fisher DE. Malignant melanoma: genetics and therapeutics in the genomic era. Genes Dev. 2006;20(16):2149-2182. doi:10.1101/gad.1437206

6. Jiang W, Liang M, Lei Q, Li G, Wu S. The Current Status of Photodynamic Therapy in Cancer Treatment. Cancers (Basel). 2023;15(3):585. doi:10.3390/cancers15030585

7. Castano AP, Demidova TN, Hamblin MR. Mechanisms in photodynamic therapy: Part one - Photosensitizers, photochemistry and cellular localization. Photodiagnosis Photodyn Ther. 2004. doi:10.1016/S1572-1000(05)00007-4

8. Beltrán Hernández I, Yu Y, Ossendorp F, Korbelik M, Oliveira S. Preclinical and Clinical Evidence of Immune Responses Triggered in Oncologic Photodynamic Therapy: Clinical Recommendations. J Clin Med. 2020;9(333):1-24. doi:10.3390/jcm9020333

9. Morais JAV, Almeida LR, Rodrigues MC, Azevedo RB, Muehlmann LA. The induction of immunogenic cell death by photodynamic therapy in B16F10 cells in vitro is effected by the concentration of the photosensitizer. Photodiagnosis Photodyn Ther. 2021;35:102392. doi:10.1016/j.pdpdt.2021.102392

10. Theodoraki MN, Lorenz K, Lotfi R, et al. Influence of photodynamic therapy on peripheral immune cell populations and cytokine concentrations in head and neck cancer. Photodiagnosis Photodyn Ther. 2017;19(May):194-201. doi:10.1016/j.pdpdt.2017.05.015

11. Shams M, Owczarczak B, Manderscheid P, David K, Gollnick SO. Development of photodynamic therapy regimens that control primary tumor growth and inhibit secondary disease. Cancer Immunol Immunother. 2015;64:287-297. doi:10.1007/s00262-014-1633-9

12. Muehlmann LA, Rodrigues MC, Paulo J, et al. Aluminium-phthalocyanine chloride

nanoemulsions for anticancer photodynamic therapy : Development and in vitro activity against monolayers and spheroids of human mammary adenocarcinoma MCF-7 cells. J Nanobiotechnology. 2015;13(36):1-11. doi:10.1186/s12951-015-0095-3
13. Rodrigues MC, Vieira LG, Horst FH, et al. Photodynamic therapy mediated by aluminium-phthalocyanine nanoemulsion eliminates primary tumors and pulmonary metastases in a murine 4T1 breast adenocarcinoma model. J Photochem Photobiol B Biol. 2020;204(July 2019):111808. doi:10.1016/j.jphotobiol.2020.111808
14. Goto PL, Siqueira-Moura MP, Tedesco AC. Application of aluminum chloride phthalocyanine-loaded solid lipid nanoparticles for photodynamic inactivation of melanoma cells. Int J Pharm. 2017;518(1-2):228-241. doi:10.1016/j.ijpharm.2017.01.004
15. Rocha MST, Lucci CM, dos Santos JAM, Longo JPF, Muehlmann LA, Azevedo RB. Photodynamic therapy for cutaneous hemangiosarcoma in dogs. Photodiagnosis Photodyn Ther. 2019;27(May):39-43. doi:10.1016/j.pdpdt.2019.05.026
16. Calori IR, Tedesco AC. Aluminum chloride phthalocyanine in MCF-7: Rationally accounting for state of aggregation of photosensitizers inside cells. Dye Pigment. 2020;173(July 2019):1-7. doi:10.1016/j.dyepig.2019.107940
17. Corrêa M, Gumieri L, Hillesheim F, et al. Photodynamic therapy mediated by aluminium-phthalocyanine nanoemulsion eliminates primary tumors and pulmonary metastases in a murine 4T1 breast adenocarcinoma model. J Photochem Photobiol B Biol. 2020;204(January):1-11. doi:10.1016/j.jphotobiol.2020.111808
18. Rodrigues GB, Brancini GTP, Pinto MR, et al. Photodynamic inactivation of Candida albicans and Candida tropicalis with aluminum phthalocyanine chloride nanoemulsion. Fungal Biol. 2020;124(5):297-303. doi:10.1016/j.funbio.2019.08.004
19. Morais JAV, Rodrigues MC, Ferreira FF, et al. Photodynamic therapy inhibits cell growth and enhances the histone deacetylase-mediated viability impairment in Cryptococcus spp . in vitro. Photodiagnosis Photodyn Ther. 2020;29(May 2019):1-5. doi:10.1016/j.pdpdt.2019.101583
20. Tatsuno K, Yamazaki T, Hanlon D, et al. Extracorporeal photochemotherapy induces bona fide immunogenic cell death. Cell Death Dis. 2019;10(8):578. doi:10.1038/s41419-019-1819-3
21. Zhu Z, Scalfi-Happ C, Ryabova A, et al. Photodynamic activity of Temoporfin nanoparticles induces a shift to the M1-like phenotype in M2-polarized macrophages. J

Photochem Photobiol B Biol. 2018;185(June):215-222. doi:10.1016/j.jphotobiol.2018.06.015
22. Hee Sook Hwang; Heejun Shin; Jieun Han; Kun Na. Combination of photodynamic therapy (PDT) and anti-tumor immunity in cancer therapy. J Pharm Investig. 2018:0. doi:10.1007/s40005-017-0377-x
23. Pan Z, Fan J, Xie Q, et al. Novel sulfonamide porphyrin TBPoS-2OH used in photodynamic therapy for malignant melanoma. Biomed Pharmacother. 2021;133:111042. doi:10.1016/j.biopha.2020.111042
24. Gurung P, Lim J, Shrestha R, Kim Y-W. Chlorin e6-associated photodynamic therapy enhances abscopal antitumor effects via inhibition of PD-1/PD-L1 immune checkpoint. Sci Rep. 2023;13(1):4647. doi:10.1038/s41598-023-30256-0
25. White JR, Gong H, Colaizy TT, Moreland JG, Flaherty H, Mcelroy SJ. Evaluation of hematologic variables in newborn C57/BL6 mice up to day 35. Vet Clin Pathol. 2016;45(1):87-95. doi:10.1111/vcp.12314
26. Wang D, DuBois RN. Immunosuppression associated with chronic inflammation in the tumor microenvironment. Carcinogenesis. 2015;36(10):1085-1093. doi:10.1093/carcin/bgv123
27. Was H, Cichon T, Smolarczyk R, et al. Effect of Heme Oxygenase-1 on Melanoma Development in Mice—Role of Tumor-Infiltrating Immune Cells. Antioxidants. 2020;9(12):1223. doi:10.3390/antiox9121223
28. Mroz P, Hashmi JT, Huang Y, Lange N, Hamblin MR. Stimulation of anti-tumor immunity by photodynamic therapy. Expert Rev Clin Immunol. 2011;7(1):75-91.
29. Castano AP, Mroz P, Hamblin MR. Photodynamic therapy and anti-tumour immunity. Nat Rev Cancer. 2006;6(July):535-545. doi:10.1038/nrc1894
30. Martin D, Rödel F, Winkelmann R, Balermpas P, Rödel C, Fokas E. Peripheral Leukocytosis Is Inversely Correlated with Intratumoral CD8+ T-Cell Infiltration and Associated with Worse Outcome after Chemoradiotherapy in Anal Cancer. Front Immunol. 2017;8. doi:10.3389/fimmu.2017.01225
31. Valero C, Zanoni DK, McGill MR, et al. Pretreatment peripheral blood leukocytes are independent predictors of survival in oral cavity cancer. Cancer. 2020;126(5):994-1003. doi:10.1002/cncr.32591
32. Grivennikov SI, Greten FR, Karin M. Immunity, Inflammation, and Cancer. Cell. 2010;140(6):883-899. doi:10.1016/j.cell.2010.01.025

33. Zhu J, Yamane H, Paul WE. Differentiation of Effector CD4 T Cell Populations. Annu Rev Immunol. 2010;28(1):445-489. doi:10.1146/annurev-immunol-030409-101212
34. Hermiston ML, Xu Z, Weiss A. CD45: A Critical Regulator of Signaling Thresholds in Immune Cells. Annu Rev Immunol. 2003;21(1):107-137. doi:10.1146/annurev.immunol.21.120601.140946
35. Raskov H, Orhan A, Christensen JP, Gögenur I. Cytotoxic CD8+ T cells in cancer and cancer immunotherapy. Br J Cancer. 2021;124(2):359-367. doi:10.1038/s41416-020-01048-4
36. Farhood B, Najafi M, Mortezaee K. CD8 + cytotoxic T lymphocytes in cancer immunotherapy: A review. J Cell Physiol. 2019;234(6):8509-8521. doi:10.1002/jcp.27782
37. Maeding N, Verwanger T, Krammer B. Boosting Tumor-Specific Immunity Using PDT. Cancers (Basel). 2016;8(10):91. doi:10.3390/cancers8100091
38. Mroz P, Vatansever F, Muchowicz A, Hamblin MR. Photodynamic Therapy of Murine Mastocytoma Induces Specific Immune Responses against the Cancer/Testis Antigen P1A. Cancer Res. 2013;73(21):6462-6470. doi:10.1158/0008-5472.CAN-11-2572
39. Deng H, Yang W, Zhou Z, et al. Targeted scavenging of extracellular ROS relieves suppressive immunogenic cell death. Nat Commun. 2020;11(1):4951. doi:10.1038/s41467-020-18745-6
40. Mao X, Sethi G, Zhang Z, Wang Q. The Emerging Roles of the HERC Ubiquitin Ligases in Cancer. Curr Pharm Des. 2018;24(15):1676-1681. doi:10.2174/1381612824666180528081024
41. Sala-Gaston J, Martinez-Martinez A, Pedrazza L, et al. HERC Ubiquitin Ligases in Cancer. Cancers (Basel). 2020;12(6):1653. doi:10.3390/cancers12061653
42. Swanson BJ, Jäck H-M, Lyons GE. Characterization of myocyte enhancer factor 2 (MEF2) expression in B and T cells: MEF2C is a B cell-restricted transcription factor in lymphocytes. Mol Immunol. 1998;35(8):445-458. doi:10.1016/S0161-5890(98)00058-3
43. Newman DM, Voss AK, Thomas T, Allan RS. Essential role for the histone acetyltransferase KAT7 in T cell development, fitness, and survival. J Leukoc Biol. 2017;101(4):887-892. doi:10.1189/jlb.1MA0816-338R
44. Gao Y, Zhao H, Mu L. LncRNA-KAT7 Negatively Regulates miR-10a Through an Epigenetic Pathway to Participate in Nonsmall Cell Lung Cancer. Cancer Biother

Radiopharm. 2021;36(5):441-445. doi:10.1089/cbr.2019.3228
45. Dong H, Zhang H, Mao X, Liu S, Xu W, Zhang Y. RBM15 Promates the Proliferation, Migration and Invasion of Pancreatic Cancer Cell Lines. Cancers (Basel). 2023;15(4):1084. doi:10.3390/cancers15041084
46. Susvirkar V, Faesen AC. Shieldin complex assembly kinetics and DNA binding by SHLD3. Commun Biol. 2023;6(1):384. doi:10.1038/s42003-023-04757-7
47. Wei Z, Shen Y, Zhou C, Cao Y, Deng H, Shen Z. CD3D : a prognostic biomarker associated with immune infiltration and immunotherapeutic response in head and neck squamous cell carcinoma. Bioengineered. 2022;13(5):13784-13800. doi:10.1080/21655979.2022.2084254
48. Yang Y, Zang Y, Zheng C, et al. CD3D is Associated with Immune Checkpoints and Predicts Favorable Clinical Outcome in Colon Cancer. Immunotherapy. 2020;12(1):25-35. doi:10.2217/imt-2019-0145
49. Kuo PT, Zeng Z, Salim N, Mattarollo S, Wells JW, Leggatt GR. The Role of CXCR3 and Its Chemokine Ligands in Skin Disease and Cancer. Front Med. 2018;5. doi:10.3389/fmed.2018.00271
50. Calabrese V, Mallette FA, Deschênes-Simard X, et al. SOCS1 Links Cytokine Signaling to p53 and Senescence. Mol Cell. 2009;36(5):754-767. doi:10.1016/j.molcel.2009.09.044
51. Zheng S, Yang B, Li L, et al. CRTAM promotes antitumor immune response in triple negative breast cancer by enhancing CD8+ T cell infiltration. Int Immunopharmacol. 2024;129:111625. doi:10.1016/j.intimp.2024.111625
52. Huang B, Han W, Sheng Z-F, Shen G-L. Identification of immune-related biomarkers associated with tumorigenesis and prognosis in cutaneous melanoma patients. Cancer Cell Int. 2020;20(1):195. doi:10.1186/s12935-020-01271-2
53. Sade-Feldman M, Yizhak K, Bjorgaard SL, et al. Defining T Cell States Associated with Response to Checkpoint Immunotherapy in Melanoma. Cell. 2018;175(4):998-1013.e20. doi:10.1016/j.cell.2018.10.038
54. Haqq C, Nosrati M, Sudilovsky D, et al. The gene expression signatures of melanoma progression. Proc Natl Acad Sci. 2005;102(17):6092-6097. doi:10.1073/pnas.0501564102
55. Eliades P, Abraham BJ, Ji Z, et al. High MITF Expression Is Associated with Super-Enhancers and Suppressed by CDK7 Inhibition in Melanoma. J Invest Dermatol.

2018;138(7):1582-1590. doi:10.1016/j.jid.2017.09.056
56. Cirenajwis H, Ekedahl H, Lauss M, et al. Molecular stratification of metastatic melanoma using gene expression profiling : Prediction of survival outcome and benefit from molecular targeted therapy. Oncotarget. 2015;6(14):12297-12309. doi:10.18632/oncotarget.3655

Annex I –

Universidade de Brasília
Instituto de Ciências Biológicas
Comissão de Ética no Uso Animal

Brasília, 16 de agosto de 2019.

DECLARAÇÃO

Declaramos que o projeto intitulado "**INVESTIGAÇÃO DOS MECANISMOS ANTICÂNCER DE DIFERENTES PROTOCOLOS DE TERAPIA FOTODINÂMICA MEDIADA POR CLORETO DE FTALOCIANINA DE ALUMÍNIO EM NANOEMULSÃO IN VIVO.".** Protocolo n.º 46/2019, sob responsabilidade do Professor Luis Alexandre Muehlmann foi avaliado e aprovado pela Comissão de Ética no Uso Animal (CEUA) da Universidade de Brasília. Este projeto foi aprovado para utilização de: *Mus musculus (180 machos)*. A presente aprovação é válida pelo período de: *01/07/2019* a *01/12/2022*.

Universidade de Brasília UnB

Dr. José Luiz Jivago de Paula Rôlo
Coordenador da CEUA – UnB

Comissão de Ética no Uso de Animais CEUA

*Este documento se restringe à avaliação ética do projeto supracitado e não substitui outras licenças e permissões que porventura se façam necessárias.

4. CONCLUSÕES E PERSPECTIVAS

Os resultados apresentados nesse trabalho revelaram a eficácia da terapia fotodinâmica (TFD) mediada por AlPcNE em induzir a morte celular imunogênica in vitro, com diferentes concentrações de fotossensibilizador. Tal descoberta é significativa pois demonstra que a TFD pode ser ajustada para modular a resposta imunitária, não se limitando apenas à eliminação direta de células tumorais. A TFD mediada por AlPcNE mostrou-se eficaz e segura no combate ao melanoma murino local, além de promover uma resposta imunológica distal contra o tumor, evidenciando um efeito abscopal.

As principais inovações da imunoterapia visam contornar as estratégias de evasão imunitária induzidas pelo câncer. Essas ferramentas reeducam o sistema imunológico do hospedeiro para detectar e eliminar células tumorais, não apenas matando diretamente as células cancerosas, mas também ajudando a induzir uma resposta imunológica contra antígenos tumorais. Esse é um campo cada vez mais promissor para estudos futuros, nos quais a TFD pode ser explorada como uma alternativa viável para a indução de respostas diretas e respostas imunológicas duradouras.

Os resultados do estudo ressaltam a eficácia da TFD no tratamento do melanoma enxertado, destacando importantes efeitos tanto no tumor primário quanto em tumores distantes, por meio do efeito abscopal. Demonstrou-se ainda que a TFD mediada por AlPcNE é capaz de induzir mudanças nos perfis de expressão gênica que podem contribuir significativamente para o desenvolvimento de novas terapias. As alterações observadas no transcriptoma sugerem que a TFD module diferentes vias no combate ao tumor e também no ambiente imunológico, promovendo uma resposta antitumoral sistêmica.

Para complementar e robustecer os resultados encontrados, serão realizados estudos com técnicas de validação adicional, como RT-PCR, para validar as alterações nos perfis de expressão gênica e entender melhor os mecanismos da resposta tumoral e imunológica que vieram à tona. Tais estudos fortalecerão o potencial terapêutico da TFD no tratamento do melanoma, abrindo caminho para o desenvolvimento de estratégias inovadoras, mais eficazes e com menos efeitos colaterais.

REFERÊNCIAS BIBLIOGRÁFICAS

1. Onitilo AA, Wittig JA. Principles of Immunotherapy in Melanoma. *Surg Clin North Am*. 2020;100:161-173. doi:10.1016/j.suc.2019.09.009
2. Hayward NK, Wilmott JS, Waddell N, et al. Whole-genome landscapes of major melanoma subtypes. *Nature*. 2017;545(7653):175-180. doi:10.1038/nature22071
3. Sung H, Ferlay J, Siegel RL, et al. Global Cancer Statistics 2020: GLOBOCAN Estimates of Incidence and Mortality Worldwide for 36 Cancers in 185 Countries. *CA Cancer J Clin*. 2021;71(3):209-249. doi:10.3322/caac.21660
4. Instituto Nacional de Câncer. Estimativa 2023: incidência de câncer no Brasil. Rio de Janeiro: INCA; 2022.
5. Weiss SA, Wolchok JD, Sznol M. Immunotherapy of melanoma: facts and hopes. *Clin Cancer Res*. 2019;25(17):5191-5201. doi:10.1158/1078-0432.CCR-18-1550
6. Hanahan D, Weinberg RA. Hallmarks of Cancer : The Next Generation. *Cell*. 2011;144(5):646-674. doi:10.1016/j.cell.2011.02.013
7. Weiss SA, Wolchok JD, Sznol M. Immunotherapy of Melanoma: Facts and Hopes. *Clin Cancer Res*. 2019;25(17):5191-5201. doi:10.1158/1078-0432.CCR-18-1550
8. Dakubo GD. Melanoma Biomarkers in Circulation. In: *Cancer Biomarkers in Body Fluids*. Cham: Springer International Publishing; 2017:1-39. doi:10.1007/978-3-319-48360-3_1
9. Baldea I, Giurgiu L, Teacoe ID, et al. Photodynamic Therapy in Melanoma - Where do we Stand? 2018:5540-5563. doi:10.2174/0929867325666171226115626
10. Chin L, Garraway LA, Fisher DE. Malignant melanoma: genetics and therapeutics in the genomic era. *Genes Dev*. 2006;20(16):2149-2182. doi:10.1101/gad.1437206
11. O'Shaughnessy MJ, Murray KS, La Rosa SP, et al. Systemic antitumor immunity by PD-1/PD-L1 inhibition is potentiated by vascular-targeted photodynamic therapy of primary tumors. *Clin Cancer Res*. 2018;24(3):592-599. doi:10.1158/1078-0432.CCR-17-0186
12. Lelliott EJ, McArthur GA, Oliaro J, Sheppard KE. Immunomodulatory Effects of BRAF, MEK, and CDK4/6 Inhibitors: Implications for Combining Targeted Therapy and Immune Checkpoint Blockade for the Treatment of Melanoma. *Front Immunol*. 2021;12. doi:10.3389/fimmu.2021.661737
13. Pastorino L, Andreotti V, Dalmasso B, et al. Insights into Genetic Susceptibility to Melanoma by Gene Panel Testing: Potential Pathogenic Variants in ACD, ATM, BAP1, and POT1. *Cancers (Basel)*. 2020;12(4):1007. doi:10.3390/cancers12041007
14. Ng MF, Simmons JL, Boyle GM. Heterogeneity in Melanoma. *Cancers (Basel)*. 2022;14(12):3030. doi:10.3390/cancers14123030
15. Guo ZS, Liu Z, Bartlett DL. Oncolytic Immunotherapy: Dying the Right Way is a Key to Eliciting Potent antitumor immunity. *Front Oncol*. 2014;4(74):1-12. doi:10.3389/fonc.2014.00074
16. Garg AD, Martin S, Golab J, Agostinis P. Danger signalling during cancer cell death : origins , plasticity and regulation. *Cell Death Differ*. 2014;21:26-38. doi:10.1038/cdd.2013.48
17. Bezu L, Gomes-da-Silva LC, Dewitte H, et al. Combinatorial strategies for the induction of immunogenic cell death. *Front Immunol*. 2015;6(187):1-11. doi:10.3389/fimmu.2015.00187
18. Fermín E. Gonzalez; Alejandra Gleisner; Felipe Falcon-Beas; Fabiola Osorio; Mercedes N. Lopez; Flavio Salazar-Onfray. Tumor cell lysates as immunogenic sources for cancer vaccine design. *Hum VACCINES Immunother*. 2014;10(11):3261-3269.
19. Garg AD, Dudek AM, Agostinis P. Cancer immunogenicity, danger signals, and DAMPs: what, when, and how? *Int Union Biochem Mol Biol*. 2013;39(4):355-367.

doi:10.1002/biof.1125
20. Sukkurwala AQ, Martins I, Wang Y, et al. Immunogenic calreticulin exposure occurs through a phylogenetically conserved stress pathway involving the chemokine CXCL8. *Cell Death Differ*. 2014;21:59-68. doi:10.1038/cdd.2013.73
21. Martins I, Tesniere A, Kepp O, et al. Chemotherapy induces ATP release from tumor cells. *Cell Cycle*. 2009;8(22):3723-3728. doi:10.4161/cc.8.22.10026
22. Fucikova J, Kline JP, Galluzzi L, Spisek R. Calreticulin arms NK cells against leukemia. *Oncoimmunology*. 2020;9(1):10-11. doi:10.1080/2162402X.2019.1671763
23. Tsunoda M, Aoki H, Shimizu H, Shichino S, Matsushima K, Ueha S. Proportional Tumor Infiltration of T Cells via Circulation Duplicates the T Cell Receptor Repertoire in a Bilateral Tumor Mouse Model. *Front Immunol*. 2021;12(October):1-12. doi:10.3389/fimmu.2021.744381
24. Palanivelu L, Liu C-H, Lin L-T. Immunogenic cell death: The cornerstone of oncolytic viro-immunotherapy. *Front Immunol*. 2023;13. doi:10.3389/fimmu.2022.1038226
25. Krysko D V., Garg AD, Kaczmarek A, Krysko O, Agostinis P, Vandenabeele P. Immunogenic cell death and DAMPs in cancer therapy. *Nat Rev Cancer*. 2012;12(12):860-875. doi:10.1038/nrc3380
26. Dennis.J.G.J. Dolmans DF and RKJ. Photodynamic therapy for cancer. *Nat Publ Gr*. 2003;3:380-387. doi:10.1038/nrc1070
27. Huis in 't Veld R V., Heuts J, Ma S, Cruz LJ, Ossendorp FA, Jager MJ. Current Challenges and Opportunities of Photodynamic Therapy against Cancer. *Pharmaceutics*. 2023;15(2):330. doi:10.3390/pharmaceutics15020330
28. Gollnick SO, Owczarczak B, Maier P. Photodynamic Therapy and Anti-Tumor Immunity. *Lasers Surg Med*. 2006;38:509-515. doi:10.1002/lsm.20362
29. Castano AP, Demidova TN, Hamblin MR. Mechanisms in photodynamic therapy: Part two - Cellular signaling, cell metabolism and modes of cell death. *Photodiagnosis Photodyn Ther*. 2005. doi:10.1016/S1572-1000(05)00030-X
30. Shen Y, Li M, Sun F, et al. Low-dose photodynamic therapy-induced increase in the metastatic potential of pancreatic tumor cells and its blockade by simvastatin. *J Photochem Photobiol B Biol*. 2020;207(May):111889. doi:10.1016/j.jphotobiol.2020.111889
31. Ash C, Dubec M, Donne K, Bashford T. Effect of wavelength and beam width on penetration in light-tissue interaction using computational methods. *Lasers Med Sci*. 2017;32(8):1909-1918. doi:10.1007/s10103-017-2317-4
32. Muehlmann LA, Rodrigues MC, Paulo J, et al. Aluminium-phthalocyanine chloride nanoemulsions for anticancer photodynamic therapy : Development and in vitro activity against monolayers and spheroids of human mammary adenocarcinoma MCF-7 cells. *J Nanobiotechnology*. 2015;13(36):1-11. doi:10.1186/s12951-015-0095-3
33. Kessel D. Photodynamic therapy : Promotion of efficacy by a sequential protocol. *J Porphyrins Phtalocyanines*. 2016;20:302-306. doi:10.1142/S1088424616500073
34. Calori IR, Tedesco AC. Aluminum chloride phthalocyanine in MCF-7: Rationally accounting for state of aggregation of photosensitizers inside cells. *Dye Pigment*. 2020;173(July 2019):1-7. doi:10.1016/j.dyepig.2019.107940
35. Goto PL, Siqueira-Moura MP, Tedesco AC. Application of aluminum chloride phthalocyanine-loaded solid lipid nanoparticles for photodynamic inactivation of melanoma cells. *Int J Pharm*. 2017;518(1-2):228-241. doi:10.1016/j.ijpharm.2017.01.004
36. Halaburková A, Jendželovský R, Kovaľ J, Herceg Z, Fedoročko P, Ghantous A. Histone deacetylase inhibitors potentiate photodynamic therapy in colon cancer cells marked by chromatin-mediated epigenetic regulation of CDKN1A. *Clin Epigenetics*. 2017;9(1):1-

16. doi:10.1186/s13148-017-0359-x
37. Rodrigues MC, Vieira LG, Horst FH, et al. Photodynamic therapy mediated by aluminium-phthalocyanine nanoemulsion eliminates primary tumors and pulmonary metastases in a murine 4T1 breast adenocarcinoma model. *J Photochem Photobiol B Biol*. 2020;204(July 2019):111808. doi:10.1016/j.jphotobiol.2020.111808